leti
cea tech

TECHNOLOGY
RESEARCH
INSTITUTE

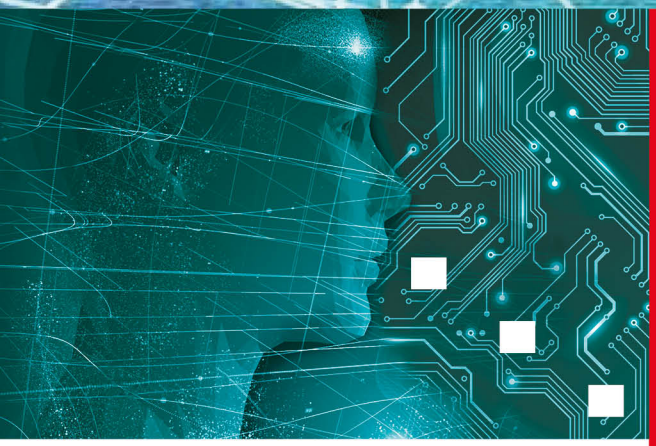

SYSTEMS

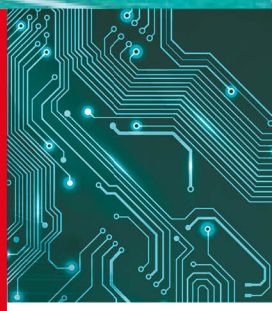

ANNUAL
RESEARCH REPORT
2018

leti
cea tech

TECHNOLOGY
RESEARCH
INSTITUTE

Committed to Innovation, Leti Creates Differentiating Solutions for its Industrial Partners.

Leti is a research institute of CEA Tech and a recognized global leader in miniaturization technologies. Leti's teams are focused on developing solutions that will enable future information and communication technologies, health and wellness approaches, clean and safe energy production and recovery, sustainable transport, space exploration and cybersecurity.

For 50 years, the institute has built long-term relationships with its industrial partners, tailoring innovative and differentiating solutions to their needs. Its entrepreneurship programs have sparked the creation of 64 start-ups. Leti and its industrial partners work together through bilateral projects, joint laboratories and collaborative research programs.
Leti maintains an excellent scientific level by working with the best research teams worldwide, establishing partnerships with major research technology organizations and academic institutions. Leti is also a member of the Carnot Institutes network*.

*Carnot Institutes network: French network of 34 institutes serving innovation in industry.

DE LA RECHERCHE À L'INDUSTRIE
cea

CEA Tech is the technology research branch of the French Alternative Energies and Atomic Energy Commission (CEA), a key player in research, development and innovation in defense & security, nuclear energy, technological research for industry and fundamental physical and life sciences.

www.cea.fr/english

Leti at a glance

€315
million budget

800
publications per year

ISO 9001
certified since 2000

Founded in
1967

Based in
France (Grenoble)
with offices in the
USA (Silicon Valley)
and **Japan** (Tokyo)

350
industrial partners

1,900
researchers

2,760
patents in portfolio

91,500
sq. ft. cleanroom space, 8" & 12" wafers

64
startups created

SYSTEMS

Based on MINATEC Campus, Systems Integration Division (DSYS) is at the strategic core of Leti's technological solutions, adding a "system perspective" on technological trends. Our research activities focus on the design and integration of innovative solutions based on emerging electronic technologies for a wide panels of applications such as factory of the future, multimedia, smart energy, smart transport, e-health, sports and leisure.

DSYS's expertise is based on four major pillars which are (i) wireless communications, (ii) innovative sensor-system design, (iii) power-management systems and (iv) security solutions for electronics and components. Our teams are using tools and know how inherited from physic, electromagnetism and electronic areas but also from signal and data processing domain ; they also take profit from state of the art facilities for achieving simulation, characterization and prototyping steps.

Thanks to its capability to work on specific application barriers, DSYS Division is particularly attractive for industrial partners who are facing the challenges of IoT , 5G and cybersecurity. It can be either SME or big companies which are looking for a high level expertise in a businesslike environment.

CONTENTS

EDITO

SEBASTIEN DAUVE,
HEAD OF DSYS SYSTEM DIVISION

This document publishes our most significant technological and innovation achievements of 2018 selected among a wide variety of scientific results, some of them conducted jointly with external partners who gave their agreement.

DSYS is committed to innovation, creating and transferring innovative solutions for its industrial partners worldwide in the domains of Energy, Sensors and Systems, Low Data Rate and Localization, Wireless High Speed Communications, Antennas and Propagation and, Security of Embedded Systems. In 2018 DSYS have been working with over 100 national and international industrial partners through bilateral projects, joint laboratories, and collaborative research. Moreover, in 2018 DSYS maintains an excellent scientific level by working with the best research teams in best academic institutions and research technology organizations at regional, national and international level, producing about 200 publications, 52 patents, tens of prototypes and 2 best papers awards in major national and international conferences.

In 2018 DSYS consolidated its contributions to the design, development and evaluation of innovative solutions for the fore coming generation of 5G (and beyond) wireless communication systems. In chapter 1 of this report, we present a selection of findings on advanced modulation/coding and spectrum/network management techniques, supported by artificial intelligence deep tech, "as well as distributed edge cloud computation and caching mechanisms. Some contributions concern 5G New Radio high-speed communications operating either below 6 GHz or in millimeter wave and sub-THz frequency domains. In chapter 2, we present complementary research results on highly resilient and ultra low power communication protocols, as well as wireless localization techniques, two major pillars of future vertical applications (factory of the future, connected intelligent transport systems…). In chapter 3, we detail innovations regarding the design, the technological realization and the performance measurement of wideband and reconfigurable antennas under stringent integration constraints, spanning from low band to millimeter and even sub-THz spectrum. Other related studies include the measurement, modeling and emulation of radio propagation in complex environments, as well as the characterization and testing of wideband, multi-band and super-directive communications.

In chapter 4 we present a selection of our scientific results in the domains of sensors' design and their dedicated signal processing and energy harvesting where we propose to exploit either MEMs capabilities for applications where low power or advanced integration present critical constraints or, to explore capabilities of nanotechnology where MEMs do not provide efficient solutions. Target applications are multiple, from Industrial IoT, multi-modal transport systems, emotional sensing to shape capture. Moreover, in chapter 4 we present our solutions and results for battery energy management.

2018 has been notably marked by a significant increase of our investigations on hardware enabled cyber security and on the identification of countermeasures to threats for the applications related to massive IoT, which have a critical impact on vertical industry needs. Our proposed solutions are detailed in chapter 5.

I would also like to thank our industrial partners, institutional fellows and academic collaborators, who have worked closely with us for many years to identify new paths towards breakthrough technologies. Finally, I would like to acknowledge the young researchers and students that join us each year to carry out some of the world's most advanced research projects and to become the next generation of innovators.

I hope you will find in DSYS's 2018 Scientific Report inspiration for your future developments and research.

SCIENTIFIC ACTIVITY

Publications

170 publications in 2018 including 43 book chapters and top journals,127 international conference communications. These include IEEE Transactions on Wireless Communications, IEEE Transactions on Antenna and Propagation, IEEE Transactions on Electromagnetic Compatibility, IEEE Transactions on Communications, IEEE Sensors & Transducers journal, IEEE Transaction on Haptics, IEEE Transactions on Very Large Scale Integration Systems, IEEE Transactions on vehicular Technology, Smart Materials and Structures journal, IEEE VTC, IEEE ICC, IEEE PIMRC, IEEE WCNC, IEEE GlobeCom, Physiological computing conference; International Workshop on SHM, PowerMEMS, etc.

Prize and awards

• Best paper award: F Wolf et al., Coherent Multi-Channel Ranging for Narrowband LPWAN: Simulation and Experimentation Results, IEEE Workshop on Positioning, Navigation, and Communications (WPNC), Bremen, Germany, 2018.
• Best poster award: P Gasnier et al., A 120°C 20G-compliant vibration energy harvester for aeronautic environments, PowerMems 2018.

Experts

1 International Expert, 2 research directors, 20 Senior Experts, 17 Experts, 8 of them holding an HDR.

Scientific committees

• National Research Agency «High performance infrastructures, software technology and science » committee.
• Technical Program committees of: JNM, COST 15104, EurAAP, IEEE EUROCON, IEEE GlobCom, EuCNC, IEEE VTC, IEEE PIMRC, IEEE WCNC, IEEE VTC, IEEE DySPAN.

Conferences and Workshops organizations

CrownCom Conference Organization in Grenoble, Workshops, Panels and special sessions organized in the following conferences: EuCAP, EuMW, EuCNC, ISWCS, IEEE ICC, IEEE WCNC, IEEE PIMRC.

International Collaborations

University of Rome (Italy) University of Bologna (Italy), University of Calgary (Canada), Université Catholique de Louvain (Belgium), Czech Technical University (Czech Republic), Fraunhofer Institute HHI (Germany), ETRI (South Korea), Tokyo Teck University (Japan).

KEY FIGURES

174 researchers

36 PhD students and post-docs

45 Temporary employees and interims

27,8 M€ budget

89,5% external funding

52 patents granted in 2018

481 patents portfolio

43 book chapters and journals

127 communications in conferences and workshops

29 Keynotes and invited talks

8 Organization of internationals conference and workshop

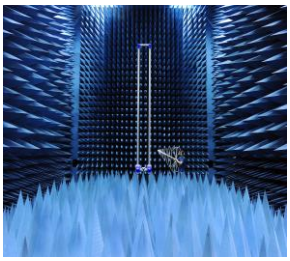

Research facilities:

3 Anechoic chambers

Magnetometer test ground
Information Technology Security Evaluation Facility (ITSEF)
Focus Ion Beam (FIB)
channel analyzer

72 Industrial partners with whom we have a bilateral contract

01 ENERGY, SENSORS AND SYSTEMS

- **Nano systems**
- **Mems Devices**
- **Energy Harvesting**
- **Battery Energy Management**
- **Emotional Sensing**
- **Shape Capture**
- **Context Recognition**

TOWARDS NANOSATELLITE MAGNETIC MISSIONS BUILT ARROUND THE NEXT GENERATION OF ASM-V SENSORS

RESEARCH TOPIC:

Optically pumped ^{4}He magnetometers; Swarm; ASM-V instrument; Nanosatellite

AUTHORS:

T. Jager, J.-M. Léger, F. Bertrand, A. Boness, W. Fourcault, G. Hulot (IPGP) and B. Faure (CNES)

ABSTRACT:

The development of an improved and miniaturized version of the scalar/vector absolute ^{4}He magnetometers (ASM-V) operated on-board the ESA Swarm satellites is now well advanced and has enabled a preliminary design of a 12U nanosatellite mission (NanoMagSat) that could complement the ESA Swarm constellation. The next generation of the laser source and of the miniaturized sensor head architecture have been investigated, operated and validated. With these upgrades, we have already demonstrated a 0.7 pT/√Hz scalar resolution and a measurement accuracy of 50 pT (1 σ).

SCIENTIFIC COLLABORATIONS: G. Hulot (IPGP, Paris, France), B. Faure (CNES, Toulouse, France)

Context and Challenges

The ASM-V instruments currently operated on-board the satellites of the ESA Swarm mission have demonstrated excellent performance since their launch in November 2013 [1-2]. To target future scientific geomagnetic missions based on nanosatellite platforms they nonetheless need further miniaturization. Supported by CNES, several development and upgrade activities focusing on both the ASM-V electronics (DPU) and the ASM-V sensor head have been performed, showing that the next generation of ASM-V instruments will meet the constraints and the performance specifications of such missions [3].

Main Results

A large proportion of the current ASM-V DPU is dedicated to a tunable fiber laser, a complex component assembly used to perform the optical pumping of the ^{4}He atoms at 1083 nm. Since the development phase of the ASM-V instrument for Swarm, new DFB fiber laser diodes at 1083 nm have become available. We have operated several of these components, confirming that an important size reduction factor (at least a factor of 10) can be achieved for this specific part of the DPU without degrading the metrological performance. This is illustrated on Fig. 1 showing a scalar noise spectrum measurement performed in ambient Earth field with an instrument using such a diode: a 0.7 pT/√Hz scalar resolution was achieved which is even better than the 1 pT/√Hz provided by the ASM-V instrument developed for the Swarm mission.

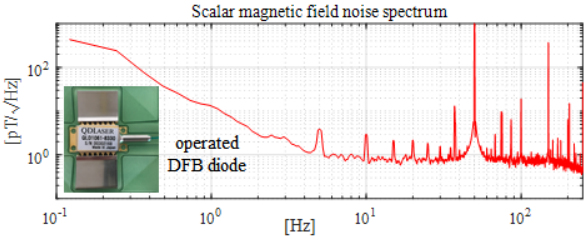

Figure 1. Scalar noise spectrum measurement performed in ambient Earth field with a 1083 nm DFB laser diode.

A major part of the sensor head improvement activities have been focused in replacing the complex {stator+rotor} isotropic structure of the ASM-V instruments built for Swarm by a monolithic one described on Fig. 2. In this new sensor architecture, a Liquid crystal Polarization Rotator (LPR) is now used to rotate the linear polarization of the incident pumping light and two pairs of RF orthogonal coils generate the RF field parallel to the polarization direction. Thanks to this new monolithic configuration, a significant size reduction of the sensor head is also achieved. A complete sensor demonstrator based on this architecture has been successfully operated in static Earth ambient magnetic field and in variable field environments with a demonstrated measurement accuracy of about 50 pT (1 σ) similar to the one obtained with the Swarm ASM-V instruments.

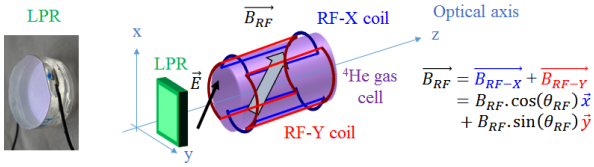

Figure 2. Isotropic sensor head architecture for the next generation of sensor with the miniaturized monolithic structure

Perspectives

These results have already enabled a preliminary design of a 12U nanosatellite mission built around the next generation of ASM-V instruments [3]. If selected, this mission could complement the Swarm one in many ways and open the path to a future low cost and permanent monitoring of the geomagnetic field.

Other improvements activities are also in progress, on the upgrade of the structure material of the ASM-V sensor head and on the optimization of the vector measurements reconstruction.

All these developments will also benefit to other types of mobile applications, such as airbone MAD or aeromagnetic survey.

RELATED PUBLICATIONS:

[1] J.-M. Léger et al., "In-flight performance of the Absolute Scalar Magnetometer vector mode on board the Swarm satellites", Earth Planets and Space, 67-57 (2015).

[2] G. Hulot et al, "Swarm's absolute magnetometer experimental vector mode, an innovative capability for space magnetometry", Geophysical Research Letters, Vol. 42, 5, 1352-1359 (2015).

[3] G. Hulot et al, "Nanosatellite High-Precision Magnetic Missions Enabled by Advances in a Stand-Alone Scalar/Vector Absolute Magnetometer", IGARSS 2018, Valencia, Spain, 22-27/07/2018.

MAGNETOENCEPHALOGRAPHY WITH OPTICALLY PUMPED 4HE MAGNETOMETERS AT ROOM TEMPERATURE

RESEARCH TOPIC:

Optically pumped magnetometers, medical imaging, MEG

AUTHORS:

Etienne Labyt (LSSC), Marie-Constance Corsi (LCHP), William Fourcault (LCHP), Augustin Palacios Laloy (LCHP), François Bertrand (LCHP), François Lenouvel (Clinatec), Gilles Cauffet (G2ELab), Matthieu Le Prado (LCHP), François Berger (INSERM U1205), and Sophie Morales (LCHP)

ABSTRACT:

We achieved the first proof of concept confirming the possibility to record magnetoencephalographic (MEG) signals with Optically Pumped Magnetometers (OPMs) based on parametric resonances of metastable ^{4}He atoms. The main advantage of this kind of OPM is the possibility to provide a tri-axis vector measurement of the magnetic field at room temperature (the ^{4}He vapor needs neither cooling nor heating). The preliminary version of the sensor used here achieves a sensitivity of 210 fT/√Hz in the bandwidth [2 Hz - 300 Hz]. MEG simulation studies with a brain phantom were cross-validated with real MEG measurements on a healthy subject.

SCIENTIFIC COLLABORATIONS: Clinatec, G2ELab, INSERM

Context and Challenges

CEA LETI has worked on helium-4 optically pumped magnetometers (OPM) for space exploration. These sensors have been launched in 2013, at the end of a **22 M€** sensor development program with European Space Agency (ESA). A declination of this sensor has been **adapted to medical biomagnetic imaging** by CEA and was awarded at the H2020 Innovation Radar Prize 2017 through the **best Early Stage Innovation**. Helium OPM bandwidth (2 kHz), dynamic range (>100 nT), power to be dissipated (0.01 W) in the sensor are one or two orders of magnitude better than alkali OPM, and a tri-axes vector measurement is achievable .

Main Results

The main advantage of this kind of OPM is the possibility to provide a tri-axis vector measurement of the magnetic field at room-temperature (the ^{4}He is neither cooled nor heated). The sensor used for this work was a preliminary version achieving a sensitivity of 210 fT/√Hz in the bandwidth [2 Hz - 300 Hz]. MEG simulation studies with a brain phantom were cross-validated with real MEG measurements on a healthy subject. For both studies, MEG signal was recorded consecutively with OPMs and Superconducting Quantum Interference Devices (SQUIDs) used as reference sensors. For healthy subject MEG recordings, three MEG proofs of concept were carried out based on the recording of auditory and visual evoked fields (AEF, VEF), and spontaneous activity. M100 peaks have been detected on evoked responses recorded by both OPMs and SQUIDs with no significant difference in latency. Concerning spontaneous activity, an attenuation of the signal power between 8-12 Hz (alpha band) related to eyes opening has been observed with OPM similarly to SQUID. All these results confirm that the room temperature vector ^{4}He OPMs can record MEG signals and provide reliable information on brain activity.

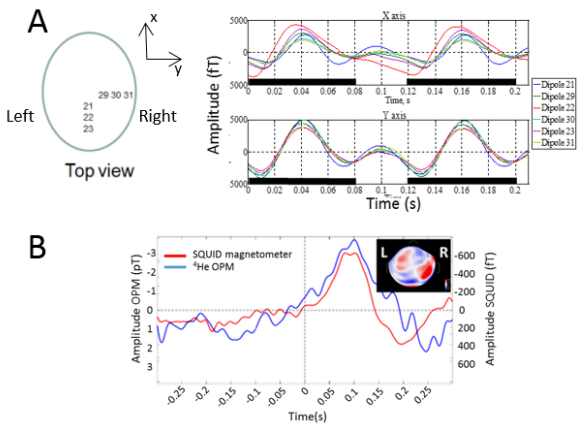

A : Averaged signals from OPMs along the X and Y axes with 6 dipoles of a MEG phantom successively excited. Dark bars correspond to dipole excitation

B : Averaged AEF recorded from one SQUID magnetometer placed in the right temporal area and superimposed, the averaged signal from ^{4}He OPM

Perspectives

Currently, a first array of 5 sensors is being developed for addressing cross-talk and electromagnetic compatibility issues in the framework of the challenge first step program. Several collaborations with hospitals (CHU La Timone - Marseille, European Hospital Erasme - Brussels) and research centers (CERMEP and CRNL - Lyon, ICM - Paris, PTB - Berlin) are emerging, for the test and the validation of this first ^{4}He OPM array for MEG imaging. Application to magnetocardiography (MCG) is also considered.

RELATED PUBLICATIONS:

Labyt E, Corsi MC, Fourcault W, Palacios-Laloy A, Bertrand F, Lenouvel F, Cauffet G, Le Prado M, Berger F, Morales S. Magnetoencephalography with optically pumped 4He magnetometers at ambient temperature. IEEE Trans Med Imaging. 2018 Jul 16. doi: 10.1109/TMI.2018.2856367.

Etienne Labyt, Augustin Palacios-Laloy, François Beato, Gaetan Lieb, Marie-Constance Corsi, William Fourcault, François Bertrand, François Lenouvel, Gilles Cauffet, François Berger, Gerald Vanzetto, Sophie Morales, Matthieu Le Prado. Proof of concept of optically pumped 4He magnetometers for MCG/MEG recordings. Conference of European MEG Society and International Society for Advancement of Clinical MEG, Poros, 2018

Etienne Labyt, Augustin Palacios-Laloy, Marie-Constance Corsi, William Fourcault, François Bertrand, François Lenouvel, Gilles Cauffet, François Berger, Sophie Morales, Matthieu Le Prado. First MEG recordings with an optically pumped 4He magnetometer at ambient temperature. 21st International Conference on BIOMAGnetism, Philadelphia, 2018

HUMAN STESS LEVEL EVALUATION USING WEARABLE SENSOR: TOWARD MULTI-TASK MULTI-USER AND PRESSURE SPECIFIC ESTIMATORS

RESEARCH TOPIC:

Affective computing, human stress estimation, wearables, physiological sensors, machine learning

AUTHORS:

Christelle Godin, Gaël Vila, Oumayma Sakri, Etienne Labyt
Sylvie Charbonnier, Aurélie Campagne

ABSTRACT:

Stress evaluation using physiological sensors need a strong database in order to choose the relevant features and models robust to activity, multi-task and multi-user. We conducted a laboratory experiment with 20 subjects in which each participant's physiological parameters were recorded doing several stress task (TSST, SECPT, MST) and the corresponding activity without stress. Several analysis were conducted in order to analyse the activity/pressure effect, the feature relevance for a multi-task model and the classification accuracy. Machine learning, statistical analysis, and fuzzy model were proposed and showed all interesting proprieties with respect to stress evaluation in real time settings goal.

SCIENTIFIC COLLABORATIONS: Gipsa-Lab, CNRS, LPNC UMR 5105, 3Univ. Grenoble Alpes

Context and Challenges

Stress and its management has become a major issue in modern societies. Systems that could automatically asses people's stress would have a lot of potential applications from prevention of long term stress related health disorders, to detecting high stress situation to avoid accidents for drivers or firefighters. Several studies designed stress estimators using physiological sensors and machine learning. Databases were constructed in laboratory conditions and estimators showed high accuracy. When used in real environments, their performances decrease. Laboratory experiments consist in simulating real life stressors. One reason of this lack of generalization capabilities of those studies is that, in laboratory experiments, only one kind of stressor was considered (simulated job interview or mental arithmetic task). Another possible reason is that stress condition is compared with rest. In this kind of experimental design, stress detection will be automatically mixed with activity detection.

Main Results

To avoid those limitations we designed a multi-task experiment. We used TSST (Trier Social Stress Test), MST (Mental Arythmetic Stress Test), SECPT (Socially Evaluated Cold Pressor Test). Each task had two conditions, one doing only the corresponding activity (counting for MST, speaking for TSST, submerge hand in water for SECPT) and the other doing the activity with the stressor. Before each experiment, rest condition was also recorded for individual baselines. 20 participants did the complete experimental protocol (3 task and 3 control sessions). All experiments were conducted with laboratory sensors (AD Instruments FE132 with ECG electrodes and MLT116F with EDA electrodes) and 6 subjects wore also Empatica E4.

Database was analyzed with three different approaches. A machine learning approach using Empatica E4 signals [1], a feature selection focusing on ability to discriminate pressure but not activity [2] and a fuzzy approach to estimate stress level using laboratory sensors [3].

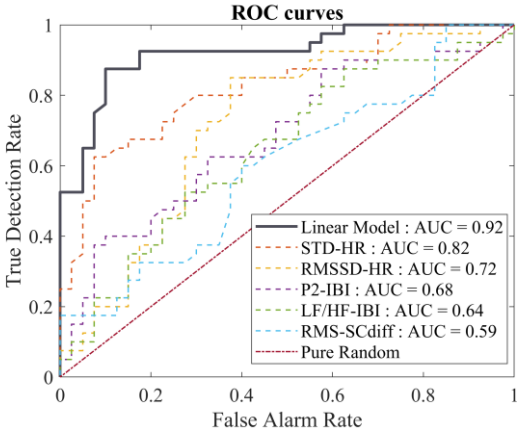

Fig 1 : Receiver Operating Characteristic for a multi-feature linear model for stress detection task.

In [1] stress/control was achieved with around 85% classification rate. Learning on TSST (resp. MST) has good validation rate on MST (resp. TSST), suggesting that MST and TSST generate similar patterns in physiological parameters. It is not the case with SECPT, but learning with TSST+SECPT has good validation rates on MST suggesting that a multi-task model is feasible.

In [2] we selected features responding for stress task but not for control ones. After this selection, a linear model was learnt at multi-user level. Its ROC curve in fig1 shows interesting proprieties like true detection rate equal to 0.5 with a null false alarm rate.

In [3] we proposed a fuzzy model calibrated by using only rest periods. This is a very interesting model personalization in real world applications.

Perspectives

Models will have to be evaluated and tuned on real world experiments.

RELATED PUBLICATIONS:

[1] O. Sakri, C. Godin, G. Vila, E. Labyt, S. Charbonnier, et A. Campagne, « A Multi-User Multi-Task Model For Stress Monitoring From Wearable Sensors », in 2018 21st International Conference on Information Fusion (FUSION), 2018, p. 761-766.

[2] G. Vila, C. Godin, S. Charbonnier, E. Labyt, O. Sakri, et A. Campagne, « Pressure-Specific Feature Selection for Acute Stress Detection From Physiological Recordings », in 2018 IEEE International Conference on Systems, Man, and Cybernetics (SMC), 2018, p. 2341-2346.

[3] S. Charbonnier, G. Vila, C. Godin, E. Labyt, O. Sakri, et A. Campagne, « A Multi-feature Fuzzy Index to Assess Stress Level from Bio-signals », in 2018 40th Annual International Conference of the IEEE Engineering in Medicine and Biology Society (EMBC), 2018, p. 1086-1089.

BROADBAND ULTRASOUND ENGINEERING WITH CARBON NANOMEMBRANES MEMS ARRAYS

RESEARCH TOPIC:

MEMS, micro-C-MUTS, carbon, membranes, mechanical properties, resonances, large bandwidth acoustic transducers

AUTHORS:

A. Ghis, S. Thibert; M. Delaunay

ABSTRACT:

Ultrathin Carbon is an innovative material providing new opportunities namely for MEMS. Both outstanding resonant patterns up to 100MHz and large deflections of 10nm thick membranes have been observed and reported. More, in a forced oscillation mode, and despite the extreme thinness, pressure waves are efficiently generated. Ultrasound generation over a large frequency range in air has recently been demonstrated. LETI is currently conducting an in-house research program on applications and technologies as these new devices can lead to breakthroughs in areas such as medical imaging or mobile devices.

SCIENTIFIC COLLABORATIONS:

Context and Challenges

Ultrasound techniques are widely used as an analysis tool, in various fields, from medical imaging to materials science. The spatial resolution of the resulting information is related in particular to the geometry of the transducers. In the case of Micromachined Ultrasonic Transducers (MUT), the active part is a vibrating membrane operated at its natural frequency. The reduction of the vibrating surface of the devices to dimensions in the micrometer range is to be associated with a decrease in the thickness of the membrane to achieve functional displacements. More, as far as the membrane material is suitable, a thickness of a few nanometers significantly rules the mechanics of these membranes, thus opening up new application opportunities, in particular by making it possible to continuously address the entire frequency range below the resonant frequency.
Amorphous carbon seems to be particularly well suited to this ultra-thin layer application as an active part of MEMS, combining elasticity and toughness with the many well-known properties of the Diamond Like Carbon (DLC) family.

Main Results

Preliminary studies were conducted with membranes suspended above 1-2µm wide long trenches. The devices have been characterized regarding to resonators performances. Resonance frequencies up to 110MHz have been observed for the narrowest devices (fig.1 left).
More, high order resonant patterns were be experimentally mapped [2] using specific AFM-based characterization method.
The results that led our present work are the measurements operated when these membranes were excited in a forced oscillation mode (fig.1 right). At very low frequency, under the electrostatic force generated by an applied voltage of a few Volts, the center of the membrane moves of several tens of nanometers. Regarding to both the thickness of the membrane (10nm) and the suspended length (1µm), this displacement is remarkably high. These measurements having been taken at ambient pressure, the membrane oscillations should be able to generate sound wave in air, even at low frequencies.

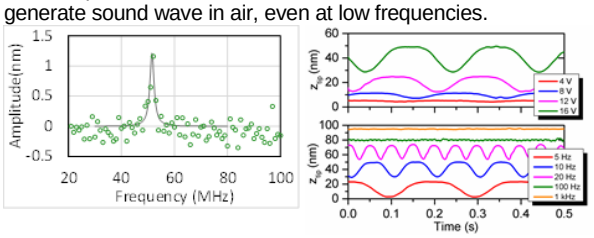

fig 1 : AFM amplitude measurements of the displacement of the center of a membrane suspended over a1.3µm large trench. left : depending on frequency; resonance is observed at 52MHz. right : depending on time at low frequencies. up : at 5Hz, for various applied voltages; low : at 16V, for various frequencies up to the AFM measurement limitation.

Arrays of several thousands of small drums (10µm in diameter), all equipped with the amorphous carbon nanomembrane are now under study. The array is driven with an alternative voltage, and we actually measure, using a microphone, an emitted ultrasound pressure wave.

Perspectives

Having broadband transducers makes it possible to think otherwise of the constraints usually associated with the use of ultrasound, especially for telemetry or tomography techniques. There is no delay in establishing a wave related to the bandwidth of the resonant transducers. Faster measurements, reduced blind zones, multiple purpose devices, and multiplex acoustic data transfer can be considered with these new broad band ultrasonic transducers.

RELATED PUBLICATIONS:

[1] Ghis, A., Thibert, S., & Delaunay, M., (2018). "Ultrathin Amorphous Carbon as Active Part of Vibrating MEMS". Eurosensors 2018. Proceedings, 2(13), 818. https://doi.org/10.3390/proceedings2130818
[2] Thibert, S., Delaunay, M., Ghis, A., (2017). "Carbon-metal vibrating nanomembranes for high frequency microresonators". Diamond and Related Materials 81, 138–145. https://doi.org/10.1016/j.diamond.2017.12.005
[3] Thibert, S., Ghis, A., Delaunay, M., (2016). "AFM study of 2D resonators based on Diamond-Like-Carbon", Nanotechnology (IEEE-NANO), 2016 IEEE 16th International Conference on. IEEE, pp. 479–482. BEST PAPER AWARD.

MOBILE CROWD-SENSING FOR INDOOR POSITIONING IN A COMMON FRAME OF REFERENCE

RESEARCH TOPIC:

Crowd-sensing, indoor positioning, pedestrian dead reckoning, Procrustes analysis

AUTHORS:

Alex PEREIRA DA SILVA, Sylvain LEIRENS

ABSTRACT:

Indoor positioning techniques have been employed in a wide number of applications and have become attractive tools for emerging technologies like Internet of Things (IoT). Numerous indoor localization methods are highly constrained since they take into account the knowledge of building information, internode distances, some absolute position information and/or Wi-Fi fingerprints. Here, we propose a less constrained crowd-sensing positioning method based only on dead reckoning information, and on relative positions of detected access points (APs). Our method comprises selection of APs, choice of a common frame of reference, and a partial Procrustes transformation (rotation and translation) applied to the trajectories of the users. By performing Monte Carlo simulations, the results show that the estimation of trajectories and position of APs performed by our crowd-sensing method is statistically accurate.

Context and Challenges

User trajectories are estimated by an embedded Pedestrian Dead Reckoning (PDR) algorithm and thus are defined by step lengths and heading angles. By setting initial position and orientation for every trajectory, it is possible to completely define every PDR trajectory in its own frame of reference. Additionally, every user detects a set of APs whose estimated positions are defined in its reference frame [2]. The sets of detected APs are not necessarily identical to one another.

The challenge is to represent position of APs and user trajectories in a common frame of reference. This way, maps of hallways and RSSI levels can be built for indoor positioning systems.

Main Results

The positions of all detected APs and users can be generally represented in a common frame of reference if every user j detects at least two APs and there exists a subset $B_j \subseteq S_j$ with at least two elements, and a set of k other users such that:

$$B_j \subseteq S_{j'} \cup \left(\bigcup_{i \neq \{j,j'\}}^{k} S_i \right)$$

where S_j is the set of APs detected by user j and j' is the user whose reference frame is selected as the common one. In order to perform the trajectory positioning of independent users, we make use of the Procrustes analysis to transform positions of trajectories from every user's reference frame to a common frame of reference. Procrustes analysis is a statistical shape analysis that compares the shape of objects, by means of translations, rotations, reflections and uniform scaling.

Our Procrustes-based method is mainly composed of five steps [1]: (1) selection of APs aiming at discarding the most uncertain ones; (2) selection of the common frame of reference as one of the users' reference frames by considering the position uncertainty of selected APs; (3) partial Procrustes-transformation (rotation and translation) applied to estimates of AP positions in reference frames of the involved users; (4) transformation of every trajectory of the users to the common frame of reference by using rotational and translational matrices; and (5) refinement of the positions of APs in the common frame of reference.

Our results have shown that the more the number of APs is used in the Procrustes transformation, the higher is the positioning accuracy in general, as shown In Figure 1 (left).

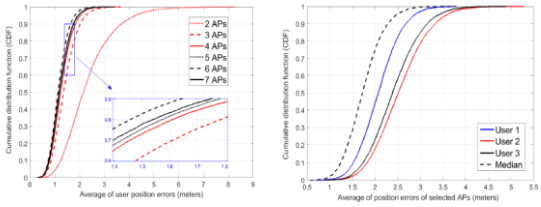

Fig. 1 CDFs of averaged user position error (left) and averaged position errors of APs (right)

However, we have seen that the introduction of high uncertain AP positions reduces the accuracy of trajectory positioning (7 APs case in Figure 1, left). By considering the average error of AP positions regarding the median of estimates performed by the users, the proposed method has also provided an improved estimate of the AP positions in a common frame of reference, as shown for 3 users in Figure 1 (right).

We have also compared the AP positions and trajectories estimated by our method to the ground-truth scenario. Statistically, the estimates are looked upon as an effective representation of the ground-truth trajectories and APs.

Perspectives

Future work might focus on handling uncertainty on PDR data (step lengths and heading changes), as well as discarding of corrupted RSSI measurements (for instance, those ones suffering high attenuation).

RELATED PUBLICATIONS:

[1] Alex Pereira Da Silva and Sylvain Leirens. "A Crowd-Sensing Procrustes-Based Method for Indoor Positioning in a Common Frame of Reference", Proc. 21st International Conference on Information Fusion (FUSION) (2018).

[2] Alex Pereira Da Silva and Sylvain Leirens. "Mobile crowd-sensing for access point localization", Proc. SPIE 10646, Signal Processing, Sensor/Information Fusion, and Target Recognition XXVII (2018).

TIME-OF-FLIGHT CALIBRATION OF AN MCT-APD SENSOR FOR A FLASH LIDAR SYSTEM

RESEARCH TOPIC:

LIDAR, active imaging, 3D imaging, Time-of-Flight, Calibration, HgCdTe, avalanche photodiode, Landing Sensor

AUTHORS:

V. E. S. Parahyba, E. de Borniol, R. Perrier, Y. R. Nowicki-Bringuier, A. Ciapponi, J. Chanussot

ABSTRACT:

Flash Imaging LiDARs (Light Detection and Ranging) are active systems that resolves depth in a scene by time-of-flight measurements and are being seen as a competitive technological alternative that presents great advantages in the space scenario. The system records full 3D-images with a single laser pulse, thus eliminating the need for a scanning device.
A first step to improve the overall quality of the measurements is the calibration of the camera. In this article we propose a calibration scheme for CEA-LETI's LiDAR that combines both intensity, range accuracy and range precision calibration and presents the first enhanced results based on data acquired under laboratory conditions.

SCIENTIFIC COLLABORATIONS: CEA-LETI DOPT, EUROPEAN SPACE AGENCY, GIPSA-LAB

Context and Challenges

A 3D camera is a device that enables the perception of depth in images. It has been described as a key component for future space missions involving automatic Guidance, Navigation and Control (GNC) of spacecraft. However, up to now, systems possibilities were limited because of the non-availability of adequate detectors.
In 2009, CEA-LETI has developed a 320x256 hybrid Focal Plane Array (FPA) for Flash Lidar Imaging. The detector array consists of 30µm pixel pitch HgCdTe APDs operating at 80K and a Read-Out Circuit (ROIC) fabricated on a standard 0.18µm CMOS process. HgCdTe APDs are particularly well-suited for applications with expected low number of photons, as it is the case for landing on extraterrestrial bodies, and for integration in 3D FPAs. Figure below describes the principle of the flash lidar depth measurement:

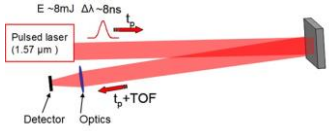

A divergent laser pulse is sent towards an observed scene and the travel time of the returning photons to the detector is measured at each pixel. Next figure is a representation of the time base used to measure the time-of-flight.

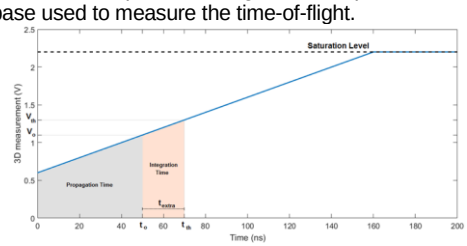

At time 0, the laser is fired and a voltage ramp is triggered to start increasing its output voltage level. At time t0 the reflected pulse reaches the detector, but the system takes until tth to reach the threshold level Vth. The consequence is a delay on the correct instant of sampling that will depend mainly on the threshold level Vth, the gain provided by the APD and the reflected pulse energy. Since in space applications we expect situations with very low number of incoming photons, a calibration scheme that accounts for this distortion is needed.

Main Results

A calibration method that fuses the 2D (intensity) and 3D (time-of-flight) information of a LiDAR system has been developed and tested. The mathematic model to rectify the 3D measurement is a quadratic polynomial function which parameters are estimated using 3 targets of known reflectivity. Figures below show the lidar depth measurement with respect to ground truth before (top) and after (below) calibration:

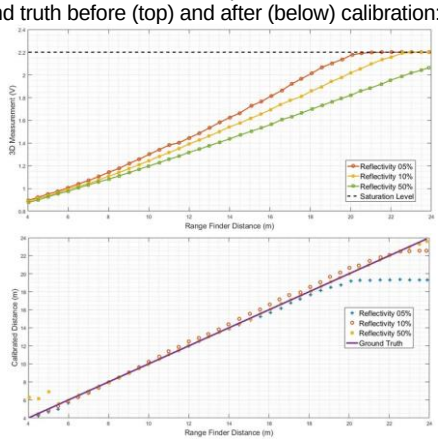

Perspectives

The prospects for future works include the expansion of the model in order to incorporate the influence of the threshold level and the gain, as well as a test campaign at a real-like scenario on ESA/ESTEC's premises.

RELATED PUBLICATIONS:

[1] De Borniol, E., Guellec, F., Rothman, J., Perez, A., Zanatta, J. P., Tchagaspanian, M., and Pistone, F., "HgCdTe-based APD focal plane array for 2D and 3D active imaging: first results on a 320 x 256 with 30 µm pitch demonstrator," In Infrared Technology and Applications XXXVI, 76603D (2010).
[2] Mourikis, A. I., Trawny, N., Roumeliotis, S. I., Johnson, A. E., Ansar, A., and Matthies, L., "Vision-aided inertial navigation for spacecraft entry, descent, and landing," IEEE Transactions on Robotics 25(2), 264-280 (2009).
[3] McManamon, P. F., Banks, P. S., Beck, J. D., Fried, D. G., Huntington, A. S., and Watson, E. A., "Comparison of Flash Lidar detector options," Optical Engineering 56(3), 031223 (2017).

SHAPE CAPTURE FOR SHM (STRUCTURAL HEALTH MONITORING)

RESEARCH TOPIC:
shape capture, MEMS applications, Structural Health Monitoring, curves and surfaces

AUTHORS:
N.Saguin-Sprynski, L. Jouanet, M. Billères, T. Stanko, S. Hahmann (LJK, INRIA), G.-P. Bonneau (LJK,INRIA)

ABSTRACT:
Shape capture has been developed for almost 15 years, and many demonstrators have been realised. Our last approach is to reconstruct curves and surfaces with only a single MEMS-embedded node. By moving the IMU along the surface, a network of local orientation data is acquired together with traveled distances and network topology. We then reconstruct a consistent network of curves and fit these curves by a globally smooth surface. We have applied this framework for 2 specific applications: the first one dedicated to surfaces in SHM, and a simplified second one in order to be embedded in a cable cabin providing the shape of its cable.

SCIENTIFIC COLLABORATIONS: Université Grenoble Alpes, CNRS (Laboratoire Jean Kuntzmann), INRIA)

Context and Challenges
Traditionally, digital models of real-life shapes are acquired with 3D scanners, providing point clouds for surface reconstruction algorithms. However, there are situations when 3D scanners fall short, e.g. in hostile environments, for very large or deforming objects.
In the last 15 years, alternative approaches to shape acquisition using data from microsensors have been developed. We consider a new setup: a device with a single IMU is moved along a virtual network of curves on the scanned surface, and the data is acquired interactively. The complete frawework has been detailed and applied with a generic demonstrator named MorphoRider. Its strength in a SHM application is tangible. We also derived this device in a cable transportation demonstrator.

Main Results
The key idea is to provide a device which can trace an unconstrained virtual network of curves on the scanned surface. This enables acquisition and reconstruction of a broader family of shapes than existing fixed-topology devices. Morphorider is equipped with one node of sensors (3-axis accelerometer and 3-axis magnetometer) providing its orientation in space, and an odometer, giving its displacement.
Any smooth surface can be scanned with this device by an operator, the additional constraint being to number the intersections of the different curves acquired on it. First, our novel method creates well-connected networks with cell-complex topology using only orientation and distance measurements and a set of user-defined constraints. Second, we address the problem of surfacing a closed 3D curve network with given surface normals. The normal input increases shape fidelity and allows to achieve globally smooth and visually pleasing shapes. A quantitative evaluation was performed by computing the error of reconstruction for our own designed surfaces. Even for complex shapes, the mean error remains around 1%. Such a device is a real innovative way for SHM because following geometric parameters along time provides very pertinent indicators about health of structures, and a new tool could be dedicated to maintenance sessions.

Figure 1 : Morphorider, real and reconstructed surface

We have also developed a demonstrator of a cable car on a reduced scale, integrating MEMS and an odometer, communicating by Bluetooth. A real time application computes and displays the trajectory when the cable car is moving along the cable. When changing the cable tension, we clearly track the shape's evolution, validating the principle of this cable shape monitoring.

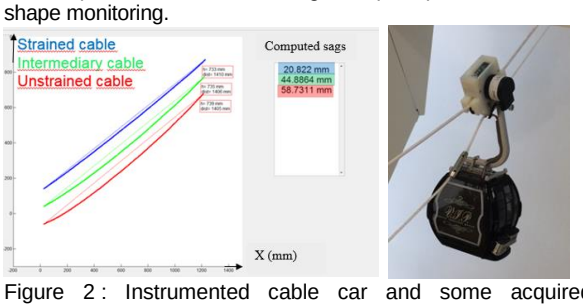

Figure 2 : Instrumented cable car and some acquired trajectories

Perspectives
Perspectives concern now the merging of modal analysis and vibrational data to our static shapes in order to perform a complete view of the health structure. We can also work on crowd sensing applications for instance to monitor a structure from collaborative measurements

RELATED PUBLICATIONS:
[1] T. Stanko, N. Saguin-Sprynski, L. Jouanet, S. Hahmann, G.-P. Bonneau, Morphorider: a new way for Structural Monitoring via the shape acquisition with a mobile device equipped with an inertial node of sensors, EWSHM2018, Manchester
[2] N. Saguin-Sprynski, L. Jouanet, M. Billères, Monitoring System for Cable transportation, Condition Monitoring 2018, Nottingham.

DATA MINING APPLIED TO TRANSPORTATION MODE CLASSIFICATION PROBLEM

RESEARCH TOPIC:

Context awareness, smart city, transportation mode, mobility, data mining, classification, wearables, sensors

AUTHORS:

Andrea Vassilev

ABSTRACT:

The recent increase in processing power and in the number of sensors present in today's mobile devices leads to a renewed interest in context-aware applications. This paper focuses on a particular type of context, the transportation mode used by a person or freight, and adequate methods for automatically classifying transportation mode from smartphone-embedded sensors. This classification problem is generally solved by a searching process which, given a set of design choices relative to sensors, feature selection, classifier family and hyper-parameters, etc., finds an optimal classifier. This process can be very time consuming, due to the number of design choices, the number of training phases needed for a cross validation step and the time necessary for one training phase. In this paper, we propose to simplify this problem by applying three data mining tools - Principal Component Analysis, Mahalanobis distance and Linear Discriminant Analysis - in order to clean the data, simplify the problem and finally speed up the searching process. We illustrate the different tools on the problem of transportation mode classification.

Context and Challenges

Recognition of the transportation modes used by a person or freight is a machine-learning problem, which is generally solved in four steps:

1) Select the relevant subsets of sensors,
2) Choose the data pre-processing, leading to features
3) Chose the Machine Learning methods and hyper-parameters
4) Train

Testing all the combinations of {subsets/features/methods} is intractable; only testing a subset of the combinations is feasible. We focus on steps 1 & 2: "*what are the interesting sensors and features ?"* and show how the following 3 Data Mining Tools can be applied to our problem:

- Principal Component Analysis (PCA)
- Mahalanobis Distance (MD)
- Linear Discriminant Analysis (LDA)

Main Results

A smartphone application was developed to collect the data of mobility. The application stores the raw sensor data such as GPS, accelerometer (ACC) and magnetometer (MAG). The subjects were asked to use it during their commute to work or any other trip and to annotate the travel mode they are using during the recording process. 22 subjects participated to the database setup. About 400 trips were recorded, representing 225 hours of traveling. Seven different transportation modes were considered: 'bike', 'plane', 'rail', 'road', 'run', 'still', 'walk'.

From the raw sensor data, signals were segmented using a 5 seconds moving window. On each window, 14 a priori relevant features were computed.

Applying PCA shows that it is possible to keep only 8 of the 14 features.

Computing a Mahalanobis Distance allows to identify and suppress 41 outliers (in red in Figure 1)

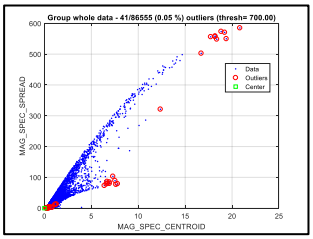

Fig. 1: outliers' detection (Mahalanobis Distance)

Finally, a Linear Discriminant Analysis shows that some features are important. For example, removing one of the 8 features, namely the variance of the norm of the accelerometer, increases the confusions between the classes (e.g. between 'run', 'bike' and 'walk', see Figure 3), compared to the nominal case with the 8 features (Figure 2).

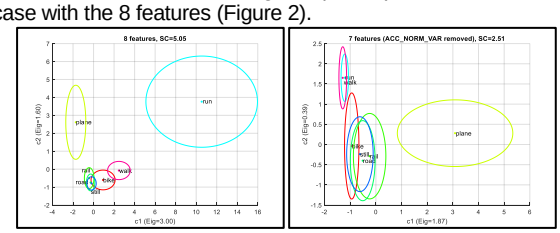

Confusions between classes; Fig. 2 (left): with 8 features. Fig. 3 (right): after removing one important feature

Perspectives

Next step is the test of non-linear techniques for dimensionality reduction such as 't-Distributed Stochastic Neighbor Embedding' (t-SNE) which seems to be particularly well suited for the visualization of high-dimensional datasets. For larger datasets, deep learning approach applied to such heterogeneous temporal signal is also to evaluate.

RELATED PUBLICATIONS:

[1] A. Vassilev, « Data Mining Applied to Transportation Mode Classification Problem », presented at 4th International Conference on Vehicle Technology and Intelligent Transport Systems, 2019, p. 36-46.

STUDY AND DESIGN OF VERY HIGH FREQUENCY (VHF) SELF-OSCILLATING INVERTER TOPOLOGIES

RESEARCH TOPIC:

Very high frequency, VHF, class ϕ2, inverter, Self-oscillating, power conversion, GaN

AUTHORS:

Rawad MAKHOUL, Xavier MAYNARD, Pierre PERICHON, David FREY, Pierre-Olivier JEANNIN and Yves LEMBEYE

ABSTRACT:

With new advancements in GaN technology, the tendency to increase the switching frequency in power converters is on the rise. Switching at very high frequency (VHF: 30MHz-300MHz) allows for smaller passive components and more compact power converters. However, although GaN components are able to switch at 100 MHz and beyond, gate drivers available in the market struggle to provide the adequate switching signal at very high frequency. Hence, there is a need for an alternative to VHF converters using those gate drivers: self-oscillating topologies.

Context and Challenges

Switching at very high frequency (VHF: 30MHz-300MHz) allows for smaller passive components and more compact power converters. However several challenges arise in the VHF range: Implementing dead times becomes challenging, usual resonant converter topologies have components in the same magnitude range as parasitic components, and gate driver chips available on the market struggle with providing the correct transistor switching signal. Hence, there is a need for an alternative to VHF converters using those gate drivers: self-oscillating topologies. The class ϕ2 inverter is a resonant inverter topology with low transistor voltage stress, fast transient response and small passive components [1] [2]. It is suitable for VHF operation. When designed to self-oscillate, it can help with avoiding the limitations introduced by gate driver chips.

Main Results

The class ϕ2 inverter is shown in fig.1: during the phase when the switch is ON, inductor L_f stores energy and resonates with capacitor C_f when the switch is OFF, generating a quasi-sinusoidal voltage across the GaN. Inductor L_{mr} and capacitor C_{mr} are designed to resonate at the second harmonic of the switching frequency in order to short-circuit the second harmonic of the drain to source voltage and therefore reduce the GaN voltage stress. Inductor L_r is a reactive power divider and sets the power delivered to the load while capacitor C_r is a DC voltage block.

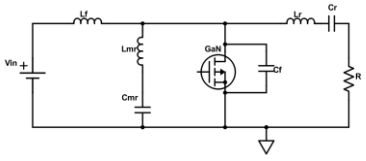

Figure 1: Class ϕ2 inverter

The proposed self-oscillating topology is shown in fig.2: C_{div1}, C_{div2}, C_o and L_{osc} constitute the self-oscillating part. R1 and R2 are the bias structure and set the gate DC voltage to the GaN threshold voltage [3] [4].

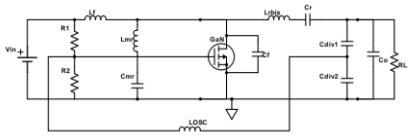

Figure 2: Self-Oscillating Class ϕ2 inverter

The simulated drain to source voltage and output voltage are shown in fig.3. It can be seen that the maximum drain to source value is about 65V (twice the input voltage) and that the output voltage is a 30MHz sinusoidal waveform.

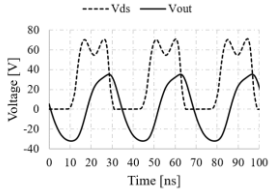

Figure 3: Drain to source and output voltage

The self-oscillating class ϕ2 inverter was built on a two-layer PCB (fig.4) in order to verify its experimental feasibility at 30MHz. Because of the critical tuning of the circuit, C0G (NP0) capacitors are used because of their stable value in time and with temperature variations. Experimental results are plotted in fig.4 and show good matching with simulation.

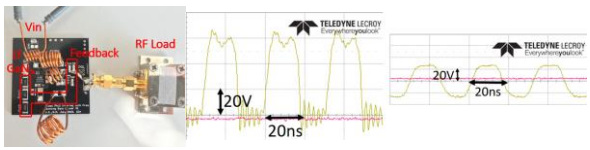

Figure 4: PCB and RF load (left), experimental waveforms (right)

Perspectives

The self-oscillating class ϕ2 inverter is expected to be the first building block of a DC/DC compact VHF converter.

RELATED PUBLICATIONS:

[1] J. Rivas, Y. Han, O. Leitermann, A.D. Sagneri, and D.J. Perreault, "A high-frequency resonant inverter topology with low-voltage stress," IEEE Transactions On Power Electronics, Vol. 23, No. 4, pp. 1759 -1771, July 2008.
[2] J. Choi, J. Xu, R. Makhoul, and J.M. Rivas, "Implementing an impedance compression network to compensate for misalignments in a wireless power transfer system", IEEE Transactions on Power Electronics, in press
[3] M.K. Kazimierczuk, V. G. Krizhanovski, J.V. Rassokhinaand, and D. V. Chernov, "Class-E MOSFET tuned power oscillator design procedure,"IEEE Transactions on circuits and systems, Vol. 52, No. 6, pp. 1138 -1147, June 2005
[4] I. S. Jacobs and C. P. Bean, "Class E high efficiency tuned power oscillator", IEEE Journal of Solid-State Circuits, vol. 16, pp. 62 - 66, 1981.

A NEW INDUCTORLESS DC-DC PIEZOELECTRIC CONVERTER

RESEARCH TOPIC:
Power conversion, Piezoelectricity, Resonator

AUTHORS:
Benjamin POLLET, Ghislain DESPESSE and François COSTA

ABSTRACT:
This paper introduces a new kind of piezoelectric DC-DC converter. A ceramic is used as an energy storage element to replace the traditional inductance. Once resonating, the system describes a cycle at each resonance period taking energy to the source, storing it and transmitting it to the load with soft switching. A resonator suitable for the converter is presented and characterized with an electrical equivalent model. A simulation representing the whole system, gives very attracting results with very high efficiency for different output powers. The converter was tested and fully validated by experimental works. An efficiency of 98 percent was reached for a 10-20 volts step up converter with an output power of 300 milliwatts.

SCIENTIFIC COLLABORATIONS: François Costa, Ecole Normale Supérieure Paris-Saclay / Laboratoire SATIE

Context and Challenges
DC/DC converters market has kept growing during the past decades representing now billions of dollars. The large diversity of their application fields (aviation, computer science, energy harvesting...) implies specific constraints and specific technological solutions. In this context, using piezoelectric materials for power conversion can be very relevant for some applications, one of them being low power with high voltage gain converters. Therefore numerous converters with piezoelectric transformers (PT) were developed. However, an inductance is necessary to obtain a high efficiency in DC/DC converters with PT. In this paper, a new inductor-less boost converter with one single piezoelectric element (no coupled piezoelectric like in PT) is presented. The material works at its resonant frequency and behaves as an energy storage element like an inductance does in classical power electronics circuits. Therefore, the storage is mechanic and not magnetic. A similar mechanics-based converter, using a variable capacitor instead of a piezoelectric resonator was proposed [2] but the piezoelectric solution is advantageous in term of quality factor, power density and ease of implementation. The presented converter is inductor-less, and has a high efficiency with a large set of possible voltage gain values.

Principle
The topology of the converter (Fig. 1.a) and its conversion cycle (Fig. 1.b) are described below.

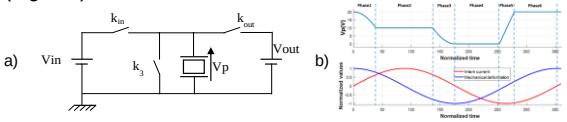

Figure 1: a) Converter Topology, b) Conversion cycle

This topology and its strategy of control represents a completely new piezoelectric converter. Compared to classical piezoelectric converter, this structure has a high efficiency level for a large range of output gains (1 to 10) and a large range of output powers (mW to W). A piezoelectric ceramic PZT, with a high coupling factor (58%) and high quality factor (>1000) is chosen and characterized by an equivalent circuit model. This model is used to study the behavior of the converter with a simulation model performed on Matlab/ Simulink. This model validates the working of this new converter and enables to understand the transient and to design a good corrector to regulate the output voltage to the desired value. Fig.2 shows the key waveforms obtained for a 10-20V 1W conversion.

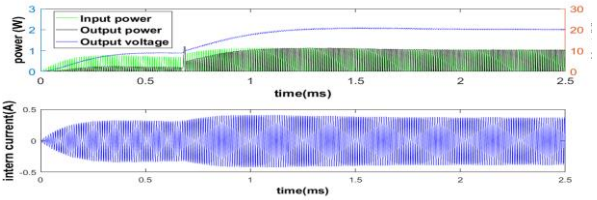

Figure 2: Simulation for a 1W output power

Main results
Finally, this new converter is fully validated in experimental operation. The control is performed by a FPGA. An efficiency of 98 % is reached for a 300mW and 10 to 20V conversion. Conversions with high efficiencies (>90%) were achieved for a large range of output powers (from 10mW to 1W) and for different gains which constitutes a significant improvement compared to existing state of the art.

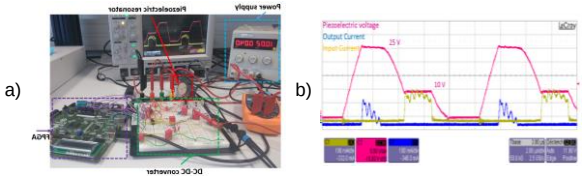

Figure 3: a) Picture of DC-DC converter b) Experiment conversion cycle for a 10-25V step up conversion

Perspectives
This new principle could be adapted to perform a step down converter, and AC-DC conversion. A PhD study started in October 2018 to study and make a very compact piezoelectric 230V_{ac} / 5 to 48V_{DC} (20W) converter usable to recharge mobile phone for example.

RELATED PUBLICATIONS:
[1] B. Pollet, F. Costa, and G. Despesse, “A new inductorless DC-DC piezoelectric flyback converter,” in proceedings of IEEE International Conference on Industrial Technology, ICIT 2018, pp. 585–590.
[2] S. Ghandour, G. Despesse, and S. Basrour, “Design of a new MEMS DC/DC voltage step-down converter,” in NEWCAS Conference (NEWCAS), 2010 8th IEEE International, 2010, pp. 105–108.
[3] S. Moon and J.-H. Park, “High Power DC–DC Conversion Applications of Disk-Type Radial Mode Pb(Zr,Ti)O3 Ceramic Transducer”, Japanese Journal of Applied Physics, vol. 50, no. 9, p. 09ND20, Sep. 2011

IMPLEMENTATION OF MONOLITHIC BIDIRECTIONAL SWITCHES IN A AC/DC DUAL ACTIVE BRIDGE IN ZVS AUTO-SWITCHING MODE

RESEARCH TOPIC:

Power electronics, GaN transistors, bidirectional switch

AUTHORS:

Léo STERNA, Othman LADHARI, Pierre PERICHON, Jean-Paul FERRIEUX, David FREY, Pierre-Olivier JEANNIN

ABSTRACT:

This paper presents the implementation of single gate bidirectional switches. In order to take fully into account the characteristics of these components, a quasi-resonant Dual Active Bridge topology has been chosen. The switches will be implemented at the primary stage to allow a direct AC/DC conversion. The quasi-resonant mode is introduced to operate in full ZVS mode at the primary bridge level. This mode involves automatic turn ON. A theoretical study validates the quasi-resonant full-ZVS automatic switching in AC/DC conversion. The driver circuit, used to guarantee ZVS automatic switching on each bidirectional switch, is then described. Finally, experimental results show the feasibility of the converter.

Context and Challenges

The AC/AC and AC/DC converters leads the power electronics designers to investigate the interest of a switching device able to support bidirectional voltage in off state. Classical examples are the matrix converters or single stage single phase AC/DC topologies [1]. Applications such as embedded battery chargers need to ensure both the insulation and an AC/DC conversion. They also have to be compact and light weight. The Dual Active Bridge converter, based on a single stage AC/DC conversion, is a relevant structure allowing compact solutions thanks to its high frequency transformer and its single conversion stage so it is possible to reduce the number of switches and associated gate drivers. Recently, based on the HEMT GaN structure, single gate bidirectional switches (SGBS), have been presented [2] allowing dividing by two the number of drivers necessary for each component. The converter described in this paper [3] takes advantage of this transistors' characteristic to operate new type of ZVS switching.

Main Results

The proposed converter topology is based on the Dual Active Bridge converter, in the particular case of direct AC/DC conversion. The converter input is directly fed with a sinusoidal voltage. The primary bridge switches are therefore bidirectional. The designed control strategy enables a PFC operation with ZVS (Zero Voltage Switching) commutations at the primary bridge.

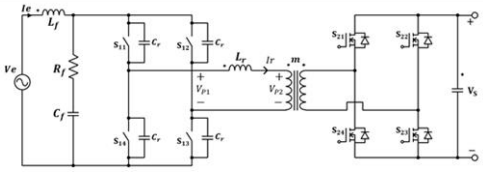

Figure 1 : Converter topology

As the bidirectional switch operates with a single gate control signal and has not any reverse conduction behavior, a specific auto-switching driver is used to guarantee ZVS switching. The auto-switching driver is designed in order to provide a particular switching behavior: "controlled" turn OFF and automatic turn ON. Two main blocks are needed: a voltage zero-crossing detection and a logic circuit. The logic unit receives an external signal which imposes turning-OFF switching and the comparator output signal.

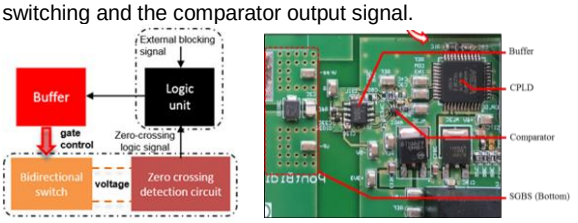

a) b)

Figure 2: a) Automatic switching driver principle b) PCB board driver implementation

The resonant switching transitions times are comprised between 600ns and 2us. The switching delay induced by the automatic switching function has to be as low as possible. The automatic-switching function is tested and validated beforehand and its performances compared with the target delay of 50ns.

The experimental results are validating the feasibility of the automatic ZVS switching concept into an AC/DC Dual Active Bridge converter operation.

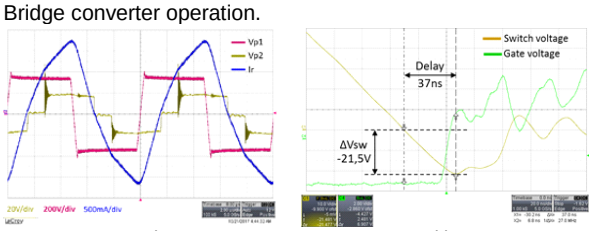

a) b)

Figure 3: a) converter characteristics waveforms ; b) automatic ZVS switching waveforms

Perspectives

In this paper, a four quadrant monolithic single gate GaN device using a novel switching mode has been implemented into an AC/DC Dual Active Bridge converter. While a discrete implementation is presented in this paper to validate the auto-ZVS principle, the final perspective is a monolithic integration of the auto-commutation electronic which should improve the dynamic performances and reduce the auto-switching delay.

RELATED PUBLICATIONS:

[1] N. D. Weise, G. Castelino, K. Basu and N. Mohan, "A Single-Stage Dual-Active-Bridge-Based Soft Switched AC–DC Converter With Open-Loop Power Factor Correction and Other Advanced Features," in *IEEE Transactions on Power Electronics*, vol. 29, no. 8, pp. 4007-4016, Aug. 2014.

[2] D. Bergogne, O. Ladhari, L. Sterna, C. Gillot, R. Escoffier and W. Vandendaele, "The single reference Bi-Directional GaN HEMT AC switch," *Power Electronics and Applications (EPE'15 ECCE-Europe), 2015 17th European Conference on*, Geneva

[3] L. Sterna, J-P Ferrieux, D. Frey ; P-O Jeannin, P. Périchon, O. Ladhari "Implementation of monolithic bidirectional switches in a AC/DC Dual Active Bridge in ZVS auto-switching mode", *2018 IEEE International Conference on Industrial Technology (ICIT)*, Lyon

MULTIFUNCTIONAL WEARABLE PLATFORMS FOR HEALTH AND ENVIRONMENTAL MONITORING: THE CONVERGENCE PROJECT

RESEARCH TOPIC:

Activity, Bio & Environmental sensors, Energy Harvesting, Heterogeneous integration on flex, Flexible electronics, Internet of Things, Low power, Wearable

AUTHORS:

E.Saoutieff, A.Faucon, S.Boisseau, JC.Souriau, A.Garnier, T.Ernst (CEA), T. Polichetti, M. L. Miglietta, B. Alfano, E. Massera, S. De Vito, G. Di Francia (ENEA), N. Marchand, T.Walewyns, L. A. Francis, S. Petre, N. André, D. Flandre (UCL), M.Greitans, A. Ancans, J. Ormanis, R. Cacurs (EDI), C. Moldovan (IMT)

ABSTRACT:

The CONVERGENCE FLAG-ERA H2020 project focuses on the development of energy efficient sensor networks exploiting the convergence of multi-parameter sensors, serving data fusion for preventive life-style and healthcare. In this perspective, we aimed at creating a wireless and multifunctional wearable system, able to monitor not only the individual physical condition (physical activity, core body temperature, electrolytes and biomarkers) but also the chemical composition of the ambient air (NOx, COx, particles). CEA research has been focused on the development of two systems platforms demonstrators: the first one dedicated to sensors and the second one to energy harvesting.

SCIENTIFIC COLLABORATIONS: EPFL, ETHZ, ENEA, UCL, HCC, TTU, G-INP, STM, IUNET, UCBM, UNICA, TAGLIAFERRI, EDI, IMT, UTBV, METU

Context and Challenges

The development of wearable platforms dedicated to prevention of life-style and healthcare and for environment monitoring is becoming important due to the importance and emergence of Internet-of-Things and Trillion-of-Sensors Planet.

The work carried out over the Convergence European project, was aimed at developing and demonstrating energy efficient sensor networks for future wearables by exploiting the convergence of multi-parameter biosensors and environmental sensors.

Main Results

CEA-LETI has developed two low power wireless demonstration platforms for wearable IoT. These platforms are versatile and compatible with sensors and energy harvesters modules developed by consortium partners.

The first one is dedicated to multi-parameter sensors and the second one to energy harvesting. A Bluetooth Low Energy communication (data collection on mobile phone) has been implemented on both platforms and the power consumption has been minimized.

Sensors platforms

Modular multi-sensors platform

- Developed for sensor data acquisition
- BLE transmission
- Low-power system (5µA to 15mA max)

The generic system platform (fig.1) is compatible with various kind of sensors: Gas, Temperature, Activity sensors and Nano-power energy harvesting ASICs module.

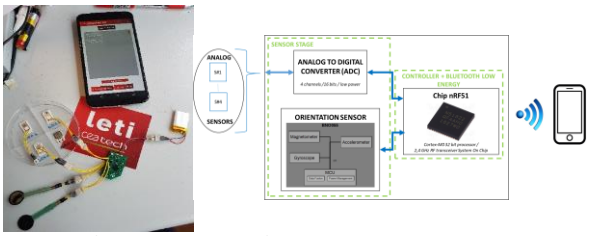

Fig. 1 (left) Rigid sensor platform tested with two gas sensors and two analogic sensors – (right) schematic of the sensor platform

Energy harvesters platforms

- developed for low-power energy harvesters (typically <10µW)
- system compatible with different energy harvesting sources (light, vibrations, flows,…)

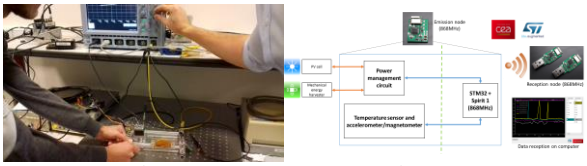

Fig. 2 (left) Rigid energy harvester platform tested with piezoelectric generator – (right) schematic of the board

Perspectives

The next steps will be focused on the future integration on a flexible system combining flexible electronics with multiple sensors (temperature, physical activity and gas sensors). Proofs of concepts will focus wrist devices and/or smart patch wearables.

RELATED PUBLICATIONS:

[1] E. Saoutieff, A. Faucon, S. Boisseau, T.Ernst, "Sensor and Energy Harvesting flexible platform", ESSDERC/ESSCIRC conference, NEREID-SINANO-Workshop "Nanoelectronics and Smart System Technologies for Future applications", Dresden, Germany, September 2018

[2] E. Saoutieff, A. Faucon, S. Boisseau, et al., "Sensors platform for health and environmental monitoring", SEMI-CONDUCTING NANOMATERIALS FOR HEALTH, ENVIRONMENT AND SECURITY APPLICATIONS, Workshop Nano2sence, Grenoble, France, November 2018

[3] T. Ernst et al., "Sensors and related devices for IoT, medicine and smart-living", VLSI, Honolulu, USA, June 2018

[4] T. Polichetti, M.L. Miglietta, B. Alfano, E. Massera, S. De Vito, G. Di Francia, A. Faucon , E. Saoutieff, S. Boisseau, T. Walewyns, N. Marchand, L. A. Francis, " A Networked Wearable Device for Chemical Multisensing", Lecture Notes in Electrical Engineering - Volume 539, Pages 17-24, 2019

[5] A. Ancans, J. Ormanis, R. Cacurs, M. Greitans, E. Saoutieff, A. Faucon, "Bluetooth Low Energy throughput in densely deployed radio environment", submitted In Elektronika IR Elektrotechnika, February 2019

OPTIMIZATION OF CM-SCALE AXIAL WATER FLOW AND THERMAL ENERGY HARVESTERS FOR DISTRICT HEATING SYSTEMS

RESEARCH TOPIC:

Energy Harvesting, Internet of Things, Smart Building, Water Flow Harvester, Thermal Energy Harvester, Water Distribution

AUTHORS:

E.Saoutieff, P.Gasnier, S.Boisseau, O.Soriano (CEA), B.Alessandri (Davidson), J.Ojer-Aranguren (Naitec), I.Rodot (SNCU)

ABSTRACT:

CEA has developed two energy harvesters demonstrators: one water flow energy harvester and one thermal energy harvester. The aims are (i) to develop smart flowmeters able to work for years without any human intervention (no battery replacement) and (ii) to improve the quality and to reduce the costs of water networks monitoring (flowrate, temperature, pressure, leakage detection, pH meters ...). Research has been focused on the optimization of a 40mm diameter water flow energy harvester based on an axial turbine (horizontal axis propeller) coupled to a customized permanent magnet generator and on a thermal energy harvester with their tests and their integrations in Montpellier's district heating system.

SCIENTIFIC COLLABORATIONS: City University, NAITEC, SERM, SNCU, CETRI, Net Technologies, CERTH, Iznab, Promar, Energetika

Context and Challenges

Challenged by climate change, district heating and cooling systems (DHCS) need to be more energy-efficient, eco-friendly with cost effective solutions to increase their adoption in buildings and cities.

The work carried out over the InDeal European project, was aimed at developing and demonstrating energy harvesting solutions to develop autonomous Smart Water Grid systems, and to make DHCS more competitive.

Main Results

Two energy harvesting proofs of concept were designed, modelled and fabricated : (i) water flow energy harvesters based on a horizontal axis microturbine, and aimed at converting locally a part of water flowing in pipes into electricity to supply in-line sensors (temperature, pressure, turbidity, pH…), and (ii) thermal energy harvester, using the temperature gradients between water and the outside to generate electricity (Seebeck modules). Both systems were then tested in laboratory and in Montpellier's DHCS (fig.1).

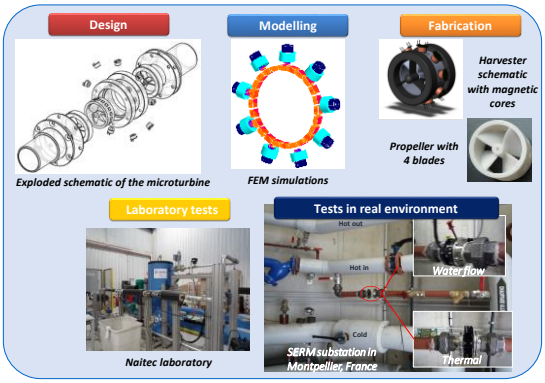

Fig. 1. Energy harvesting solutions development

This is the first work to propose the optimization of a centimeter-scale water flow harvester as well as its long-term characterization in a real application case. High output powers at high flow rates (490mW@9m^3.h^{-1}) in both cold and hot water with very low pressure losses in the pipe (<50 mbars) were measured with a mean power of 5mW. The proportionality between the rotation speed of the turbine$_T$ and the flow is demonstrated, which enables the use of this energy harvester as an autonomous flowmeter. After 4 months of test in heating system substation (fg.2), the presence of fouling and dirtying on the propeller did not degrade its good operation.

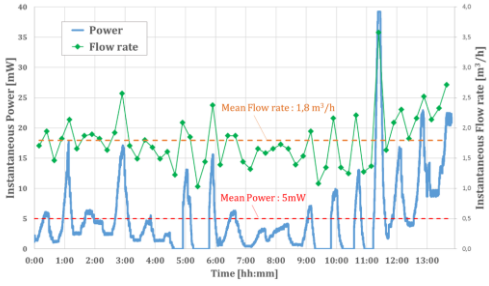

Fig. 2. Energy harvesting solutions development

Output powers up to 34,8mW were measured in Montpellier's DHCS with the Thermal Energy Harvesters thanks to a high ΔT (water temperature of 56°C / substation temperature of 17.5°C). The easiness of installation (stopping the flowrate is not required since the harvesters can be set around the pipes), the absence of fooling and the high output power at high temperature gradients are key points for integration in Smart Water Grid System.

Perspectives

The next steps will be focused on the development of new propellers for water flow energy harvesters with coatings to reduce fouling and to increase their lifetime in harsh environments.

RELATED PUBLICATIONS:

[1] P. Gasnier, E Saoutieff, O. Soriano, B. Alessandri, J. Ojer-Aranguren, S. Boisseau, "Cm-Scale Axial Flow Water Turbines for Autonomous Flowmeters: an Experimental Study", Smart Materials and Structures, 27 115035 (12pp), 2018

[2] E. Saoutieff, P.Gasnier, S.Boisseau, J.Oyer-Aranguren, I.Rodot, "Performances of a cm-scale water flow energy harvester in real environment for autonomous flowmeters", Proc. PowerMEMS, Daytona Beach, USA, 2018

[3] E. Saoutieff, P.Gasnier, S.Boisseau, "Energy Harvesting for Autonomous Sensors", EnerGaïa, Montpellier, 2018

A CM-SCALE, LOW WIND VELOCITY AND 250°C-COMPLIANT AIRFLOW-DRIVEN HARVESTER FOR AERONAUTIC APPLICATIONS

RESEARCH TOPIC:

Airflow energy harvesting, aeronautic environments, electromagnetic microturbine

AUTHORS:

P Gasnier, J Willemin, S Boisseau, B Goubault De Brugière, G Pillonnet

ABSTRACT:

This work reports the design, fabrication, and testing of a centimeter-scale ($Ø_{rotor}$=35mm), 250°C-compliant microturbine for aeronautic applications. Dedicated to low-speed airflows (≈3 m/s and down to 2 m/s), this device is the first flow-driven harvester withstanding such high temperatures and high vibration levels (10^7 cycles at 20G). Furthermore, the proposed harvester exhibits the highest output power per unit cross sectional area compared to prior art in the cm-scale and low velocity ranges.

SCIENTIFIC COLLABORATIONS: CEASARLab –SAFRAN/CEA joint laboratory, funding received from the European Union's FP7 CLEANSKY No. 632614 HiTEAS.

Context and Challenges

Airflows are a powerful source of ambient energy that can be used to supply Wireless Sensor Nodes from 1-2m/s. Even if airflow harvesters exploiting aeroelastic flutter phenomena [1] can be an alternative to lift-based rotors, horizontal axis propellers still outperform fluttering devices in terms of aerodynamic efficiencies or cut-in speeds. The harvester introduced hereafter has been designed to supply a wireless sensor system interfacing with aeronautic-grade pressure/strain transducers [2]. Thus, in order to withstand severe aeronautic environment constraints such as high temperatures and vibrations amplitudes, particular materials and specific design rules have been used. Furthermore, in recent years, many works have been proposed on the miniaturization of classical wind turbines, from 2cm to 6cm rotor diameters but most of them show low performances at low-speeds and/or exhibit large cross-sectional areas. Our work also aims to compete with previous electromagnetic-based microturbines whose cross-sectional areas are below 30cm² (Ø<6cm).

Main Results

Our prototype (figure 1) is a horizontal axis wind turbine coupled to a coreless permanent magnet generator which converts mechanical rotations into electricity.

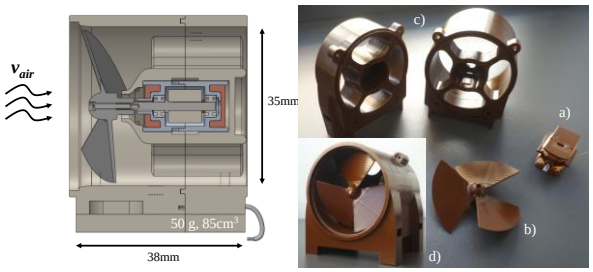

Figure 1 : Cross-sectional view of our harvester and a) to c) main parts and d) photograph of the final harvester

The device is composed of several mechanical parts screwed and/or glued together as depicted in figure 1. The coreless alternator (figure 1.a) includes a machined shaft (Aluminum), a 250°C tolerant copper wire wrapped around two casings slotted together and a drilled cylindrical SmCo magnet with radial orientation glued to the shaft. A 35mm diameter three-blade propeller (figure 1.b) is screwed to the shaft and converts the kinetic power of the air into a rotation movement. The propeller, the alternator's casing and the carter (figure 1.c) have been machined in a high-performance polyimide-based plastic (Vespel®) withstanding 260°C.

Thanks to finite element simulations, the Von Mises stress of all parts (propeller alone and assembled device) at 20G have been kept below 20MPa for all their resonant frequencies in the x, y and z directions.

Four harvesters have been assembled and characterized at room temperature in a wind tunnel at various wind velocities (2 to 4 m/s) and up to 10 m/s. The harvesters have a cut-in speed of 2.5m/s, outputs 350µW @ 2 m/s and up to 4.5mW @ 4 m/s at maximum power points. Regarding the power density, our harvester exhibits the highest performances compared to prior art in the cm-scale (Ø<6cm) and low velocity (v_{air}<5 m/s) ranges. This is moreover the first one to be compatible with the harsh aeronautic environments, that is to say high temperatures (250°C) and high accelerations (20G).

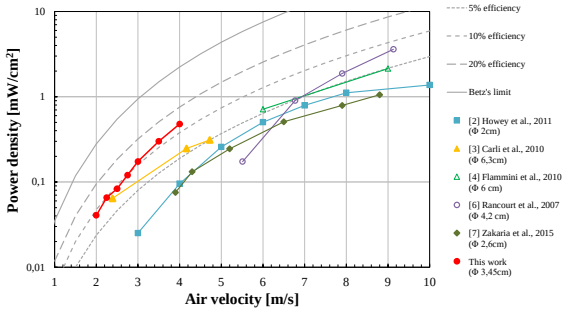

Figure 2 : Performance comparison for airflow harvesters reported in the literature

Perspectives

This harvester provides a practical solution to harvest power from low-speed airflows in harsh environments where batteries cannot operate, as well as more conventional applications like inside buildings equipped with ventilation (HVAC). The next works will consist in working on innovative propeller designs and on the carter/propeller interactions thanks to FEM simulations to enhance even more the output power of the device.

RELATED PUBLICATIONS:

[1] Perez M, Boisseau S, Gasnier P, Willemin J and Reboud J L 2015 An electret-based aeroelastic flutter energy harvester Smart Mater. Struct. 24 035004

[2] Grezaud R, Sibeud L, Lepin F, Willemin J, Riou J C and Gomez B 2017 A robust and versatile, -40C to +180C, 8Sps to 1kSps, multi power source wireless sensor system for aeronautic applications Symposium on VLSI Circuits pp C310–1

[3] Gasnier P, Willemin J, Boisseau S, Goubault De Brugière B, Pillonnet G, 2018, A cm-scale, low wind velocity and 250°C compliant airflow-driven harvester for aeronautic application, PowerMems2018

A 120°C 20G-COMPLIANT VIBRATION ENERGY HARVESTER FOR AERONAUTIC ENVIRONMENTS

RESEARCH TOPIC:

Vibration energy harvesting, Piezoelectric generators, harsh environments, aeronautics

AUTHORS:

P. Gasnier, S. Boisseau, M. Boucaud, M. Gallardo, J. Willemin, A. Morel, D. Gibus, M. Moreau

ABSTRACT:

This paper reports the design, fabrication and testing of a piezoelectric energy harvester operating at 90°C and withstanding 120°C and 20G of acceleration. This harvester, along with its dedicated power management circuit, has been designed to supply a 3-channel Acceleration Measurement System (AMS) for the structural health monitoring of an aircraft engine. This aeronautic-compliant bimorph harvester outputs 6.83mW at 1G, up to 246mW at 8G of acceleration and exhibits a maximum Normalized Power Density of 1,25mW.cm^{-3}.g^{-2} at 90°C.

SCIENTIFIC COLLABORATIONS: SAFRAN Power Units

Context and Challenges

Autonomous wireless sensor nodes operating in harsh environments, especially at high temperatures, are of particular interest for aerospace and aeronautic sectors. Indeed, Structural Health Monitoring (SHM) at various locations of an aircraft engine may help identifying and estimating structural faults or ageing phenomena (e.g. bearings). But some locations on/inside the engine can be very difficult to monitor, either because of their accessibility or because their temperatures are too high for a battery to operate. Particularly at small-scale, vibration energy harvesting has revealed a great innovation potential to supply wireless sensors nodes in such harsh environments. In this work, we use the piezoelectric principle to convert the engine's vibrations into electricity in order to supply a 3-channel Acceleration Measurement System (AMS) used to monitor the vibration level of the engine.

Main Results

The harvester is based on a piezoelectric bimorph cantilever (Fig. 1.a) tuned on a constant engine rotation frequency (≈70000 rpm, 1167Hz).

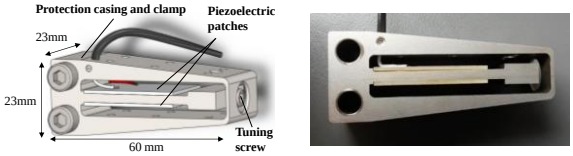

Figure 1. a) 3D schematic of the harvester with its dimensions, b) Photograph of the assembled harvester

A 2-degree-of-freedom (2DOF) analytical model was used to design the harvester. It enabled to optimize the dimensions (piezoelectric and substrate's thicknesses, lengths) to reach the best global electromechanical coupling while respecting the constraints of the application (resonant frequency, volume, output power). We used Finite Element method (COMSOL) on the optimal geometry to check the validity of our optimization and made slight adjustments to tune its resonant frequency to 1167Hz at 90°C and to limit the maximum stress to 10MPa at 20G, i.e. far below the piezoelectric material's depolarization stress. The final prototype (Fig. 1.b) was fabricated with an electrical discharge machining process with dimensional controls after its fabrication. To characterize the harvester, frequency sweeps at optimal resistive load and constant input acceleration were performed in a climatic chamber at 90°C and 120°C. Two ageing tests at 20G were also performed at 90°C and then at 120°C: the harvester was excited for 10^7 cycles on its first resonant mode. At 90°C, the harvester exhibits the following performances (Fig 2): 6.8mW@1G, 36.1mW@3G, 70.7mW@5G and 135mW@8G when excited at 1167Hz.

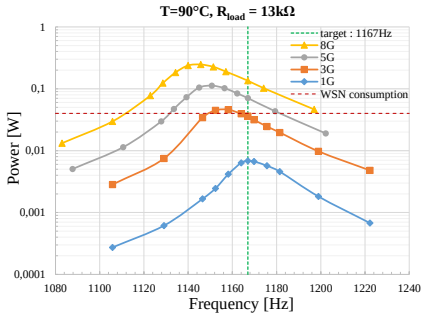

Figure 2. a) Electrical power as a function of the input frequency on an optimal resistive load for various acceleration values at 90°C.

Finally, we validated the operation of the complete system (harvester, PMC, AMS) which was successfully tested on a real engine's bench where acceleration measurements of 3 aeronautic-compliant accelerometers were performed autonomously (Fig 3).

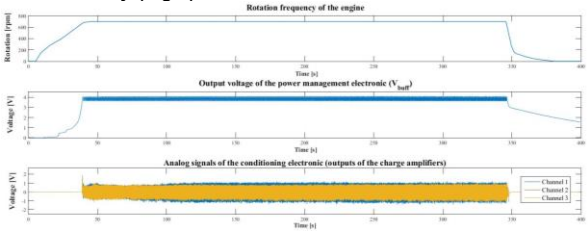

Figure 3. Autonomous measurements in real conditions: rotation frequency of the engine, output voltage of the power management electronic and the conditioning stage (prop. to the acceleration).

Perspectives

To the best of our knowledge, this autonomous system is the first one in prior art implementing a high acceleration (20G) and temperature (120°C) compliant piezoelectric harvester tested and validated in real conditions.

RELATED PUBLICATIONS:

[1] Gasnier P., Boucaud M., Gallardo M., Willemin J., Boisseau S., Morel A., Gibus D., and Moreau M. 2018 A 120°C 20G-compliant vibration energy harvester for aeronautic environments *J. Phys. Conf. Ser.*(PowerMems2018)

[2] Gasnier P, Willemin J, Chaillout J, Condemine C, Despesse G, Boisseau S, Gouvernet G and Barla C 2012 Power conversion and integrated circuit architecture for high voltage piezoelectric energy harvesting 10th IEEE International NEWCAS Conference pp 377–80

[3] Gasnier P, Willemin J, Boisseau S, Despesse G, Condemine C, Gouvernet G and Chaillout J 2013 An autonomous piezoelectric energy harvesting IC based on a synchronous multi-shots technique Proceedings of the ESSCIRC pp 399–402

MODELING AND DESIGN OF HIGHLY-COUPLED PIEZOELECTRIC ENERGY HARVESTERS FOR BROADBAND APPLICATIONS

RESEARCH TOPIC:

Vibration energy harvesting, Broadband Vibration

AUTHORS:

David GIBUS, Pierre GASNIER, Adrien MOREL, Sébastien BOISSEAU and Adrien BADEL

ABSTRACT:

This paper reports a method to design highly-coupled piezoelectric energy harvesters with frequency tuning capabilities using nonlinear electrical techniques. A cantilever beam with two PMN-PT patches has been optimized thanks to both analytical modelling and Finite Element Methods (FEM). The prototype exhibits a strong electromechanical coupling (k^2=17.6%) and a figure of merit (k_m^2Q=12.4) which allow an operating frequency bandwidth corresponding to 22% of the resonance frequency value.

SCIENTIFIC COLLABORATIONS: Adrien Badel, Université Savoie Mont Blanc / Laboratoire SYMME

Context and Challenges

Vibration energy harvesting appears as a relevant solution to deliver electrical energy to sensors where batteries cannot be used or need to be complemented. Piezoelectric systems based on mechanical resonators are interesting for their high power density at small scale. However, the frequency bandwidth limits are still an important issue. Electrical nonlinear methods have recently been proposed to enlarge the harvesting bandwidth by tuning the resonant frequency of linear piezoelectric harvesters. In opposition to nonlinear mechanical harvesters, these techniques are not dependent on the input excitation level and are based on the influence between the mechanical resonator dynamics and the electrical circuit. For that purpose, the use of highly-coupled piezoelectric generators was shown to be mandatory to enlarge the frequency response. However, few works in prior art have studied such generators, since increasing the electromechanical coupling (k^2) beyond a certain value did not show any interest to improve the maximal harvested power, and because the bandwidth was rarely studied.

Main Results

In 2014, Badel and Lefeuvre [1] introduced a strongly coupled (k^2=53%) cantilever-based PZN-PT harvester with a long tip mass, but no design method was proposed. One of the motivations for this work was to understand why such a simple structure (hence easy to manufacture) gets such high coupling.

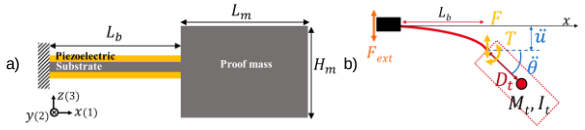

Figure 1: a) Clamped-free beam, b) beam during bending

Our device implements a long tip mass (Fig 1). Nevertheless, the single degree of freedom (SDOF) model is inaccurate for this particular geometry and the commonly-used distributed parameter model is inappropriate for optimization and needs numerical resolutions to compute the resonance frequencies and to deduce the coupling. Thus, we propose a 2-degree-of-freedom (2-DOF) model to design highly-coupled bimorph cantilevers with a long tip mass. In opposition to other works, in addition to the analysis of the deflection *u* and the force *F* performed in the SDOF model, the effect of the rotation θ_{Lb} of the tip mass and the resultant torque *T* are analyzed.

The model is used to find the geometrical parameters (Fig 1) that maximize the first vibration mode coupling coefficient for given PMN-PT piezoelectric patches (45×10×0.5mm). It also enables to explain why such geometries are advantageous. In complement, a 3D FEM analysis has also been used to refine the device optimization.

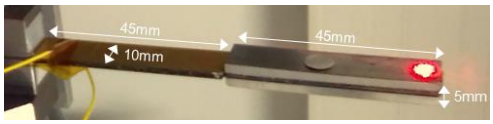

Figure 2: Fabricated prototype under test (h_s=h_p=0.5mm)

Our prototype exhibits a coupling of k^2=17% and a figure of merit k_m^2Q=12.4. The harvester provides a maximal power of 32.7µW @ 0.02g and a bandwidth equal to 8.4% of the resonant frequency by tuning the resistive load.

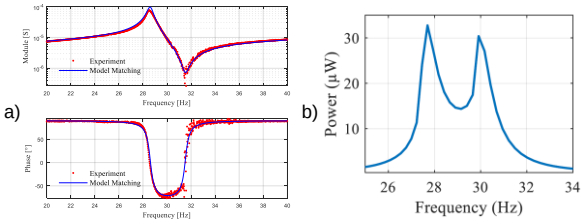

Figure 3: a) measured admittance of the prototype and b) measured power vs frequency at optimal resistive load under 0.02g acceleration.

Perspectives

With these characteristics, we expect a 22% operating frequency bandwidth when associated with a non-linear interface circuit such as FTSECE [1] or SC-SECE [2], which is one of the best performances in the state of art performed with a easy-to-manufacture, vibration energy harvester.

RELATED PUBLICATIONS:

[1] Badel A and Lefeuvre E 2014 Wideband Piezoelectric Energy Harvester Tuned Through its Electronic Interface Circuit J. Phys. Conf. Ser. 557 012115
[2] Morel A, Gasnier P, Wanderoild Y, Pillonnet G and Badel A 2018 Short Circuit Synchronous Electric Charge Extraction (SC-SECE) Strategy for Wideband Vibration Energy Harvesting IEEE International Symposium of Circuits And Systems (ISCAS)
[3] Ahmed-Seddik B, Despesse G, Boisseau S and Defay E 2013 Self-powered resonant frequency tuning for Piezoelectric Vibration Energy Harvesters J. Phys. Conf. Ser. 476 012069
[4] Gibus D, Gasnier P, Morel A, Boisseau S and Badel A, Modelling and design of highly coupled piezoelectric energy harvesters for broadband applications 2018 J. Phys. Conf. Ser PowerMems2018

PIEZO-POTENTIAL GENERATION IN FLEXIBLE CAPACITIVE GAN-WIRE BASED SENSORS: MULTIPHYSICS DESIGN MODELS AND DEVICE IMPLEMENTATIONS

RESEARCH TOPIC:

Nanosystem, flexible sensor, GaN wire, piezoelectricity, finite element modelling

AUTHORS:

E. Pauliac-Vaujour, A. El Kacimi, O. Delléa, E. Saoutieff, J. Eymery

ABSTRACT:

As part of our integrated sensor system activity, we develop novel and complex integrated sensor solutions for instrumented surfaces for a panel of possible applications such as automotive, predictive maintenance, wearables, health, sports and wellness, etc. Flexible piezoelectric devices, based on a continuous composite film of GaN wires, provide promising touch or shape reconstruction interfaces for further integration with structural electronics and additive fabrication processes In all these applications.Evolutive design models underpin the full potential of these adaptive structures as a function of their targeted implementations.

SCIENTIFIC COLLABORATIONS: CEA-LITEN, CEA-IRIG

Context and Challenges

Our group investigates some novel and evolutionary multi-scale, multi-modality, energy efficient system architectures, which feature and combine some of the latest technologies in terms of sensing, energy harvesting, communication, etc. One research area is in so-called "structural electronics", and in particular, we develop flexible systems operating electroactive materials, such as piezoelectric GaN wires, for widening system capabilities in terms of sensing (high performances, surface distribution, etc.) while optimising the overall system volume, or energy consumption for example. Multiphysics design models, in particular, are powerful tools for such purposes.

Main Results

We have developed and tested several configurations of GaN wire-based piezoelectric devices for flexible applications, including horizontally [1] and vertically [2] integrated flexible sensors (HIFS, VIFS, Fig. 1a,b). For example, we assembled a capacitive VIFS based on a scalable fabrication process by peeling [2] which reproducibly generated 2V signals under manual finger compression and was stable over thousands of compression and release cycles (Fig. 1b).

These configurations enabled us to robustify our finite element (FE) models from the elementary GaN wire to a complete multi-wire unit cell (Fig. 2). By use of this predictive model, sensor characteristics could be optimised as a function of the targeted solicitation mode (compression for touch detection, traction for stress or curvature, etc.). The impact of parameter variability on the device performance can be evaluated both at the wire level (geometry, orientation, doping) and at the device level (wire density, choice of stack materials and stack layer characteristics, geometry, contact position, etc.).

Perspectives

Arrays of such "sensitive surfaces" with dedicated electronic interfaces and reading circuits are aimed to be implemented in ultra-low-power and fully flexible systems for force and deformation mapping in a variety of applications. For this purpose, all preliminary developments were carried out so as to ensure future compatibility with additive fabrication technics and printed electronics, and hence to favour applicability.

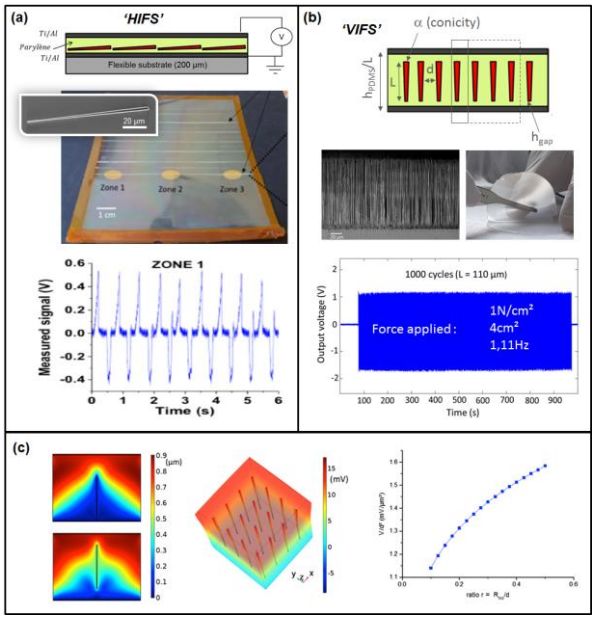

Figure 1: (a) and (b), from top to bottom: schematics of HIFS / VIFS devices; SEM image of GaN wire(s); flexible device with (a) patterned lines of GaN composite topped with electrode and (b) as grown vertical wires; generated piezo-potential under compression-release cycles. (c) from left to right: FE simulation of a single wire unit with two different composite stackings; 3D tilted view of a multi-wire-in-PDMS structure (including electrodes) under 5nN/µm² compressive strain; generated potential per unit area as a function of wire density in the multi-wire structure [2].

RELATED PUBLICATIONS:

[1] A. El Kacimi, E. Pauliac-Vaujour, O. Delléa, J. Eymery, "Piezo-potential generation in capacitive flexible sensors based on GaN horaizontal wires", *Nanomaterials* **8**, 426 (2018).

[2] A. El Kacimi, E. Pauliac-Vaujour, J. Eymery, "Flexible capacitive piezoelectric sensor with vertically aligned ultralong GaN wires", *ACS Applied Materials & Interfaces* **10** *(5)*, pp 4794-4800 (2018).

O2 LOW DATA RATE AND LOCALIZATION

- **Localization and Navigation Techniques**
- **Advanced Coding for LPWA Networks**
- **Body Area Networks**

ADAPTIVE LPWA NETWORKS BASED ON TURBO-FSK

RESEARCH TOPIC:
Low Power Wide Area, IoT, PHY, MAC, Adaptive networks

AUTHORS:
A. Guizar, M. Maman, F. Dehmas, V. Mannoni, V. Berg

ABSTRACT:
In order to meet the contradictory requirements of long range, low power consumption and adaptive throughput, LPWA networks require a decision module to select the most appropriate RF/PHY configuration and to cover the large variety of LPWA applications. In this study, we define a new adaptive LPWA network exploiting the flexibility of the Turbo-FSK waveform. The most relevant configurations are selected from the PHY and MAC layers point of view. At the PHY layer, a trade-off between data rate, spectral efficiency, energy consumption and range is considered while the MAC layer deals with the reliability, latency, network capacity, multi-user access (number of users, traffic intensity). Different massive deployment strategies are evaluated by simulation in terms of reliability, network capacity, battery lifetime and end-to-end latency.

Context and Challenges
To tackle the problem of massive Machine-to-Machine (M2M) communications in cellular networks, Low Power Wide Area (LPWA) Networks were proposed for large-scale applications needing long range communication and low power consumption. The three current challenges for LPWA MAC and Network layers are (i) flexible and hybrid MAC supporting device heterogeneity (e.g., scheduled access for devices with periodic packets and random access for devices with very few communication messages per day), (ii) flexible network architecture from low-power star topology adapted to low-traffic and sparse network to Device-to-Device (D2D) communications for high traffic loads and dense networks and (iii) decision module based on cognitive functionalities to identify the most appropriate configuration for a given scenario. This decision module will exploit the flexibility introduced by RF/PHY layers and the network architecture in order to improve system efficiency, capacity and QoS

Main Results
Our first contribution [1] focuses on the decision module to identify and select the most appropriate configurations of a flexible solution. For that purpose, we propose a methodology to select the relevant configuration from the PHY and MAC point of views and then, a global network adaptation strategy according to one or several criteria: energy, throughput, range or channel access (massive or sparse). The flexible solution is based on Turbo-FSK. It combines an orthogonal modulation (FSK), a linear modulation (PSK) and a convolutional code. A configuration using 4 FSK, 1 PSK with 4 repetitions will be called (4,1,4)

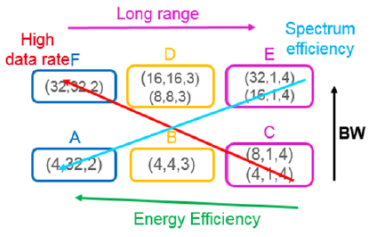

Figure 1: 6-states decision module exploiting Turbo-FSK flexibility

Our second contribution focuses on massive deployment strategy of LPWA networks [2]. For that purpose, we have developed a large scale network simulator [3] that provides the network performance (abacus) depending on application requirements (e.g., number of users, traffic intensities). Our simulation is adapted to flexible PHY and multiple waveforms and it provides spectrum model with an accurate interference model. The MAC and upper layer performance can be evaluated in terms of reliability, network capacity, latency and energy consumption for massive access scenarios. Thanks to this simulation framework, we evaluate the different Turbo-FSK configurations with different traffic loads and deployment strategies and we show the importance of heterogeneity management in LPWA networks.

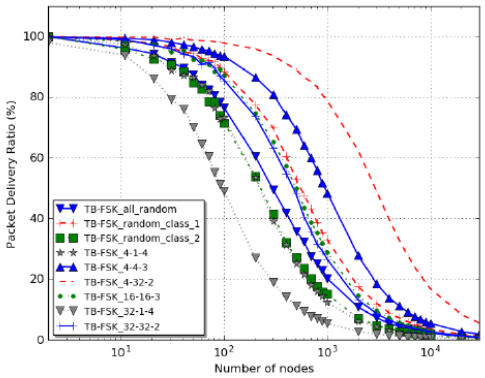

Figure 2: Packet Delivery Ratio as a function of the number of nodes sending a 100-Bytes packet each second in heterogeneous and homogeneous networks.

Perspectives
Our future work will focus to evaluate cognitive capabilities for centralized or distributed strategies. In the centralized approach, the Base Station needs to learn from the network to identify its global performance and status (i.e. dense or sparse) and can help nodes with low reliability (e.g. nodes at the edges having low PDR). In the distributed approach, nodes could activate their cognitive capabilities to detect the channel availability and adapt to the application (e.g. optimizing its energy consumption, sending a critical packet, performing real-time transmissions).

RELATED PUBLICATIONS:

[1] A. Guizar, M. Maman, V. Mannoni, F. Dehmas and V. Berg, "Adaptive LPWA Networks based on Turbo-FSK: from PHY to MAC Layer Performance Evaluation", GLOBECOM2018
[2] A. Guizar, L. Suraty, M. Maman and V. Mannoni, "Massive Deployment Evaluation of adaptive LPWA Networks using Turbo-FSK", WiMob2018
[3] CEA-LETI, “Wsnet simulator v4.0.” https://github.com/CEA-Leti/wsnet/, 2018.

FIELD VALIDATIONS OF V2V-AIDED COOPERATIVE VEHICULAR LOCALIZATION

RESEARCH TOPIC:

Cooperative localization, field trials, GPS continuity, V2V connectivity, ITS-G5, hybrid data fusion

AUTHORS:

Gia Minh Hoang, Benoît Denis, Jérôme Härri, Dirk Slock

ABSTRACT:

We herein account for proof-of-concept validations of a cooperative vehicular localization involving up to three cars in a real highway scenario. The proposed cooperative Bayesian filtering framework enables to combine ITS-G5 vehicle-to-vehicle (V2V) awareness messages, on-board GPS data and accurate ranging measurements based on the Impulse Radio Ultra Wideband (IR-UWB) technology. Experimental results show that a steady-state accuracy level down to 30 cm can be achieved through cooperation, despite locally poor -or even temporarily lost- GPS conditions. On this occasion, the superiority of particle filtering over Extended Kalman filtering in this context has also been illustrated, mitigating the erratic measurement noises observed under typical car mobility.

SCIENTIFIC COLLABORATIONS: EURECOM (Sophia Antipolis, France)

Context and Challenges

Cooperative vehicular localization, which mainly relies on Vehicle-to-Vehicle (V2V) communications and hybrid data fusion techniques, has been emerging as a promising solution to fulfill the needs of future Intelligent Transport Systems (ITS). One major aim is to improve Global Positioning Systems (GPS) in terms of both localization accuracy and service continuity. However, only rare experiments have been conducted in real driving conditions so far to validate this concept.

Main Results

In the proposed Cooperative Localization (CLoc) approach, vehicles broadcast their own absolute positions over V2V communication links (e.g., conveyed in ITS-G5 messages) and behave as so-called virtual anchors to assist their neighbors. Cooperative formulations of both Extended Kalman and Particle Filters (resp. EKF and PF) have been developed so as to fuse locally (i.e., at each vehicle) (i) positional awareness information received from neighbors, (ii) on-board GPS data and (iii) additional V2V range-dependent radio measurements performed with respect to the same neighbors (Fig. 1).

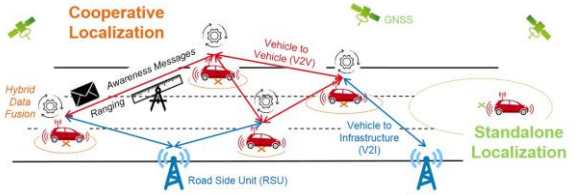

Fig. 1: Illustration of V2V-aided cooperative localization.

Regarding the latter radio measurements, the received signal strength of V2V ITS-G5 messages has been first integrated into the Bayesian filter observation (besides on-board GPS data). Relying on preliminary field trials conducted in a highway scenario, quite interesting performance gains could already be illustrated in comparison with standard GPS (e.g., reducing the 2-D location error by 50% in average, even though not going below 1m) [1]. Alternatively, more accurate V2V ranging measurements have been considered in new offline proof-of-concept validations [2]-[3], based on the round trip time of flight estimation of Impulse Radio - ultra Wideband (IR-UWB) signals. Quasi-constant localization accuracy around 0.3 m has thus been observed in the steady-state fusion regime (i.e., after initial convergence), despite poor on-board GPS data (i.e., with errors up to 1.3 m) or even under temporary GPS loss, thus confirming the relevance of V2V-aided cooperative approaches to improve both localization accuracy and service continuity (Fig. 2).

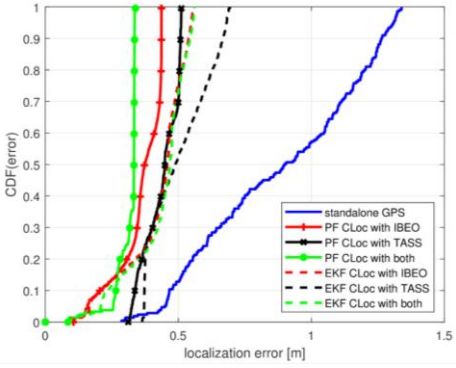

Fig. 2: CDF of 2-D location error for standard GPS (blue) or cooperative fusion of V2V IR-UWB range measurements wrt. 1 neighbor's RTK (red), 1 neighbor's standard GPS (black) or both (green), through PF (solid) and EKF (dashed).

Perspectives

Context-switching decision rules have also been investigated to select the optimal fusion strategy (and the adequate combination of algorithms accordingly) at any time/place [4], depending on operating conditions (i.e., on-board technologies, connectivity…) and a priori service requirements (e.g., accuracy class). Besides, the resilience of underlying V2V communication protocols against malicious attacks is today under question, calling for new specific cross-layer security mechanisms.

RELATED PUBLICATIONS:

[1] S. Severi, et al. "Beyond GNSS: Highly Accurate Localization for Cooperative-Intelligent Transport Systems", Proc. IEEE WCNC'18, Barcelona, April 2018

[2] G.M. Hoang, et al. "Cooperative Localization in VANETs: An Experimental Proof-of-Concept Combining GPS, IR-UWB Ranging and V2V Communications", Proc. IEEE WPNC'18, Bremen, Oct. 2018

[3] G.M. Hoang, et al. "Bayesian Fusion of GNSS, ITS-G5 and IR-UWB Data for Robust Cooperative Vehicular Localization", to appear in Comptes Rendus physique de l'Académie des Sciences, Special Issue on Localization, 2019

[4] S.K. Datta, et al. "IoT and Microservices Based Testbed for Connected Car Services", Proc. IEEE SmartVehicles'18, Chania, June 2018

TOWARDS PRECISE RADIO LOCALIZATION FOR LPWAN: COHERENT MULTI-CHANNEL RANGING

RESEARCH TOPIC:

Low Power Wide Area Network (LPWAN), precise narrowband radio localization, frequency hopping

AUTHORS:

F. Wolf, S. de Rivaz, F. Dehmas, J.-P. Cances (Université de Limoges

ABSTRACT:

Precise radio based positioning for low power wide area networks is a challenging research area due to narrowband signals and multipath propagation. Multi-channel ranging provides improved temporal resolution by coherent processing.
While this technique has been applied to short range radio standards, no application to long range radio devices exists. Theoretical performance bounds have been evaluated, ranging algorithms are benchmarked by numerical simulation and a transceiver testbed is developed to provide a proof-of-concept towards precise narrowband ranging for low power wide area networks.

SCIENTIFIC COLLABORATIONS: XLIM - Université de Limoges, Limoges, France.

Context and Challenges

Long range low power radio devices are designed for wireless sensor network (WSN) and Internet of Things (IoT) applications, where low-cost devices with high energy constraints exchange data over several kilometers. Low power wide area network (LPWAN) radio technologies (e.g. NB-IoT, LoRa, Sigfox) apply narrowband modulation schemes, offering high receiver sensitivity for long range communication.
Precise localization, based on the inherent radio signals of these radio nodes will enable new applications and enhance network management. However, accurate positioning remains challenging due to hardware imperfections (e.g. carrier frequency offset), low temporal resolution of narrowband signals and multipath propagation scenarios. State-of-the-art research and solutions have focused on either low complexity, low precision localization techniques (e.g. received signal strength, RSS; time-of-arrival, ToA) or on high precision methods (phase-of-arrival, PoA) applied to short range communication.

Main Results

Coherent multi-channel ranging allows aggregating multiple sequentially transmitted narrowband signals to a virtual increased bandwidth, making it compatible with LPWAN radio transceivers.
A detailed signal model for a two-way packet exchange has been derived in [1]. Numerical evaluation of theoretical asymptotical precision bounds (Cramer Rao lower bounds, CRLB) in line-of-sight and multipath propagation illustrates that ranging precision can be decoupled from instantaneous signal bandwidth.

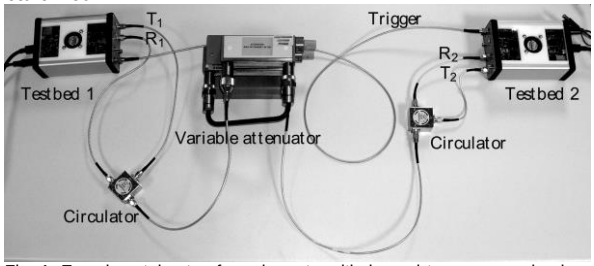

Fig. 1: Experimental setup for coherent multi-channel two-way ranging in a cabled frequency flat AWGN channel.

To investigate the feasibility of coherent multi-channel ranging experimentally, a transceiver testbed (Figure 1), comprising a radio front-end and a field programmable gate array (FPGA) has been developed [2]. This transceiver is designed to maintain phase coherence over the virtual multi-channel bandwidth.

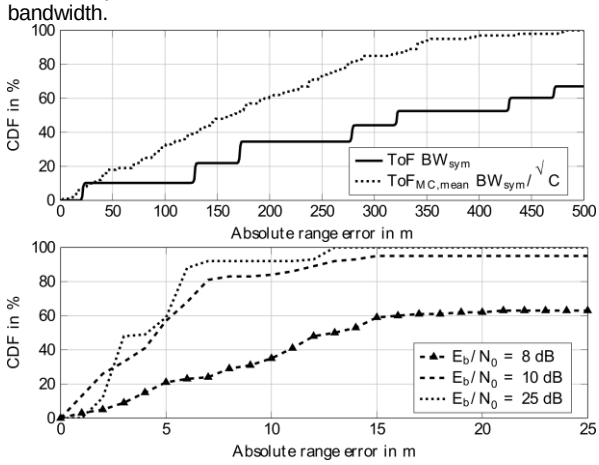

Fig. 2: Measured time-of-flight (ToF) range error (top) and multi-channel phase-of-flight (PoF) range error (bottom).

Experimental results demonstrate ranging performances in a cabled frequency flat AWGN channel. Time-of-flight (ToF) ranging with a 10kHz BPSK signal achieves 500m ranging error (Figure 2, top) whereas phase coherent ranging with a total of 16 channels and a 200kHz channel spacing attains errors below 15m (Figure 2, bottom).

Perspectives

Further work will characterize ranging errors in real outdoor long range scenarios. Directional antenna setups will be considered to mitigate multipath. Differential topologies are studied. Acquired data can serve as input to machine learning or deep neural network based algorithms to enhance ranging precision.

RELATED PUBLICATIONS:

[1] F. Wolf, C. Villien, S. de Rivaz, F. Dehmas and J.-P. Cances , "Improved Multi-Channel Ranging Precision Bound for Narrowband LPWAN in Multipath Scenarios", 2018 IEEE Wireless Communications and Networking Conference (WCNC), Barcelona, Spain, April 2018
[2] F. Wolf, J.-B. Doré, X. Popon, S. de Rivaz, F. Dehmas and J.-P. Cances, "Coherent Multi-Channel Ranging for Narrowband LPWAN: Simulation and Experimentation", 2018 15th Workshop on Positioning, Navigation and Communications (WPNC), Bremen, Germany, Oct. 2018

STUDY OF LOCALIZATION-COMMUNICATION TRADEOFFS IN mmWAVE 5G NETWORKS

RESEARCH TOPIC:

mmWave radio, beam selection, 5G, wireless localization, stochastic geometry, in-street deployment, multi-service provision

AUTHORS:

R. Koirala, G. Ghatak, B. Denis, A. De Domenico, D. Dardari, B. Uguen, M. Coupechoux

ABSTRACT:

Considering a typical in-street network deployment, we herein explore non-trivial operating tradeoffs between data communication and localization services in future 5G mmWave systems. More specifically, based on theoretical performance bounds and analytical tools from stochastic geometry, we come up with optimal beam selection strategies and resource partitioning schemes (e.g., in terms of allocated power or time), given a priori requirements in terms of down link rate coverage probability and/or localization errors.

SCIENTIFIC COLLABORATIONS: Univ. of Bologna (Cesena, Italy), Univ. Rennes 1 - IETR (Rennes, France), Telecom ParisTech (Paris, France)

Context and Challenges

Foreseen 5G communication systems operating in the millimeter wave domain beyond 20 GHz (mmWave) benefit from unprecedented localization capabilities, which are perceived today as a major enabler to guarantee both high data rates and service coverage (e.g., easing beam selection and alignment during the initial access phase and enabling dynamic users tracking under mobility). However, the provision of joint mmWave communication and localization services is subject to non-trivial operating tradeoffs, which are yet hardly addressed in state-of-the-art.

Main Results

Considering a canonical mmWave network deployed along the streets of a city, where the base stations (BSs) jointly provide positioning and data communication services, we have studied practical tradeoffs between localization errors and data rates based on theoretical performance bounds in [1]. More specifically, leveraging on tools from stochastic geometry, we have assess the "average" performance of localization and communication, by exploiting the a priori distribution of the distances separating the users from their serving BSs. First, we have derived the Cramer-Rao lower bound (CRLB) related to the estimation of these distances. Then, we have obtained the expressions of both signal to noise ratio (SNR) and rate coverage probabilities for a typical user, as a function of the power splitting factor between communication and localization services. Based on the previous CRLB characterizing distance estimation, an upper bound on the probability of beam-misalignment has thus been computed. This upper bound has been further used to determine the minimum antenna beamwidth that limits beam misalignment. Finally, we have prescribed the operator with a set of rules to select the adequate power splitting factor between localization and communication services so as to support a priori quality of service requirements, given the previously optimized beamwidth and an a priori BS density.

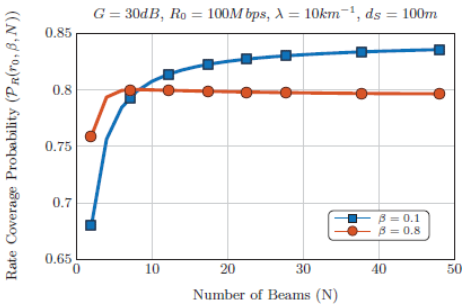

Fig. 1: Rate coverage probability as a function of the number of beams available in the alphabet, for different time sharing strategies between localization and data services (β representing the fractional time devoted to communication)

One step ahead in [2], relying on the same kind of formalism and theoretical framework (all except but assuming time sharing rather than power sharing between the two services), we have formulated the average beam selection error as a function of position uncertainty and accordingly, both SINR and rate coverage probabilities (Fig. 1). Finally, based on the previous expressions, we have introduced a multi-service optimization policy enabling beamwidth selection to maximize the rate coverage probability, given the respective amounts of time devoted to localization and communication. On this occasion, we have illustrated even more concretely the complex relationship binding the two services. In particular, we have shown how allocating more resource to localization leads to lower beam selection errors, whereas the resulting limitation in communication resource could adversely reduce downlink data rates (and vice-versa).

Perspectives

Besides beam selection, future works should address dynamic location-based beam alignment (at the user also) for even more efficient access and continuous users tracking.

RELATED PUBLICATIONS:

[1] G. Ghatak, R. Koirala, A. De Domenico, B. Denis, D. Dardari, B. Uguen, M. Coupechoux, "Positioning Data-Rate Trade-off in mm-Wave Small Cells and Service Differentiation for 5G Networks", IEEE Vehicular Technology Conference 2017 – Spring (IEEE VTC-Spring'17), Porto, June 2018

[2] R. Koirala, G. Ghatak, B. Denis, B. Uguen, D. Dardari, A. De Domenico, "Throughput Characterization and Beamwidth Selection for Positioning-Assisted mmWave Service", IEEE Asilomar Conference on Signals, Systems, and Computers 2018 (IEEE ASILOMAR'18), Pacific Grove, Oct. 2018

PERFORMANCE EVALUATION OF LARGE SCALE LORA DEPLOYMENTS

RESEARCH TOPIC:

LoRa network, IoT, PHY, MAC, Adaptive networks

AUTHORS:

M. Nunez Ochoa, A. Guizar, M. Maman and A. Duda (LIG)

ABSTRACT:

The LoRa technology has emerged as an interesting solution for low power, long range IoT applications by proposing multiple "degrees of freedom" at the physical layer. This flexibility provides either a long range at the cost of a lower data rate or higher throughput at the cost of low sensitivity, so a shorter range. In this study, we investigate the performance of homogeneous networks (i.e. when all the nodes select the same LoRa configuration) and heterogeneous networks (i.e. when each node selects its LoRa configuration according to its link budget or their needs) for large scale deployments (up to 10000 nodes per gateway. Then we analyze the flexibility of LoRa and propose various strategies to adapt its radio parameters (such as the spreading factor, bandwidth, and transmission power) to different deployment scenarios.

Context and Challenges

Over the past few years, new approaches called Low Power Wide Area (LPWA) networking technologies have emerged. Among them, LoRa has been widely adopted due to its maturity and the opening of the system. The main LPWA research directions are about large scale networks to support massive number of devices, interference issues, link optimization and adaptability. The potential of an adaptive LoRa solution in terms of spreading factor, bandwidth, transmission power, and topology is still not well studied or exploited. Thus, new protocols and strategies are required to improve LoRa scalability. The first step is to understand heterogeneous network deployments when devices use different spreading factor. The second step is to propose adaptive strategies.

Main Results

In [1], we study the performance of homogeneous (i.e. when all the nodes select the same LoRa configuration) and heterogeneous networks (i.e. when each node selects its LoRa configuration according to its link budget) for large scale deployments (up to 10000 nodes per gateway). For that purpose, we have developed an accurate model of the PHY/MAC LoRa based on the extended WSNet simulator [3]. The LoRa model takes into account spectrum usage, co-channel rejection due to quasi-orthogonality of the LoRa spread spectrum modulation, and the gateway capture effect. The simulation results give an insight on reliability (Fig.1), network capacity, and energy consumption as a function of the number of nodes and traffic intensity. The comparison shows the benefits of deployment heterogeneity.

In [2], we analyze LoRa flexibility and propose some strategies to adapt its radio parameters (e.g., spreading factor, bandwidth, and transmission power) to different deployment scenarios (i.e. star and mesh topologies). Our simulation results show that in a star topology, we can achieve the optimal scaling-up/down strategy of LoRa radio parameters to obtain either a high data rate or a long range while respecting low energy consumption. In mesh networks, energy consumption is optimized by exploiting various configurations and the network topology (e.g., the number of hops, the network density and the cell coverage).

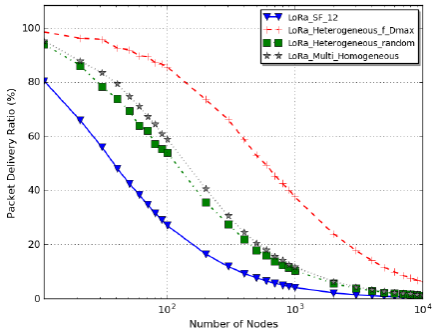

Figure 1: Packet Delivery Ratio as a function of the number of devices generating a 50 Bytes packet each 60s.

Finally, we propose a strategy (Fig.2) exploiting both star and mesh topologies (boosting the use of high data rate modes)

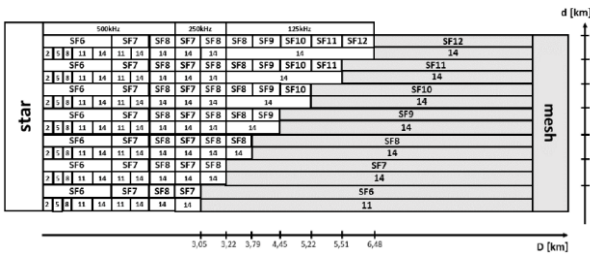

Figure 2: (SF, PTX, Topology) adaptation strategy

Perspectives

Our future work will focus decision modules that optimally select the mode according to the scenario criteria (e.g., network congestion, energy efficiency, data rate), the radio environment (e.g., link budget, level of interference, device mobility) and the network infrastructure (i.e. by increasing the number of gateways). This multi-gateway adaptation will maximize the overall capacity of the global network by exploiting the orthogonality of various spreading factors and the spatial reuse of the communication.

RELATED PUBLICATIONS:

[1] M. Nunez, L. Suraty, M. Maman and A.Duda, "Large Scale LoRa Networks: From Homogeneous to Heterogeneous Deployments", WiMob2018
[2] M. Nunez, A. Guizar, M. Maman and A.Duda "Evaluating LoRa Energy Efficiency for Adaptive Networks: From Star to Mesh Topologies", WiMob2017
[3] CEA-LETI, "Wsnet simulator v4.0." https://github.com/CEA-Leti/wsnet/, 2018.

RESOURCE SHARING STRATEGIES FOR MULTIUSER LOCALIZATION IN mmWAVE 5G NETWORKS

RESEARCH TOPIC:

Beamforming optimization, fairness strategies, multi-user resource allocation, mmWave radio, wireless localization, 5G

AUTHORS:

Remun Koirala, Benoît Denis, Bernard Uguen, Davide Dardari, Henk Wymeersch

ABSTRACT:

We herein describe practical resource sharing schemes for multi-user localization applications in mmWave multicarrier MIMO systems. To this aim, beamforming is optimized at the base station with respect to theoretical localization performances while various fairness criteria are considered, enabling localization-optimal power allocation over both multiple users and subcarriers, depending on the a priori application requirements.

SCIENTIFIC COLLABORATIONS: Univ. Rennes 1 - IETR (Rennes, France), Univ. of Bologna (Cesena, Italy), Chalmers Univ. of Technology (Gothenburg, Sweeden)

Context and Challenges

In the context of 5G communication networks (5G), the millimeter wave (mm-Wave) radio technology, which operates within large available bandwidths at high frequencies (i.e., above 20 GHz), is expected to fulfill unprecedented needs in terms of data rates and channel load. Benefitting from both directional antenna systems and sparse multipath channels, mmWave systems also offer unprecedented localization capabilities besides high data rates. However, practical resource allocation strategies (i.e., over time/frequency, over users…) still need to be defined so as to optimize localization performance as a function of the underlying application and/or use cases (e.g., multi-user vs. single-user, 2D vs. 1D…).

Main Results

Based on former works characterizing the theoretical performance bounds of downlink location estimation for a single user [1], the mmWave localization-optimal beamforming problem has been reformulated in a multi-user context [2]. We have first generalized the Cramer Rao Lower Bound expressions of delay, angle of departure (AoD) and angle of arrival (AoA) estimates, while considering multiple subcarriers. Then, we have defined an equivalent localization error cost for beamforming optimization, as a weighted combination of the previous bounds, where the weights can be timely tuned for flexible power allocation across the subcarriers (e.g., with the possibility to arbitrarily favor 1D or 2D estimation). Finally, through mathematical transformations, the resulting optimized beamformer has been injected into the expressions of both Position and Orientation Error bounds (PEB/OEB) to evaluate a posteriori the performance of two main resource sharing schemes (over multiple users), namely the min-max and proportional fairness strategies. The former ensures a minimum localization error requirement to each user (Fig. 1), whereas the latter provides favorable users with proportionally more resources and thus, with better localization accuracy. Monte Carlo simulations confirm that proportional (resp. min-max) fairness is mainly relevant in case of large (resp. small) spread between users' operating conditions (e.g., wrt. signal to noise ratio) (Fig. 2).

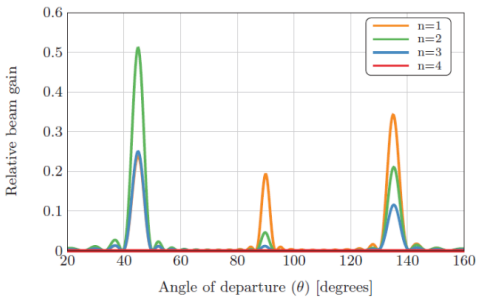

Fig. 1: Ex. of normalized beam gain optimization per subcarrier (wrt. the total gain) with a min-max fairness strategy for 3 users (resp. at 45°/40m, 90°/28m, 135°/40m).

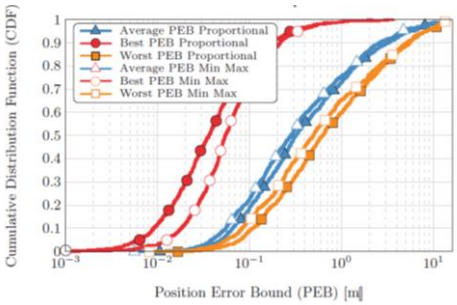

Fig. 2: CDF of position error bounds per user (best, worst and average performance) for different fairness strategies.

Perspectives

Relying on both localization-optimal and rate-optimal beamformers, we will explore relevant operating tradeoffs between localization and data services in both single-user and multi-user multi-carrier mmWave MIMO contexts, while considering various time-frequency resource division schemes.

RELATED PUBLICATIONS:

[1] R. Koirala, B. Denis, D. Dardari, B. Uguen, "Localization Bound Based Beamforming Optimization for Multicarrier mmWave MIMO", IEEE Workshop on Positioning, Navigation and Communications 2017 (IEEE WPNC'17), Bremen, Oct. 2017.

[2] R. Koirala, B. Denis, B. Uguen, D. Dardari, H. Wymeersch, "Localization Optimal Multi-user Beamforming for Multi-Carrier mmWave MIMO Systems", IEEE Personal, Indoor, and Mobile Radio Communications 2018 (IEEE PIMRC'18), Bologna, Sept. 2018.

TURBO-FSK: A FLEXIBLE AND POWER EFFICIENT MODULATION FOR THE INTERNET-OF-THINGS

RESEARCH TOPIC:

Low Power Wide Area (LPWA), Internet of Things (IoT), Physical layer, low sensitivity

AUTHORS:

Yoann Roth, Jean-Baptiste Doré, and Vincent Berg

ABSTRACT:

Turbo-FSK is a constant envelope modulation with orthogonal alphabet that allows to operate at very low levels of receiver power (high sensitivity performance) and very low levels of energy per bit Eb. The scheme combined with a linear alphabet and puncturing is not only efficient but also flexible. We demonstrated that it is adapted to the constraints of cellular LPWA transmissions. Flexibility in terms of spectral efficiency, asymptotic performance with regard to Shannon's limit and the constant envelope property of Turbo-FSK make the scheme a serious contender for the 5th generation of cellular physical layer dedicated to the IoT.

SCIENTIFIC COLLABORATIONS: Laurent Ros, Université Grenoble Alpes, CNRS, GIPSA Lab

Context and Challenges

When designing new solutions for Low Power Wide Area (LPWA) networks, coexistence and integration into existing cellular frameworks should be considered to ease the deployment procedure and reduce costs. Turbo-Frequency Shift Keying (FSK) was proposed as a potential physical layer for LPWA networks. Flexible extension of the initial Turbo-FSK is evaluated by combining orthogonal and linear properties, the
It allows achieving higher levels of spectral efficiencies. In addition to the more spectrally efficient alphabet, a puncturing mechanism which trades performance for a shorter transmitted sequence is introduced. These improvements increase the flexibility of the scheme and makes it a serious contender for future 5G IoT schemes.

Main Results

In the context of LPWA networks, reaching low levels of sensitivity and containing the power consumption at the device level is a major concern. Turbo-FSK with a constant envelop reduces linearity constraints imposed on the power amplifier. It has been demonstrated that an efficiency of 90% can be achieved when considering class B amplifier [1]. The modulation scheme is defined by a relatively large number of possible configurations. Asymptotic non-exhaustive study has been realized, and demonstrated interesting properties [2]. While a very large number of possible mappings of the codewords on the trellis are possible, it is more beneficial to maintain some orthogonal properties between the transitions of the trellis. Puncturing allows for an increase in spectral efficiency at the expense of some performance loss. It can also reduce the error floor for a given spectral efficiency, at the expense of an increase in complexity. The comparison to the maximum achievable spectral efficiency (Fig. 1.) reveals that Turbo-FSK maintains an energy efficiency close to Shannon's limit [2]. When compared to the Turbo Code (TC) used for the NB-IoT solution, Turbo-FSK is more flexible and can provide a better energy efficiency when low spectral efficiencies are considered.

The possibility to use the Turbo-FSK modulation scheme has been evaluated for the use in a transmitter and a receiver based on an OFDM architecture [3]. Simulations demonstrated that the proposed schemes achieve performance close to TC-OFDM in AWGN conditions and Rayleigh fading channels for both static and mobility conditions. This further reinforce the usage of the scheme for future 5G cellular applications of the IoT.

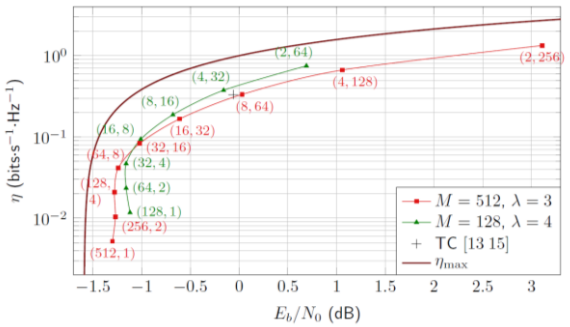

Figure 1: Spectral efficiency versus threshold for various configurations of the Turbo-FSK modulation scheme – Comparison to Turbo-Code and Shannon'

Perspectives

Combination of the physical layer with non-orthogonal multiple access (NOMA) scheme should be considered for IoT applications to increase cell capacity and power consumption of the IoT data transaction.

RELATED PUBLICATIONS:

[1] Yoann Roth, Jean-Baptiste Doré, Laurent Ros, Vincent Berg. "5G Contender Waveforms for Low Power Wide Area Networks in a 4G OFDM Framework". ICT 2018, 25th International Conference on Telecommunications, June 2018, Saint-Malo, France.

[2] Yoann Roth, Jean-Baptiste Doré, Laurent Ros, and Vincent Berg, "Coplanar Turbo-FSK: A Flexible and Power Efficient Modulation for the Internet-of-Things," Wireless Communications and Mobile Computing, vol. 2018, Article ID 3072890, 17 pages, 2018

[3] 1Y. Roth, JB. Doré, L. Ros, V. Berg, "Contender Waveforms for Low Power Wide Area Networks in a Scheduled 4G OFDM Framework", EURASIP journal on Advances in Signal Processing, EURASIP Journal on Advances in Signal Processing 2018:43, june 2018

TURBO-FSK, A PHYSICAL LAYER FOR LPWA: SYNCHRONIZATION AND CHANNEL ESTIMATION

RESEARCH TOPIC:

IoT, LPWA, Turbo-FSK, Physical layer, Synchronization, channel estimation

AUTHORS:

F. Dehmas, V. Mannoni, V. Berg, J.-B. Doré

ABSTRACT:

Turbo Frequency Shift Keying (Turbo-FSK) has been considered as a promising physical layer for low power wide area applications. Its constant envelope at the transmitter combined with performance close to the Shannon's limit enable to achieve a high energy efficiency. Synchronization and channel estimation approach based on a specifically built preamble and adapted to the performance of this new modulation is presented. Simulations have been performed for both time and frequency synchronization as well as channel estimation. Less than 1 dB degradation in comparison to perfect detection is achieved for the most severe types of channels.

SCIENTIFIC COLLABORATIONS: no

Context and Challenges

Internet of Things (IoT) is rapidly expanding and more than twenty billion devices are expected to be connected through wireless systems by 2020. Low Power Wide Area (LPWA) network technologies whose LoRa and NB-IoT are two leaders, constitute an important part of the IoT by providing a long range and low power wireless connectivity.

Long range is achieved by ensuring a very low level of sensitivity. Low energy consumption is achieved by selecting a constant envelope modulation for the efficiency of the power amplifier (PA).

Turbo-FSK is a new waveform with performance close to Shannon's limit for low spectral efficiency. As a consequence, signal-to-noise (SNR) ratio at the receiver can be well below 0 dB imposing significant performance constraints on time and frequency synchronization as well as on channel estimation. However precedent publication considered only perfect synchronization and channel estimation.

Main Results

A preamble based synchronization has been considered [1]. It is based on a Zadoff-Chu sequence that has been modified to have a spectrum in accordance with the turbo-FSK modulation. This sequence has a constant envelope (to keep the low power property of TurboFSK) and good autocorrelation properties. As low SNR synchronization is needed, accumulations on several sequences are required. To be resistant to carrier frequency offset (CFO), a differential accumulation is done and to avoid the need of a start of frame delimiter, the repeated sequence is weighted by the cumulative product of a Zadoff-Chu sequence. Thus the resulting differential cross correlation has a single peak with low side lobs.

Two different approach have been proposed for pilots dedicated to channel estimation: a time domain approach [1] with a modified Zadoff-Chu sequence as in preamble (thus with constant envelope); a frequency domain approach [2] with also a Zadoff-Chu sequence. In the first case, the shape of the spectrum drives to a less accurate estimate at the borders of the band. In the second case, the envelope is no longer constant so an additive sequence is added to reduce the variations of the envelope. Channel estimation is based on Wiener filters (in frequency domain to reduce the noise and in time domain to interpolate and average).

With synchronization and channel estimation, performance is given in Figure 1. The performance loss is limited to 1 dB in AWGN or typical urban (ETU) channel.

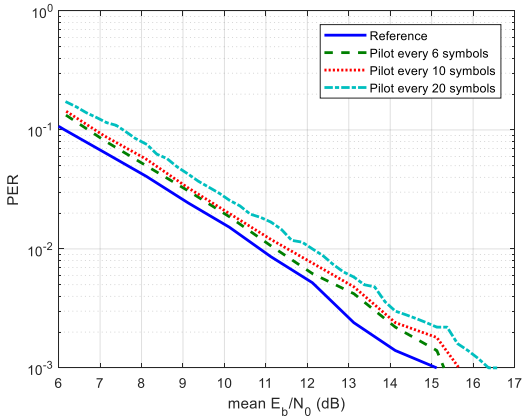

Figure 1: PER for ETU channel including synchronization, CFO estimation and correction, channel estimation

Perspectives

This signaling and associated algorithms will be tested at INRIA in the CorteXlab thanks to software defined radio demonstrators. Multi-user capability of the Turbo-FSK with the proposed preamble will also be evaluated.

RELATED PUBLICATIONS:

[1] F. Dehmas, V. Mannoni, V. Berg. "Turbo-FSK, a physical layer for LPWA: Synchronization and Channel estimation". EUCNC 2018 - European Conference on Networks and Communications, Jun 2018, Ljubljana, Slovenia

[2] J.-B. Doré, V. Berg, "Turbo-FSK: a 5G NB-IoT Evolution or LEO Satellite Networks", 2018 6th IEEE Global Conference on Signal and Information Processing, November 26–29, 2018. Anaheim, California, USA

O3 WIRELESS HIGH SPEED COMMUNICATIONS

- **Millimeter Waves**
- **Full Duplex**
- **Advanced Coding**
- **Spectrum and Heterogeneous Network Management**

FILTER-BANK OFDM TRANSCEIVERS FOR WIRELESS COMMUNICATIONS

RESEARCH TOPIC:
5G, B5G, PHY layer, waveform design

AUTHORS:
David Demmer, Jean-Baptiste Doré

ABSTRACT:
5G paves the way to service-centric adaptation radio link. The transmitted signal is configured according to the service it provides and the propagation impairments it suffers from. However, in 5G the multi-service multiplexing leads to a poor bandwidth use. Indeed, the 5G waveform is responsible for large out-of-band emission and therefore large guard bands are required between bands of different numerologies. We investigate the use of waveforms based on filter-bank as an alternative of legacy 5G technology. Such waveforms prove to be an enabling technology for an efficient multi-service multiplexing. This result would ease the support of real-time numerology adaptation as one base station could provide different services in the same cell.

SCIENTIFIC COLLABORATIONS: CNAM, Paris.

Context and Challenges
The fifth Generation New Radio (5G-NR) standard proposes to adapt the waveform configuration to the provided service and the used carrier frequency. By doing so, the requirements for each service can be satisfied. However, the waveform Cyclic Prefix Orthogonal Frequency Division Multiplexing (CP-OFDM) is still used and it has been observed in [1] that multiplexing the different services can only be ensured with a huge compromise in the spectral efficiency. In this work we demonstrate that an ubiquitous multi-service support is possible using a dedicated waveform technology. Such contribution is interesting for the downlink as a base station could provide different services in the same band while being 5G NR compliant.

Main Results
OFDM-precoded filter-bank waveforms have been initially studied for research on 5G waveforms. One of them is the Block Filtered-OFDM. This modulation scheme provides subband filtering and ensures near complex orthogonality allowing a straightforward reuse of advanced techniques developed for OFDM. It implies that BF-OFDM receiver satisfies the transparency condition, meaning that it can perform the signal demodulation without any knowledge on the filtering and/or windowing performed at the transmitter side. We have demonstrated the benefits of the proposed approach especially in a scenario multiplexing different numerologies [1][2]. As an example, we have considered a scenario composed of a 8-resource block-wide interfering user of numerology $\mu = 2$ over an one-subcarrier user of interest of numerology $\mu = 0$. The performance evaluation is done by measuring the Mean Square Error (MSE) at the receiver side. Different technologies are compared, namely OFDM (5G waveform), OFDM with windowing (wOFDM and WOLA) as well as BF-OFDM. The results are given in Figure 1. One can observe that the performance is improved with a windowed receiver and even significantly for the BF-OFDM. Therefore, one can say that BF-OFDM both provides great results for the inter-numerology co-existence scenario and efficient implementation of a multi-service base station. Besides, the results highlight the complementary of the processing performed at the transmitter and receiver.

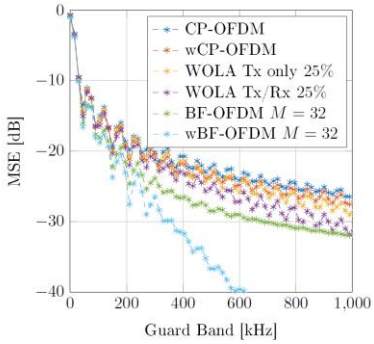

Fig. 1: Multi-service co-existence performance results.

Perspectives
An efficient support of multi-service links has become a challenge to overcome for future cellular technologies. 5G NR gives a first practical implementation but with weaknesses. Our current contributions proposed to alleviate the difficulties of such challenges by considering an adequate subband-confined waveform: BF-OFDM. This waveform ensures the reuse of know-how digital communications advanced techniques and relies on a simple 5G NR receiver. Moreover, with a proper characterization and filter design, it is possible to build a base station providing simultaneously different services within a single channel. The spectral efficiency is improved w.r.t legacy 5G NR implementation while keeping a backward compatibility with the standard. One could envisaged, in the future, to extend the concept of multi numerologies transmission toward dynamic waveforms configurations settings depending on the communication requirements and link quality.

RELATED PUBLICATIONS:
[1] D. Demmer, R. Gerzaguet, J.-B. Doré, and D. Le-Ruyet, “Analytical study of 5G NR eMBB co-existence,” in 2018 25th International Conference on Telecommunications (ICT), June 2018, pp. 186–190
[2] D. Demmer, R. Zakaria, J.-B. Doré, R. Gerzaguet, and D. Le-Ruyet, “Filter-bank OFDM transceivers for 5G and beyond,” in Asilomar Conference on Signals, Systems, and Computers, 2018, Nov 2018.

ASSESSMENT OF 5G-NR PHYSICAL LAYER FOR FUTURE SATELLITE NETWORKS

RESEARCH TOPIC:

Integration of satellite networks into 5G.

AUTHORS:

N. Cassiau, L. Maret, J.-B. Doré, V. Savin, D. Kténas.

ABSTRACT:

The performance of recently released 5G New Radio (NR) physical layer (PHY) with typical satellite scenarios were assessed. Four typical propagation channels in Ka band were considered and implementation constraints were modeled. It was demonstrated that for open rural and high speed train scenarios, 5G-NR PHY may be used as is. Higher speed scenarios (e.g. aeronautical) can benefit from the 5G-NR mode that allows very short symbols. Finally, we showed that amendments should be considered in the standard for supporting 2-state channels (like suburban).

Context and Challenges

5G-NR (New Radio) standard release 15 is now available. It is accepted that satellite systems will be an integral part of 5G. Nevertheless, the standard does not yet include specifications dedicated to them. It is therefore legitimate to ask whether the current specifications of this new standard, from the point of view of the physical layer (PHY), are suitable for satellite transmissions. In this study, the performance of the 5G-NR PHY, in terms of error rates and synchronization, were thus evaluated with typical satellite scenarios and implementation constraints.

Main Results

Four representative geostationary satellite scenarios were selected. Scenario S1, 60 km/h Land Mobile Satellite (LMS) suburban, is modelled by a two-state channel (adopted by the standardization for performance evaluation). Scenario S2 is also a vehicular channel, but in an open environment with a receiver speed of 100 km/h. Scenario S3 is the aeronautical model, with a speed of 1000 km/h. Finally, scenario S4 is railway channel with 300 km/h train speed. For all scenarios, the downlink direction is considered and the carrier frequency is in the Ka band.

Five implementation constraints were considered: i) phase noise, ii) non linearities of the power amplifier with a true Output BackOff of -3.6 dB for 16-QAM modulation, iii) analog Output MUltipleXing (OMUX) filter, iv) a carrier frequency offset (CFO) of 5 ppm and v) a sampling frequency offset (SFO) of 10 ppm.

Table 1. CNR required to reach TBLER=10^{-3} [dB], 20 MHz (and 40 MHz) bandwidth.

Scenario	μ	MCS 4 QPSK 0.3	MCS 9 QPSK 0.66	MCS 14 16QAM 0.54
S1 LMS suburban	{2,3}	> 20 (>20)		
	4	>17.8 (>20)	>20 (>20)	>20 (>20)
S2 Open rural	2	0.9 (0.5)	5.2 (5.8)	10.3 (10.6)
	3	1.8 (1)	6.2 (5.6)	11 (10.2)
	4	2.8 (1.9)	7.3 (6.5)	11.9 (10.8)
S3 Aero	2	error floor		
	3	error floor)	error floor	error floor
	4	2.5 (1.5)	7.8 (6.5)	19.5 (17)
S4 Train	2	5.2 (5.1)	10 (10.3)	14.8 (14.5)
	3	6 (5.4)	10.5 (10.1)	15 (14.2)
	4	6.6	11.3	15.7 (15.1)

The error rate performance are presented in Table 1. This table shows the Carrier-to-Noise-Ratio (CNR) required to reach a target Transport-Block-Error-Rate (TBLER) of 10^{-3}. In the considered satellite scenarios, typical CNR values observed at the receiver are around 14 dB, a three-color code has therefore be adopted: in S1, the performance are limited by the channel deep fading; in S2, the channel is nearly an Additive White Gaussian Noise channel, therefore the target TBLER can be reached with a CNR lower than 14 dB, even with the highest Modulation and Coding Scheme (MCS); S3 can benefit from the 4 times shorter symbol duration of numerology 4 (with respect to numerology 2) to deal with the very high Doppler; finally the target TBLER can be reached with QPSK modulation for S4, whatever the numerology, and nearly reached with 16-QAM.

Time and frequency synchronization strategies were also designed: first, before starting the OFDM symbol synchronization, a detection of the numerology is done by running 5 parallel autocorrelation blocks configured for the 5 different supported numerologies. Then different processes for time and frequency synchronization were implemented: i) a time-domain OFDM symbol synchronization is performed using a 1-bit autocorrelation on CP-length windows; ii) the autocorrelation peak is then used to get a first estimation of the fractional part of CFO which is digitally compensated in time-domain; iii) a detection of Primary Synchronization Signals (PSS) is implemented in frequency domain, based on a cross-correlation on the 127 PSS subcarriers. It allows to get an estimation of the integer part of CFO and to detect the start of a Primary Broadcast Channel SS-Block. Further Secondary SS detection allows to perform the frame timing. These strategies were proven to provide excellent detection and false alarm performance in all the studied scenarios.

Perspectives

The results demonstrate that the 5G NR physical layer as it is standardized today can fulfil the satellite communication requirements for scenarios without shadowing and for which receiver speed is not too high (train for example). When the receiver speed is very high (aeronautic case), system can benefit from the high numerologies introduced in 5G standard: very short OFDM symbols allow to obtain good performance. In channels with shadowing (like LMS suburban), CNR in shadowing locations is too low to demodulate signal, whatever the numerology. It suggests, for future works, to study the introduction of new FEC schemes including deep time interleaving function and/or larger LDPC codeword sizes, which is limited to 8 kbits in the release 15.

Finally, synchronization performance show that numerology and OFDM symbol detection probabilities are performing well whatever the numerology strategy, except for channels with shadowing for which a higher bandwidth with more samples per OFDM symbol improves these detections.

RELATED PUBLICATION:

[1] N. Cassiau, L. Maret, J.-B. Doré, V. Savin, D. Kténas, "Assessment of 5G NR Physical Layer for Future Satellite Networks," 2018 6th IEEE Global Conference on Signal and Information Processing (GlobalSIP), Anaheim, California, USA, November 26–29, 2018.

ADVANCED DESIGN FOR LAYERED LDPC DECODERS

RESEARCH TOPIC:

TELECOM (LDPC codes, hardware implementation)

AUTHORS:

Valentin Savin

ABSTRACT:

This work proposes a holistic approach that addresses both the message mapping in memory banks and the pipeline related data hazards in layered Low-Density Parity-Check (LDPC) decoders. It relies on (i) a residue-based layered scheduling that reduces the pipeline related hazards, and (ii) off-line algorithms for optimizing the message mapping in memory banks and the message read access scheduling. The hardware usage efficiency of our layered decoder is improved by 3%-49% when only the off-line algorithms are employed, and by 16%-57% when both the residue-based layered architecture and the off-line algorithms are used.

SCIENTIFIC COLLABORATIONS: Politehnica University Timisoara (Romania); ENSEA, Cergy-Pontoise (France)

Context and Challenges

A key property of Low-Density Parity-Check (LDPC) decodes is represented by their capability to accommodate different degrees of parallelism yielding different throughput-cost trade-offs (Fig. 1). In this work, we study off-line algorithms to optimize the memory access, combined with built in architecture support for mitigating pipeline related hazards, targeting Quasi-Cyclic (QC)-LDPC decoders using layered scheduling.

Main Results

In [1], we propose a number of off-line algorithms for both the message mapping and read access scheduling problems, such that the decoder hardware usage efficiency is maximized: (1) a genetic Travelling Salesman Problem (TSP) solver for coarse grain message read access scheduling minimizing pipeline stalls; (2) a hyper-graph coloring using a Modified Misra-Griess algorithm for memory mapping; (3) a fine grain message read access scheduling algorithm for in-layer message processing re-ordering that further minimizes the pipelined related stalls. We further propose a new residue-based layered decoding that relaxes the access scheduling constraints associated to the pipeline related hazards, and implement it using FPGA's. Optimization through code construction for layered architectures with pipelined processing and memory organized in single-port banks if also proposed in [2].

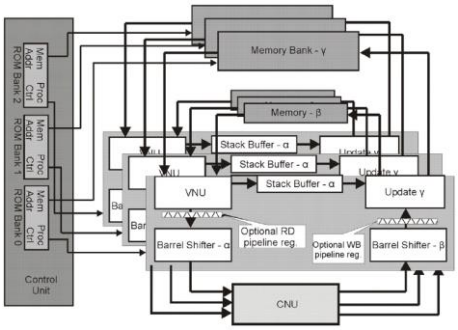

Fig. 1: Generic layered QC-LDPC architecture with n=3 single port memory banks.

The proposed improvements have been assessed for both WiMAX and DVB-S2x codes, with coding rates varying from 1/2 to 5/6. Several values of the layered architecture parameters have been considered, including the parallelism degree at processing unit level (n_{banks}), the memory access and pipeline update delay ($n_{latency}$), and the maximum overlapping update sequence length (n_{Ω}) for the proposed residue-based layered decoding. According to our evaluation, the proposed solutions improve the hardware usage efficiency of the layered LDPC decoder by 3%-49% when only the off-line algorithms are employed, and by 16%-57% when both the residue-based layered architecture and the off-line algorithms are used.

Implementation results are presented in Table I for various parameters of the layered architecture and proposed residue-based layered decoding. Throughput to Area Ratio (TAR) is the ratio between the throughput and the implementation cost expressed in slices. The implementation results show that the residue based layered scheduling decoder implementations (corresponding to $n_{\Omega} > 0$) have a superior TAR in spite of additional register files and pipelining implementation cost overhead. It is worth noting that the architecture we employ has a wide range of features that allow a high degree of flexibility: reversed write-back policy, generic barrel shifters for routing, as well as generic parallelization degree at processing unit level.

Table I: Implementation results for WiMAX and DVB codes

Decoder	$\langle n_{banks}, n_{latency}, n_{\Omega} \rangle$						
	$\langle 3,2,0 \rangle$	$\langle 5,2,0 \rangle$	$\langle 5,3,1 \rangle$	$\langle 3,4,\infty \rangle$	$\langle 5,4,\infty \rangle$	$\langle 5,2,0 \rangle$	$\langle 5,4,\infty \rangle$
Code size[bit]	2304 (WiMAX rate 3/4)					64800	
Device	Virtex-7 VC707 (xc7vx485tffg1761-2)						
Slices	8576	13070	16938	12496	18748	55511	59874
Slice regs.	15543	17017	26706	26925	35013	76008	112613
Slice LUTs.	29688	46136	59952	40700	63832	188145	198810
No. BRAMs	40.5	67.5	67.5	40.5	67.5	252.5	252.5
f_{max}[Mhz]	90.9	75.1	95.2	142.8	125	45.5	80
n_{iter}	10						
I_G[cc]	33	21	22	31	22	189	173
T[Mbps]	634.7	824.9	997	1061.7	1309	1525.7	2996.5
T^N[Gbps]	6.34	8.24	9.97	10.77	13.09	15.26	29.96
TAR[Mbps/slices]	0.74	0.63	0.58	0.84	0.69	0.27	0.50

Perspectives

Proposed solutions to high-throughput LDPC decoding stand out as suitable candidates for the new generation of communication systems, expected to reach Tbit/s over wireless links. The impact of the proposed solutions for ASIC designs will be investigated in future works.

RELATED PUBLICATIONS:

[1] O. Boncalo, G. Kolumbán-Antal, A. Amaricai, V. Savin, and D. Declercq, "Layered LDPC Decoders with Efficient Memory Access Scheduling and Mapping and Built-in Support for Pipeline Hazards Mitigation", *IEEE Transactions on Circuits and Systems I: Regular Papers*, accepted for publication.

[2] O. Boncalo, G. Kolumbán-Antal, D. Declercq, and V. Savin, "Code-design for efficient pipelined layered LDPC decoders with bank memory organization", *Microprocessors and Microsystems, Elsevier*, vol. 63, pp. 216-225, September 2018.

ENHANCED DECODING OF MULTILEVEL POLAR CODED MODULATION

RESEARCH TOPIC:

TELECOM (Polar codes, multilevel coded modulations)

AUTHORS:

Ludovic Chandesris, Valentin Savin

ABSTRACT:

This work investigates a new approach to decoding (higher order) multi-level polar coded modulations. We show that the structure of Successive Cancellation based polar decoders, can be efficiently exploited to improve the decoding performance. The proposed lasting decoders work continuously along all the bit-levels of the coded modulation. At the cost of a slight increase of the complexity, these decoders offer significantly better performance, and make the rate-allocation problem very simple. Finally, it is shown that multi-level polar coded modulations offer a clear advantage as compared to bit-interleaved polar coded modulations.

SCIENTIFIC COLLABORATIONS: ENSEA, Cergy-Pontoise (France)

Context and Challenges

Bit-Interleaved Coded Modulation (BICM) and Multilevel Coded Modulation (MLCM) are known as the two main approaches for higher-order coded modulations. While from an information theory perspective, MLCM provides the optimal combination of binary coding and higher order modulation, it requires the use of a wide range of coding rates, which in turn results in a difficult joint rate allocation and code optimization problem. Nevertheless, with polar codes, this “rate-allocation” task is no longer obstacle, as it can be efficiently solved by density evolution, and it has been shown that MLCM provides an advantage with respect to BICM under Successive Cancellation (SC) decoding. In this paper, we investigate the use of more powerful polar decoders and show that their structure can be efficiently exploited to improve the decoding performance.

Main Results

We define a lasting strategy for SC-based decoders, such as SC-List or SC-Flip, where the decoding process works continuously along all the bit-levels [1]. The proposed lasting SC-List decoder (illustrated in Fig. 1), propagates the decoding paths from one bit-level to the next one, thus increases the probability for the correct path to be kept in the list. As a result, the decoding of the higher bit-levels may impact the decisions taken on previous bit-levels. Similarly, a lasting Dynamic-SC-Flip (D-SC-Flip [2]) decoding can also be applied to MLCM in a very natural way.

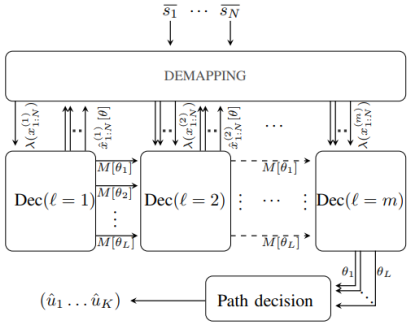

Fig. 1: Lasting SC-List decoding in MLCM

Moreover, in case of Cyclic Redundancy Check (CRC) assisted decoding, lasting decoders requires only one global CRC code, instead of one CRC per bit-level. We show in [1] that this allows increasing the decoding performance (due to higher number of frozen bits), while the rate allocation and code construction problem can effectively be solved by using density evolution.

Fig. 2 compares the different decoding strategies in MLCM and BICM. We consider an Additive White Gaussian Noise (AWGN) channel, with 16-Quadrature Amplitude Modulation (QAM). The number of coded QAM symbols is fixed to N = 256, and the coding rate is 1/2. It can be seen that the MLCM setup provides a significant advantage over BICM, under SC decoding. Moreover, this advantage is maintained under more powerful decoders, as SC-List and D-SC-Flip, when their lasting version is used. The D-SC-Flip employs a CRC of 16 bits and the number of additional attempts is fixed to T = 10, while the CRC Assisted (CA)-SCL has a list of size L = 8 and a CRC of 8 bits. Thus, MLCM offers a clear advantage with the powerful lasting CA-SCL decoder as well as with the low complexity lasting D-SC-Flip decoder.

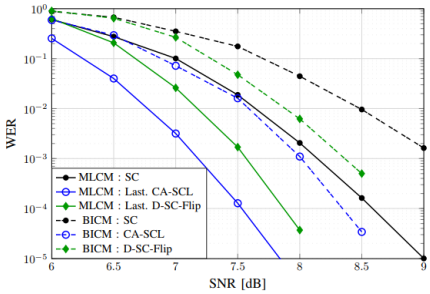

Fig. 2: Different decoding strategies in MLCM vs BICM

Perspectives

We have shown that the sequential nature of polar decoders can be effectively exploited to build lasting decoders, significantly outperforming the conventional MLCM decoding strategy. Future work will investigate the use of lasting decoders under probabilistic constellation shaping, known to allow a significant capacity increase over conventional modulation schemes.

RELATED PUBLICATIONS:

[1] L. Chandesris, V. Savin, and D. Declercq, “Lasting Successive-Cancellation based Decoders for Multilevel Polar Coded Modulation”, *IEEE International Conference on Telecommunications (ICT)*, Saint-Malo, France, June 2018.

[2] L. Chandesris, V. Savin, and D. Declercq, “Dynamic-SCFlip Decoding of Polar Codes”, *IEEE Transactions on Communications*, vol. 66, no. 6, 2018.

SUB-THZ SPECTRUM AS ENABLER FOR ULTRA-HIGH SPEED WIRELESS NETWORKS

RESEARCH TOPIC:
B5G, Thz/Tbps, PHY layer

AUTHORS:
Bicaïs Simon, Doré Jean-Baptiste

ABSTRACT:
The radio spectrum above 90 GHz offers opportunities for huge signal bandwidths, and thus unprecedented increase in the wireless network capacity, beyond the performance defined for the 5G technology. Today this spectrum is essentially exploited for scientific services, but attracts much interest within the wireless telecommunications research community, following the same trend as in previous network generations. The aim of our work is to elaborate new waveforms able to efficiently operate in the 90–300 GHz spectrum. The researches rely on three complementary works: the definition of relevant communication scenarios (spectrum usage, application, environment, etc); the development of realistic models for the physical layer (propagation channel and RF equipment's); and the elaboration of efficient modulations.

Context and Challenges
In this work, we introduce and evaluate new radio technologies that would operate in the 90-200 GHz spectrum. The migration of 5G networks towards radio access systems that support several hundreds of Gbit/s is envisaged for the future generation of wireless technologies [1]. Ultimate goal is the definition of a solution that would reach 1 Tbit/s. Taking into account the adversary nature of a communications channels in frequencies above 90 GHz, we focus on scenarios in which the connected nodes (end user, relay, access point, gateway) are in line-of-sight (LoS) or nearly LoS (i.e. only light obstruction). We propose to revisit the PHY-layer by looking back on single-carrier (SC) modulations, thus allowing for improved spectral efficiency and reduced power consumption (i.e. from lower PAPR). Indeed, LoS transmission and the use of very directive antennas make the propagation channel favorable to SC. Besides, the propagation and RF impairments at frequencies above 90 GHz are investigated and modelled. This will serve three objectives: 1) implement realistic link and system-level simulators; 2) design the new air interface based on well-understood physical constraints; 3) evaluate and demonstrate B5G scenarios.

Main Results
We address the design of optimum receivers affected by phase noise [2] [3]. We first derive the optimum decision metric for symbol detection under the assumption of a Gaussian phase noise and a high signal-to-noise ratio. The modeling of phase noise (PN) through the Gaussian distribution is mathematically convenient and thus often exploited to pursue simple analytical analyses. In fact, it appears to be an appropriate PN model for mm-wave systems. When considering wide bandwidth systems, the oscillator noise floor represents the greatest contribution to the overall PN. In contrast to state-of-the-art approaches, we propose to represent the demodulation over the phase noise channel within a complete metric space. The provided framework enables us to propose a simple detection metric achieving optimum detection performances. Upon the proposed metric, we derive computable probabilistic demapper values to exploit state-of-the-art channel decoding algorithms [2] [3]. Computable probabilistic demapper values cannot be defined from existing literature's metrics. It has been shown that the proposed polar metric, in comparison to the usual Euclidean distance, leads to performance gains for coded systems (see Fig 1). Eventually, we propose the necessary channel estimation scheme to perform the proposed demodulation. This work shows that knowledge of the channel statistics can be capitalized to enhance performance of both coded and uncoded systems.

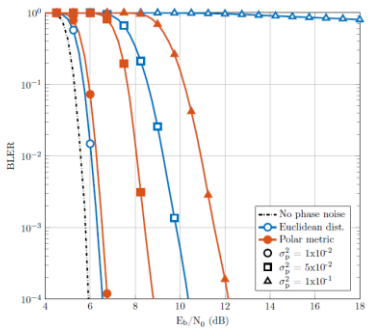

Fig. 1: Comparison of a LDPC coded 16-QAM performance exploiting LLR based either upon the Euclidean distance or on the polar metric.

Perspectives
Preliminary results have demonstrated the benefits of designing dedicated signal processing for sub-THz channels. Tough conventional modulation schemes present very poor performances for such channels. Therefore, we are currently addressing the problem of designing robust communications impaired by phase noise. This should be broken down into two questions: how signal constellations can be optimized for phase noise? How RF architectures may be adapted for sub-THz applications? The ambition is to propose new modulation schemes and RF architectures to enable robust communications in a wide range of scenarios adapted to sub-THz spectrum.

RELATED PUBLICATIONS:
[1] J. Doré et al., "Above-90GHz Spectrum and Single-Carrier Waveform as Enablers for Efficient Tbit/s Wireless Communications," 2018 25th International Conference on Telecommunications (ICT), St. Malo, 2018, pp. 274-278.
[2] S. Bicaïs, J. Doré and J. L. Gonzalez Jimenez, "On the Optimum Demodulation in the Presence of Gaussian Phase Noise," 2018 25th International Conference on Telecommunications (ICT), St. Malo, 2018, pp. 269-273.
[3] S. Bicaïs, J. Doré and J. Luis Gonzalez Jimenez, "Adaptive PSK Modulation Scheme in the Presence of Phase Noise," 2018 IEEE 19th International Workshop on Signal Processing Advances in Wireless Communications (SPAWC), Kalamata, 2018, pp. 1-5

PROACTIVE COMPUTATION CACHING POLICIES FOR 5G-AND-BEYOND MOBILE EDGE CLOUD NETWORKS

RESEARCH TOPIC:
5G, multi-access edge cloud, caching

AUTHORS:
Nicola di Pietro and Emilio Calvanese Strinati

ABSTRACT:
Computation caching is a novel strategy to improve the performance of computation offloading in mobile edge cloud networks. It consists in storing in local memories situated at the edge of the network the already processed results of popular computational tasks that users offload to the mobile edge cloud. The goal is to avoid redundant and repetitive processing of the same tasks, thus streamlining the offloading process and improving the exploitation of resources. Here, three computation caching policies are evaluated and compared. They are based on the popularity of offloadable tasks, the size of their inputs, and the size of their results. We show how combining together those three parameters is effective to design well-performing computation caching policies.

Context and Challenges
In multi-access edge cloud networks, Serving Small Cells (SSCs) endowed with radio access technology, computing units, and local cache memories are charged by User Equipments (UEs) to run computational tasks on their behalf. This procedure is called *computation offloading* [4]. In this context, the paradigm of *computation caching* was recently introduced [1], [2], [3]. It exploits the SSC's memory to store the results of offloadable computations, so that they can be simply retrieved from the cache instead of being recomputed each time they are requested. Thus, redundant and repetitive processing is decimated, with several advantages: drastically reducing computation time, saving energy for both UEs and SSCs, etc. Here, we compare three different computation caching metrics. The important novelty is the introduction of a policy [1] that simultaneously takes into account three different characterizing parameters of an offloadable task: its popularity, the size of its input, and the size of its result.

Main Results
The cost of task offloading includes: i) the cost of uploading the computation inputs from the UE to the SSC; ii) the cost of executing the computation at the SSC. Depending on the application, "cost" can mean energy consumption, time delay, etc. Whenever a pre-computed task result is cached, the task itself does not need to be run at the SSC and its input does not need to be uploaded by the UE. Consequently, the two cost components mentioned above are zeroed. To maximize this cost reduction for a given fixed list of tasks, a caching policy is by definition a rule to decide which task results to cache in the (finite) memory available at the SSC. To do so, a "cacheability" metric μ is assigned to each task and a caching policy consists in caching the results of the tasks with the highest μ, until the cache is full. We compared the outcomes of three metrics:
i) $\mu = p$ [3], ii) $\mu = p * I$ [2], iii) $\mu = p * I/O$ (novel metric [1]), where p is the popularity of a task, I is its input's size (in bits), and O is its result's size (in bits). Our numerical results, based on Zipf popularity patterns [1], show that the third metric significantly improves the effectiveness of computation caching.

Figures are plotted as a function of the SSC's cache size, expressed as a percentage of the total cacheable data. The first figure shows the percentage of task input data that does not need to be neither uploaded to nor elaborated at the SSC, because the corresponding results were cached and already available for downloading. This corresponds to a cost reduction, both for the UE and for the SSC. The second figure, instead, shows the ratio between the average number of offloaded tasks per hour with and without computation caching. In both simulations, the third metric yields the best numerical results.

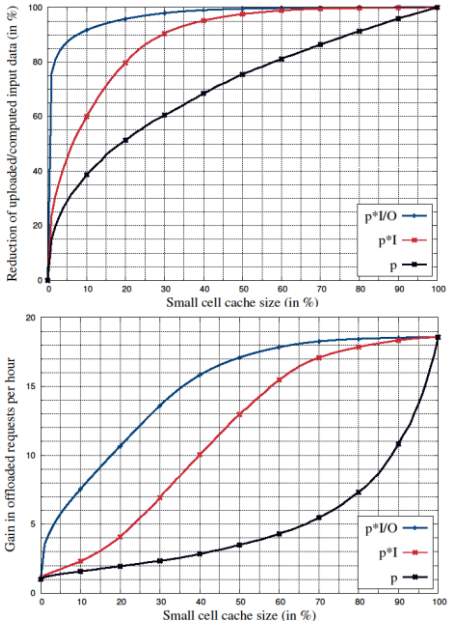

Perspectives
Future developments of this work will focus on its extension to more complex scenarios, involving more UEs and cooperating small cells with embedded intelligence.

RELATED PUBLICATIONS:
[1] N. di Pietro, E. Calvanese Strianti, "Proactive computation caching policies for 5G-and-beyond mobile edge cloud networks," in Proc. EUSIPCO, Rome, Italy, 2018.
[2] J. Oueis, E. Calvanese Strinati, "Computation caching for local cloud computing," presented at WCNC, 5G TACNET Workshop, San Francisco, USA, 2017.
[3] M. S. Elbamby, M. Bennis, and W. Saad, "Proactive edge computing in latency-constrained fog networks," in Proc. EuCNC, Oulu, Finland, 2017.
[4] S. Wang, X. Zhang, Y. Zhang, L. Wang, J. Yang, and W. Wang, "A survey on mobile edge networks: Convergence of computing, caching and communications," IEEE Access, vol. 5, pp. 6757-6779, 2017.

AN ARTIFICIAL INTELLIGENCE FRAMEWORK FOR SLICE DEPLOYMENT AND ORCHESTRATION IN 5G NETWORKS

RESEARCH TOPIC:

5G, Artificial Intelligence, Resource Management, Unsupervised Learning, Reinforcement Leaning

AUTHORS:

Ghina Dandachi and Antonio De Domenico

ABSTRACT:

Network slicing is a key enabler to successfully support 5G services with specific requirements and priorities. In this paper, we propose an Artificial Intelligence (AI) framework for cross-slice admission and congestion control that considers communication, computing, and cloud storage resources with the aims of optimizing resources utilization and maximizing the operator revenue. The proposed reinforcement learning algorithm offers outstanding advantages over traditional static and optimization-based approaches by automatically adapting the controller decisions to the system changes.

SCIENTIFIC COLLABORATIONS: UNIVERSITY OF TECHNOLOGY SYDNEY, AUSTRALIA, NANYANG TECHNOLOGICAL UNIVERSITY (NTU), SINGAPORE

Context and Challenges

To efficiently support use cases with heterogeneous requirements, the 5G systems will deploy a novel architecture where the network infrastructure is logically split into different instances, i.e., network slices, each designed for a specific service and running in the cloud environment. In this context, depending on the network load and service requirements, the 5G systems will need to manage communication and cloud resources smartly. Moreover, it is necessary to take into account the priorities and constraints of different slice requests. Then, we propose a new architecture for joint cross-slice admission control and congestion control to maximize the operator revenues while considering different slice types and resource requirements.

Main Results

In this work, we classify the slice requests into two types, i.e., guaranteed quality-of-service (GS) and best effort (BE) according to the associated requirements. Then, we introduce a cross-slice Admission Control (AC) that optimizes the trade-off between resource utilization and slice dropping probability [1]. We also introduce a cross-slice Admission and Congestion Control (CSACC) that limits the dropping of slice requests, especially when the system becomes overloaded [2]. The CSACC can scale down resources allocated to slices with low priorities, so that slices with high priorities can be admitted. Both the AC and the CSACC are based on SARSA, a well-known online reinforcement-learning algorithm, aiming to find a stationary policy that associates a given system state with a proper action such that the expected aggregated reward is maximized. In this case, the reward is related to the revenues that an operator perceives when is able to deploy a new service through its network. Although the reinforcement learning model can be successfully used to address small-scale problems, it becomes impractical in realistic cases, as computational requirements of reinforcement learning grow exponentially with the number of state variables.

We have also designed a Slice Analytics (SA) function, which attempts to assign a new slice request to an existing network slice instance in order to maximize the resource sharing across slices and accelerate the slice deployment [2]. Fig. 1 shows the average reward (in terms of accepted slices) obtained by our system when using these strategies. We can notice that the CSACC leads to a large reward gain as compared to the AC for low values of GS request arrival probabilities. In contrast, the gain brought by the SA increases with the GS request arrival probability. Moreover, we observe that when using CSACC with SA, the reward gain with respect to the simple AC is larger than the sum of the gains lead by each single strategy. This gain is due to the large reduction in the BE dropping probability.

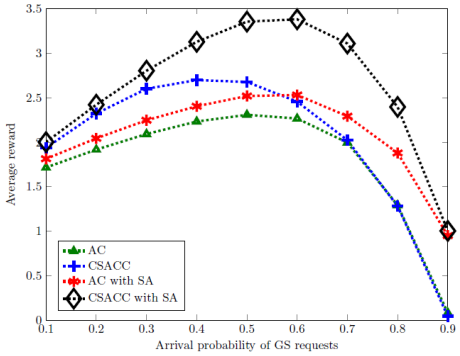

Fig. 1: Average reward for different schemes as a function of the GS arrival probability.

Perspectives

In future studies, we will focus on a system dealing with slice requests characterized by more heterogeneous requirements and priorities. Moreover, we will investigate how to optimize the sizing of the system, in terms of required resources, such that the slice dropping probability is further minimized.

RELATED PUBLICATIONS:

[[1] D. T. Hoang, D. Niyato, P. Wang, A. De Domenico, and E. Calvanese Strinati, “Optimal Cross Slice Orchestration for 5G Mobile Services,” Proc. IEEE VTC Fall, Aug. 2018.

[2] G. Dandachi, A. De Domenico,D. T. Hoang, and D. Niyato, "An Artificial Intelligence Framework for Slice Deployment and Orchestration in 5G networks," submitted to IEEE JSAC SI on Machine Learning in Wireless Communication

OPTIMAL VIRTUAL NETWORK FUNCTION DEPLOYMENT FOR 5G NETWORK SLICING IN A HYBRID CLOUD INFRASTRUCTURE

RESEARCH TOPIC:

5G, Network virtualization, Resource Management,

AUTHORS:

Antonio De Domenico

ABSTRACT:

Network virtualization is a key enabler for the 5G systems for supporting the novel use cases related to the vertical markets. In this context, we investigate the joint optimal deployment of Virtual Network Functions (VNFs) and the allocation of computational resources in a hybrid cloud infrastructure by taking into account the requirements of the 5G services and the characteristics of the cloud nodes. To achieve this goal, we analyze the relations between functional placement, computational requirements, and latency constraints, and formulate an integer linear programming problem, which can be solved by using a standard solver.

SCIENTIFIC COLLABORATIONS: Department of Electrical and Computer Engineering, University of Toronto, Toronto, Canada, Chinese Academy of Sciences, Beijing, China,

Context and Challenges

A network slice is composed of a chain of Virtual Network Functions (VNFs), which represent the software implementation of the traditional network functions (NFs), such as coding/encoding, and can be efficiently reconfigured through the ETSI MANO and NFV frameworks. In contrast to all previous works, our analysis takes into account the type of mobile service associated with each network slice as well as the different requirements of the related VNF chains. Then, we propose a framework for jointly optimizing the computational resource allocation and the deployment of VNF chains with heterogeneous requirements. This optimization is done in a hybrid cloud infrastructure composed by edge clouds and central cloud with different capacities and latencies. [1,2]

Main Results

We consider the scenario with a mix of VNF chains: mMTC, eMMB, and two URLLC services. We compare the performance of the optimal deployment scheme with two baseline solutions denoted as fixed split and fixed service. In the first solution, the VNFs of each chain, independently of the type of service, are split in the same manner. Specifically, the VNFs up to the lower MAC, which have stringent latency and computational requirements, are deployed in the edge cloud, while the other VNFs are instantiated in the central cloud. In contrast, in the fixed service scheme, the chains with largest computational requirements are deployed at the central cloud, while the chains with the most stringent latency constraints are allotted to the edge cloud. In Fig. 1, we can observe the maximum number of slices that can be deployed on the cloud Infrastructure, when using the proposed solution and the baseline schemes, for different distances of the central cloud from the access network. We can see that the proposed optimal scheme greatly enhances the number of VNFs chains that can be successfully deployed with respect to the two static solutions, even when the central cloud is located near the edge cloud. Specifically, for a distance of 30 km, the optimal solution leads to a gain of 37.5% and 120% in terms of the number of deployed chains. These gains further increase when the distance between the central cloud and the edge cloud increases. Overall, we can observe that when the number of VNF chains (or equivalently the distance of the central cloud and the edge cloud) increases, the proposed scheme brings the desired flexibility to balance the cloud load (i.e., moving VNFs from one cloud to another) and make computational resources available for the chains with more stringent requirements.

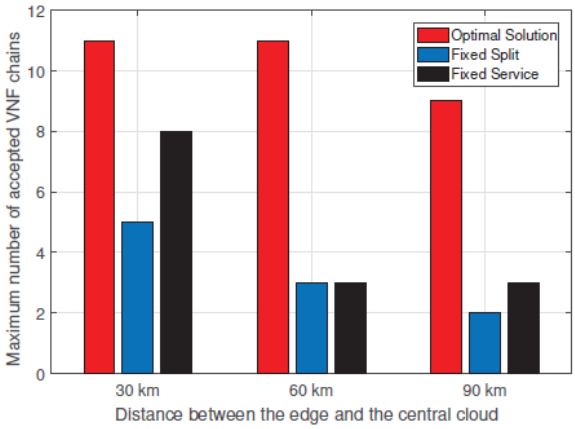

Fig. 1: Maximum number of accepted VNF chains as a function of the distance between the edge cloud and the central cloud.

Perspectives

In future works, we shall consider dynamic settings, where AI based solutions learn the trends of the computational requests, and proactively distribute the requests through the clouds, in order to prevent service outage.

RELATED PUBLICATIONS:

[[1] A. De Domenico, Y.-F. Liu, and W. Yu, "Optimal computational resource allocation and network slicing deployment in 5G hybrid C-RAN," IEEE ICC, May 2019
[2] A. De Domenico, Y.-F. Liu, and W. Yu, "Optimal Virtual Network Function Deployment for 5G Network Slicing in a Hybrid Cloud Infrastructure," submitted to IEEE JSAC.

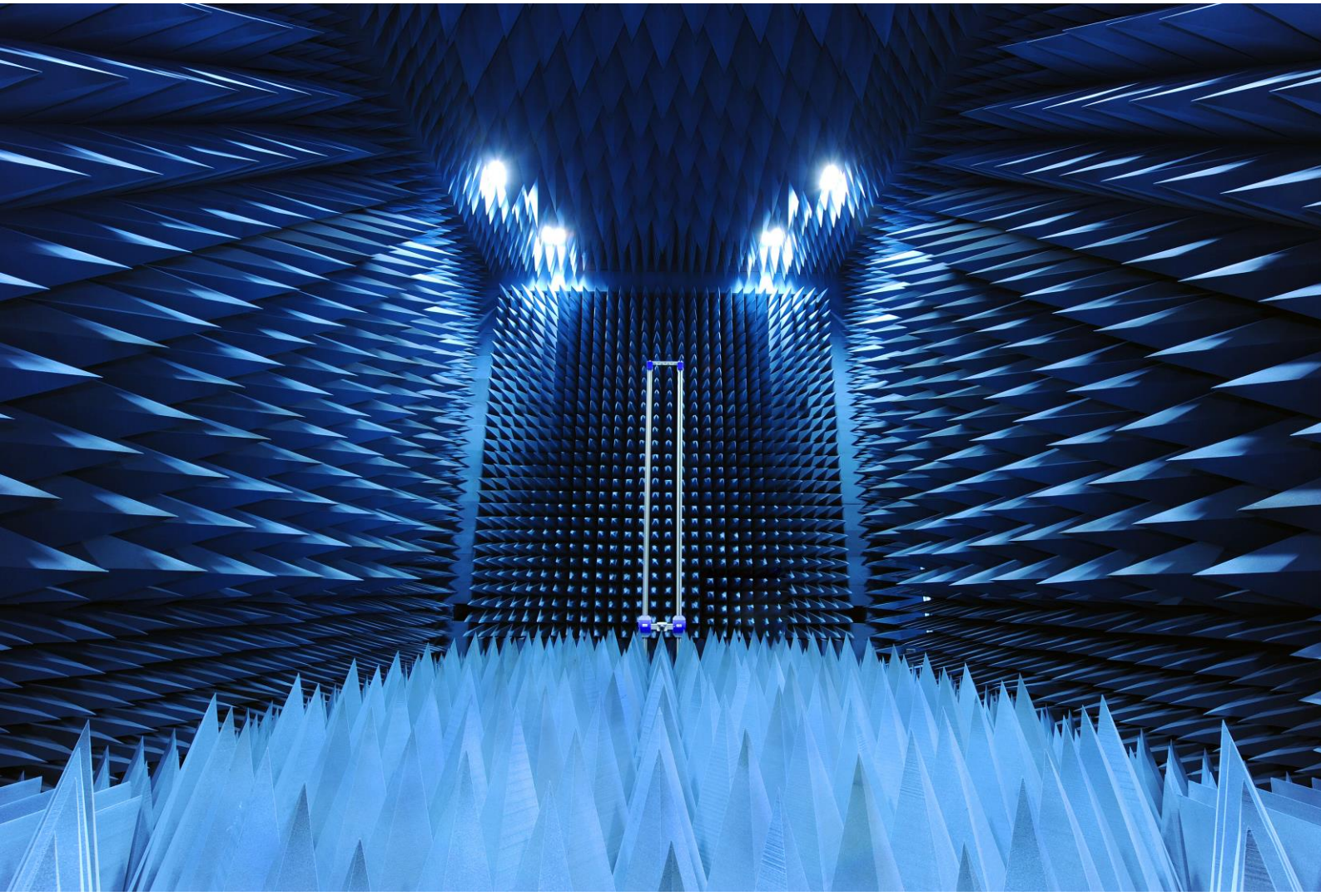

04 ANTENNAS AND PROPAGATION

- **Antennas Design, Characterization and Experimentation**
- **Reconfigurable Transmit Array**
- **Low Profile Antennas**
- **Channel Modelling**
- **Environment Mapping**

A VERY HIGH BIT RATE BIDIRECTIONNAL COMMUNICATION AT 13.56 MHZ FOR CONTACTLESS SYSTEMS

RESEARCH TOPIC:
RFID, Very High Bit Rate, ISO14443

AUTHORS:
M. Descharles, J. Reverdy, T. Thomas, A. Faucon, H. Glodkowski, E. Blanchard

ABSTRACT:
This paper presents a very high bit rate bidirectionnal communication at 13.56 MHz for contactless systems such as medical implants or remote sensors. The tag RFID front-end is a CEA chip that integrates a phase demodulator. The communication from the reader to the tag is achieved with a bit rate up to 10.17 Mbits/s using phase modulation and thanks to new modulator and power generator architectures. From tag to reader, a bit rate up to 3.39 Mbits/s is achieved using amplitude modulation (ISO14443). This high bit rate birectionnal communication allows RFID tag to embed more features as sensors or actuators.

SCIENTIFIC COLLABORATIONS: Clinatec

Context and Challenges
The need of RFID smart applications such as e-passports, NFC, medical implant, payment or remote sensors continuously increases. Personal information exchanged (biometrical data, payment data etc..) need a higher level of security which increase the transferred data. Telemetry, measurement and data recording (sensor tags, medical implant) also contribute to the growing amount of data. Remote sensors systems keep requiring more precision or more sensors, which lead again to a large increase of the amount of data. The transmission data rate has to be increased to allow more and more data to be transmitted. CEA has worked on a bidirectional RFID communication at 13.56 MHz that could be used in medical implants.

Main Results
The communication from reader to tag is achieved using phase modulation as specified in ISO14443. It has been shown [1] that phase modulations for VHBR can be robust even if the quality factor of the antenna is high. The phase modulation is realized with a comparison between a 13.56 MHz sinusoid and thresholds computed by the FPGA. The modulated signal drives a specific power stage that comprises two identical N-MOS and a balun Guanella structure. This "D-class" architecture offers more robustness and dynamic [2].

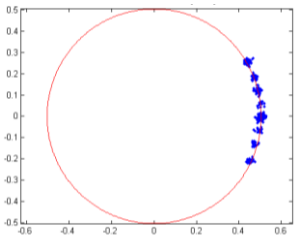

Fig. 1. Filter output emitted PSK constellation at 10.17 Mbits/s

The tag embeds an analog front-end chip designed by the CEA, a low-power FPGA and a microcontroller that are remote power-supplied by the RF field from the reader.
The RFID front-end handles a patented phase demodulator with a 307ps (1.5°) resolution [3] which allows an uplink communication from reader to tag up to 10.17 Mbits/s. This result has been achieved without any predistorsion or equalization algorithm.
The communication from the tag to the reader uses amplitude modulation specified in ISO14443. The CEA-LETI tag front-end can retromodulate the RF field at 3.39 Mbits/s. The demodulation on the reader is done by a marketed chip (ST25R3911).

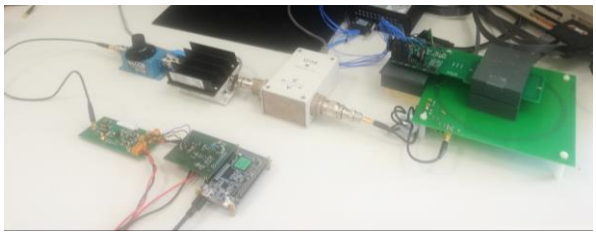

Fig. 2. Photograph of the global system: emitter and receiver (10.17 Mbits/s uplink and 3.39Mbits/s downlink)

Perspectives
A new optimized antenna system is currently under analysis. It should allow the best compromise between bandwidth and power transmission. This novel antenna design should also provide a live channel estimation and then allow the implementation of a predistorsion algorithm in the reader processor. A predistorsion algorithm in the reader avoids equalization in the chip [4] which consumes volume and energy.

RELATED PUBLICATIONS:
[1] Berg V., Doré JB., Frassati F., "ISO/IEC 14443 VHBR: unfluence of the proximity antennas on the PCD-to-PICC data link performance", International EURASIP Workshop on RFID Technology, 2015
[2] Thomas T., Josselin V., "High-Frequency generator", Patent US9548706, 2017
[3] Lachartre D., "Demodulator and system for transmitting modulated informations, in particular for radio-frequency identification tag", Patent FR2945398, 2010
[4] Doré JB., Touati N., Pebay-Peroula F., "MLSE Detector for beyond VHBR contactless air interface", IEEE 2012 International conference on RFID - Technologies and Applications (RFID-TA), 2012

CIRCULARLY-POLARIZED TRANSMITARRAYS WITH FIXED BEAM AT KA-BAND

RESEARCH TOPIC:

Fixed-beam transmitarray, high-gain antennas, mmWave, SATCOM, 5G

AUTHORS:

Fatimata Diaby, Antonio Clemente, Kien Pham (IETR, UR1), Laurent Dussopt, Ronan Sauleau (IETR, UR1)

ABSTRACT:

This paper presents the simulation, optimization and demonstration of a collimated-beam and a quad-beam transmitarray operating at Ka-band. Both transmitarrays are based on a 3-bit unit-cell implementing both phase-shift and linear-to-circular polarization conversion functions. The collimated-beam transmitarray presents a measured gain of 33.8 dBi (corresponding to an aperture efficiency of 51.2%) and a 3-dB gain bandwidth larger than 15.9%. The quad-beam transmitarray phase distribution has been optimized by a genetic algorithm code coupled with an analytical tool. The array is designed to radiate four beams at $\theta_0 = \pm 25°$ in the horizontal and vertical planes at the frequency of optimization.

SCIENTIFIC COLLABORATIONS: IETR, University of Rennes 1 (UR1)

Context and Challenges

Transmitarrays or discrete lenses are an attractive antenna technology for a plethora of applications at microwave and millimeter-wave frequencies. In particular, they can be used to implement high-gain backhauling/fronthauling for 5G mobile networks at Ka- (24.25-27.5, 27.5-28.35 or 37-40 GHz), V- (66-76 GHz) and E-bands (71-76 and 81-86 GHz) or relatively low-cost SATCOM-on-the-move terminals at Ku- and Ka-bands.

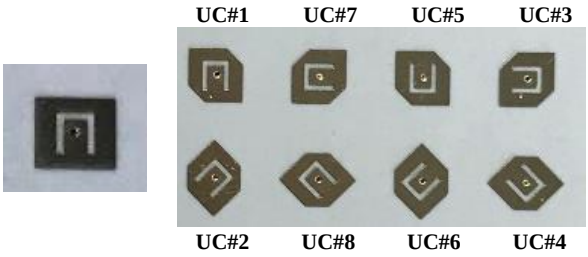

Fig. 1. Photographs of the proposed 3-bit unit-cell (UC) at Ka-band. (a) Bottom (Rx), and (b) top (Tx) patches.

Main Results

A collimated-beam and a quad-beam transmitarrays are presented and demonstrated here. Both antennas are based on a 3-bit circularly-polarized unit-cell [1]. The transmitting layer of the proposed unit-cell ensures phase-shift and polarization transformation at the same time (Fig. 1). The 1600-element square transmitarray (Fig. 2(a)) is illuminated by a 10-dBi linearly-polarized standard gain horn placed at a distance of 134 mm (corresponding to F/D = 0.67 and an edge taper illumination of about 10 dB) [2]. The 489-element circular quad-beam transmitarray (Fig. 2(b)) is optimized at 29 GHz using a genetic algorithm code coupled with our analytical simulation tool [2[,]3]. A measured gain of 33.8 dBi, an aperture efficiency of 51.2%, and a 3-dB gain bandwidth better than 15.9% have been obtained in the case of the focused-beam transmitarray.

Instead the quad-beam transmitarray is designed to radiate four simultaneous beams at $\theta_0 = \pm 25°$ with a gain around 18 dBi.

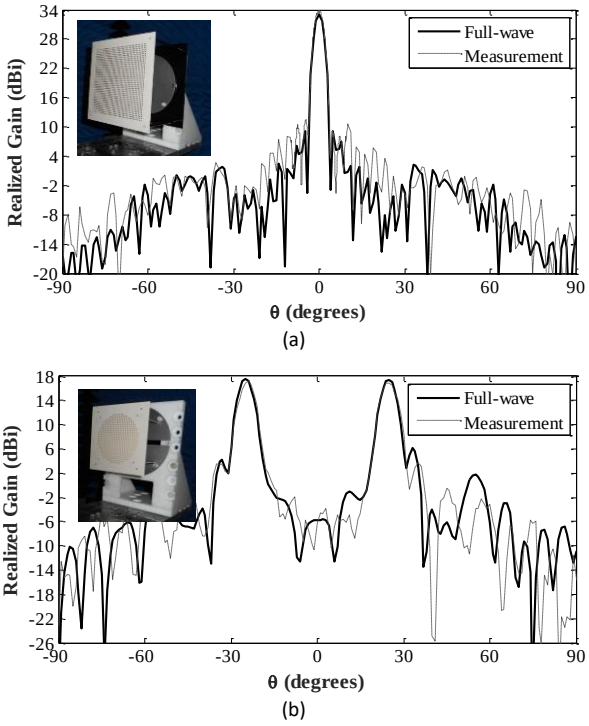

Fig. 2. Measured and simulated gain radiation patterns of the (a) focused-beam and (b) quad-beam transmitarrays.

Perspectives

Dual-band and dual circularly-polarized transmitarray with low-profile topology will be designed in the future.

RELATED PUBLICATIONS:

[1] F. Diaby, A. Clemente, L. Di Palma, L. Dussopt, K. Pham, E. Fourn, and R. Sauleau, "Wideband circularly-polarized 3-bit transmitarray antenna in Ka-Band," in *Proc. 11th European Conf Antennas Propag.* (EuCAP 2017), 2017.

[2] F. Diaby, A. Clemente, K. Pham, R. Sauleau, and L. Dussopt, "Circularly-polarized transmitarray antennas at Ka-band," IEEE *Antennas Wireless Propag. Lett.*, vol. 17, no. 7, pp. 1204-1208, Jul. 2018.

[3] F. Diaby, A. Clemente, K. Pham, R. Sauleau, and L. Dussopt, "Synthesis and experimental characterization of a single-feed quad-beam circularly-polarized transmitarray at Ka-band," *39th ESA Antennas Workshop*, 2018.

ELECTRONICALLY RECONFIGURABLE 2-BIT UNIT-CELL AND STEERABLE TRANSMITARRAY AT KA-BAND

RESEARCH TOPIC:

Transmitarray antennas, electronically reconfigurable antennas, beamforming, beam steering, 5G, SATCOM

AUTHORS:

Fatimata Diaby, Antonio Clemente, Laurent Dussopt, Ronan Sauleau (IETR, UR1), Kien Pham (IETR, UR1)

ABSTRACT:

This paper presents the design, optimization, fabrication and experimental characterization of an electronically steerable transmitarray with 2 bits of phase quantization per unit cell. The proposed transmitarray operates in linear polarization at Ka-band and is composed of 14×14 reconfigurable unit-cells. The transmitarray is realized in standard Printed Circuit Board technology considering a six-metal layer dielectric stack-up. Four p-i-n diodes are integrated on each unit-cell to control the radiated field phase distribution across the transmitarray aperture. The prototype demonstrates experimentally pencil beam scanning over a 120×120-degree window, a maximum gain at broadside of 19.8 dBi, and a 3-dB fractional bandwidth of 16.2%.

SCIENTIFIC COLLABORATIONS: IETR, University of Rennes 1 (UR1)

Context and Challenges

The demonstration of relatively low-cost and innovative antenna technologies for user terminals with electronically beam-steering capabilities is a key element in the development of the future Internet of Space (IoS) and 5th Generation (5G) mobile terrestrial network ecosystems. In this context, satellite constellations and communication systems operating at Ka-band play a fundamental role to increase the system bandwidth and consequently the achievable data rate.

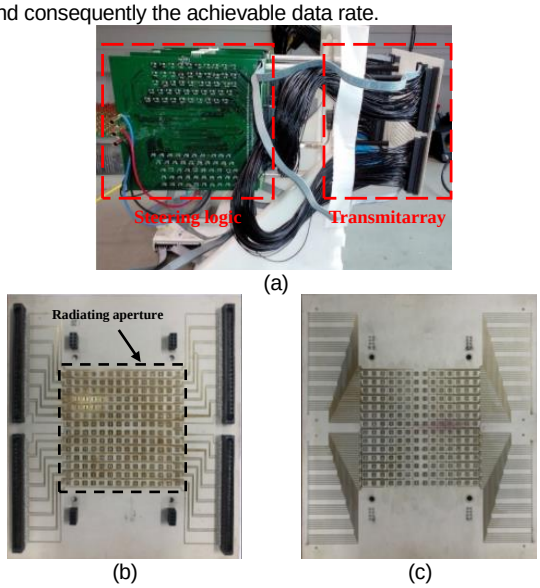

Fig. 1. Photograph of the realized linearly polarized reconfigurable 2-bit transmitarray at Ka-band.

Main Results

Thanks to their spatial feeding architecture and the possibility to control easily the phase distribution on the array aperture [1], transmitarrays (TAs) are excellent alternatives for beam steerable applications. A TA is typically composed of one or several focal sources illuminating an array of unit-cells (flat lens). Each unit-cell consists of a first antenna array working in receive mode and connected (through phase shifters) to a second array working in transmission mode. Here a 2-bit electronically reconfigurable unit-cell and TA prototype are presented at Ka-band (Fig. 1). The proposed antenna is based on the reconfigurable unit-cell architecture previously reported in our conference work [2]. To the best of our knowledge, the TA prototype described here is one of the largest (14×14 unit-cells) 2-bit electronically-reconfigurable TA presented in the open literature at Ka-band, and its radiation efficiency is among the highest reported so far (around 48%). The excellent scanning capabilities of the antenna are demonstrated up to 60° in E- (and H-) planes in Fig. 2 [3]. The scan loss at ±60° reaches about 5 dB due to the gain variation of the unit-cell radiation pattern for the same angular range.

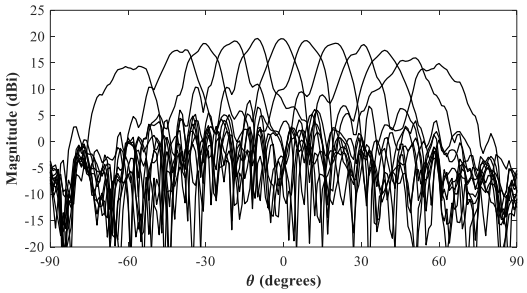

Fig. 2. Measured scanning capability of the proposed antenna at Ka-band.

Perspectives

The realized TA is based on a single focal feed including a 10-dBi gain horn. This horn is located at a distance 48 mm from the array, which corresponds to an F/D ratio of 0.67. Innovative architecture for ultra low-profile TAs are under development.

RELATED PUBLICATIONS:

1] L. Di Palma, A. Clemente, L. Dussopt, R. Sauleau, P. Potier, and P. Pouliguen, "Circularly-polarized reconfigurable transmitarray in Ka-band with beam scanning and polarization switching capabilities," *IEEE Trans. Antennas Propag.*, vol. 65, no. 2, pp. 529-540, Feb. 2017.

[2] F. Diaby, A. Clemente, L. Di Palma, L. Dussopt, K. Pham, E. Fourn, and R. Sauleau, "Design of a 2-bit unit-cell for electronically reconfigurable transmitarrays at Ka-band," in Proc. *European Radar Conf. (EuRAP 2017)*, Nuremberg, Germany, 11-13 Oct. 2017.

[3] F. Diaby, A. Clemente, R. Sauleau, K. Pham, and L. Dussopt, "Electronically-steerable transmitarray at Ka-band with 2 bits of phase quantization," *39th ESA Antennas Workshop*, 2018.

EXPERIMENTAL CHARACTERIZATION OF A CIRCULARLY-POLARIZED 1-BIT UNIT-CELL FOR BEAM STEERABLE TRANSMITARRAYS AT KA-BAND

RESEARCH TOPIC:

Transmitarray antennas, mmWave, SATCOM, circular-polarization, waveguide simulator

AUTHORS:

Luca Di Palma, Antonio Clemente, Laurent Dussopt, Ronan Sauleau (IETR, UR1), P. Potier (DGA), and P. Pouliguen (DGA)

ABSTRACT:

We propose here an experimental characterization procedure applied to a 1-bit reconfigurable transmitarray unit-cell working in circular polarization at Ka-band. The transmission phase of the unit-cell is controlled on the receiving side by switching two p-i-n diodes integrated on the radiating element. The circular polarization is generated on the transmitting side with a truncated corner patch antenna. A specific waveguide characterization setup and related procedure have been developed to extract the unit-cell S-matrix. The proposed setup includes non-standard waveguide sections, ad-hoc transitions and an Ortho-Mode Transducer (OMT). The experimental results demonstrate a good agreement with full-wave simulations with a discrepancy of less than 0.1 dB on the measured minimum insertion loss of 1.65 dB at 29 GHz. A 3-dB bandwidth larger than 12% has been measured.

SCIENTIFIC COLLABORATIONS: IETR, University of Rennes 1 (UR1), DGA

Context and Challenges

Thanks to their spatial feeding architecture, printed transmitarrays (TAs) have been massively studied in the last years for applications up to the sub-millimeter-wave band. A TA is composed of a focal system illuminating an array of elements (unit-cells). Beam-forming functions can be easily implemented by electronically control the transmission phase of each unit-cell. Even if several high-performance fixed-beam TAs have been successfully demonstrated, only a few demonstrations of full electronically reconfigurable architectures have been presented in the open literature. In our recent paper [1], we implemented a circularly-polarized (CP) electronically reconfigurable TA based on a sequentially-rotated linearly-polarized (LP) 1-bit unit-cell [2] enabling simple polarization switching. This TA exhibits a significant directivity loss due to the generation of the circular polarization from the sequential rotation of orthogonal LP unit cells. Unit-cells working directly in circular polarization can be developed in order to improve aperture efficiency.

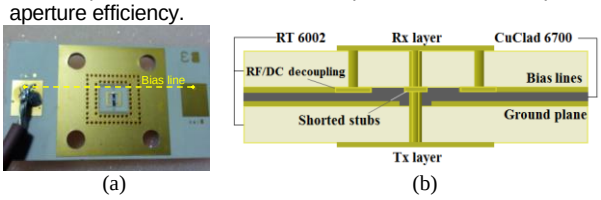

(a) (b)

Fig. 1. (a) Photographs of the fabricated CP electronically reconfigurable unit-cell. (b) Etched dielectric stack-up.

Main Results

In [3], we describe a CP electronically reconfigurable unit-cell (Fig. 1) and an experimental characterization procedure based on waveguide simulators (Fig. 2(a)). The proposed method allows to verify the transmitarray performance at unit-cell level during preliminary development phases (Fig. 2(b)). This enables to individuate possible issue and re-optimize the design without the need of manufacturing and anechoic chamber test of the whole TA panel that often consists of thousands of elements. The unit-cell operates at Ka-band (27.5 GHz - 31.0 GHz) and has been designed on the dielectric stack-up shown in Fig. 1(b). The receiving (Rx) layer is composed of a rectangular patch loaded by an O-shaped slot and two p-i-n diodes; this active patch is linearly-polarized. It is worth to notice that this choice allows the use of a simple and wideband LP focal source. In the transmitting layer (Tx), a square patch loaded by a U-shaped slot with truncated corners is designed in order to generate circular polarization. A 1-bit phase quantization is achieved by opportunely controlling the two diodes [2].

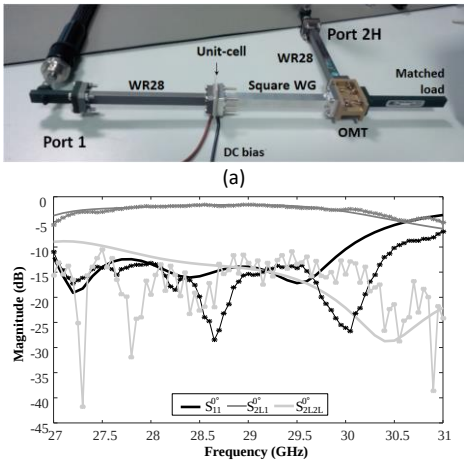

(a)

(b)

Fig. 2. (a) Photographs of the waveguide setup. (b) Magnitude of the simulated (line) and measured (line and symbols) scattering parameters of the reconfigurable unit-cell.

Perspectives

Dual CP unit-cells and TAs will be developed in the future.

RELATED PUBLICATIONS:

[1] L. Di Palma, A. Clemente, L. Dussopt, R. Sauleau, P. Potier, and P. Pouliguen, "Circularly-polarized reconfigurable transmitarray in Ka-band with beam scanning and polarization switching capabilities," *IEEE Trans. Antennas Propag.*, vol. 65, no. 2, pp. 529-540, Feb. 2017.

[2] L. Di Palma, A. Clemente, L. Dussopt, R. Sauleau, P. Potier, and P. Pouliguen, "1-bit reconfigurable unit-cell for Ka-band transmitarrays," *IEEE Antennas Wireless Propag. Lett.*, vol. 15, pp. 560-563, 2016.

[3] L. Di Palma, A. Clemente, L. Dussopt, R. Sauleau, P. Potier, and P. Pouliguen, "Experimental characterization of a circularly-polarized 1-bit unit-cell for beam steerable transmitarrays at Ka-band," *IEEE Trans. Antennas Propag.*, vol. 67, no. 2, pp. 1300-1305, Feb. 2019.

INDOOR ENVIRONMENT-ADAPTIVE MAPPING WITH BEAMSTEERING MASSIVE ARRAYS

RESEARCH TOPIC:
Radar, millimiter wave, massive array

AUTHORS:
Francesco Guidi, Andrea Mariani, Anna Guerra, Davide Dardari, Antonio Clemente, Raffaele D'Errico

ABSTRACT: Beamsteering massive arrays have been recently proposed for indoor environment mapping in next 5G scenarios, thanks to their capability to better penetrate materials with respect to current laser or vision-based systems. From the perspective of integrating radars in small portable devices, architectures based on non-coherent processing of raw measurements represent a viable solution to overcome the limitations of current indoor radio mapping techniques, which entail a too high processing or receiver complexity. Here, we investigate the capability of low-complexity mobile radars, equipped with mm-wave massive arrays, to adapt to the environment in order to reconstruct it, by adjusting a threshold with respect to the collected data and the radiation pattern. Measurement results show the effectiveness of the proposed approach.

SCIENTIFIC COLLABORATIONS: **UNIVERSITY OF BOLOGNA, ITALY**

Context and Challenges

The joint use of millimeter-waves (mm-wave) and massive arrays technologies has recently shown the capability to pack a large number of antennas onto a small area, thus paving the way for a future integration in next generation portable devices (e.g. 5G).
Thanks to the possibility to better penetrate materials than laser and vision-based systems, mm-wave massive arrays could be integrated into such systems. Towards this direction, devices moving in indoor environments could assist the user navigation even in scarce visibility conditions or could enable the creation of indoor maps, where Global Positioning System (GPS) fails, without exploiting signals coming from ad-hoc infrastructures

Main Results

In this work we introduced a new adaptive scheme for indoor environment mapping, not requiring a high complexity processing (as, for example, the CLEAN-inspired algorithms) that keeps the overall complexity as low as possible to ease the integration into portable devices.
The proposed approach first accounts for a traditional thresholding phase (*phase 1*) and, successively, for a new thresholding phase (*phase 2*) to mask unwanted side-lobe contributions.
This new thresholding strategy is able to adapt itself to the measured signals, overcoming the limitations mainly related to the need of having a-priori knowledge of the backscattering properties of the indoor environment.

To validate the previously described system, we now exploit as a case study the mm-wave measurement campaign. In particular, measurements were collected centered at 60 GHz with 6 GHz bandwidth, and transmitarrays (TAs) with 400 elements and only one bit for phase compensation were adopted. Such arrays represent a practical solution when array complexity has to be kept as low as possible while preserving good directional radiation properties. To meet the requirements of the considered mobile radar, 37 steering directions were considered ranging from −90° to +90° with a step of 5°. Measurements were conducted in two indoor environments, that is an office room and a corridor. They were chosen due to their different backscattering characteristics, since the room is dense of furniture, whereas the corridor can be considered as a furniture-free and tunnel-shaped environment, with a completely different geometry. In Fig. 1 we show the estimated map at the output of two phases. Results are collected from different radar position obtained by moving the radar of 0.5 m along the y-axe.
Thanks to the adaptive threshold, the similarity score is improved of approximately the 36% in corridor and the 78% in the room, with respect to the noise threshold. Thus, it is experimentally verified that our algorithm, designed for the detection of a unique target, still performs well in environments showing different backscattering characteristics thanks to the adoption of extremely narrow beam arrays. This further motivates the importance of adopting massive instead of non-massive arrays.

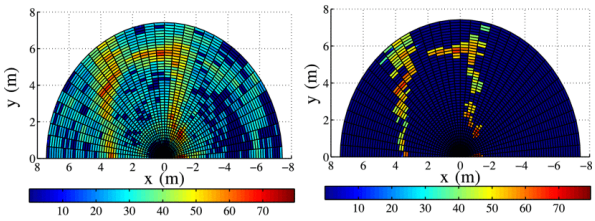

Fig. 1 Reconstructed map with noise threshold (left) and with adaptive threshold (right)

Perspectives

In this work we proposed the design of a radar, suitable for small-size and low-complexity devices, capable of self-estimating a threshold for cleaning measured data during the beamsteering operation without requiring a-priori information of the environment. We showed the feasibility of the proposed approach by exploiting measurements collected with real 400-element massive arrays at mm-wave. It has been experimentally verified that the presented algorithm allows to mitigate the side-lobes effect in dense scatterers scenarios paving the way for future personal radar devices.

RELATED PUBLICATIONS:
[1] F. Guidi, A. Mariani, A. Guerra, D. Dardari, A. Clemente and R. D'Errico, "Indoor Environment-Adaptive Mapping With Beamsteering Massive Arrays," in IEEE Transactions on Vehicular Technology, vol. 67, no. 10, pp. 10139-10143, Oct. 2018.

WIDEBAND LOW-PROFILE TRANSMITARRAY ANTENNA FOR BACKHAULING AT 60 GHZ

RESEARCH TOPIC:
Transmitarray antennas, high-gain antennas, 5G networks

AUTHORS:
A. Clemente, M. Smierzchalski, M. Huchard (Radiall), C. Barbier (Radiall), T. Le Nadan (Radiall)

ABSTRACT:
In this paper, the design and experimental characterization of a low-profile transmitarray operating at V-band (57 – 66 GHz) have been presented. A quad-feed based architecture has been selected to reduce the antenna profile maintaining high gain and wideband behaviors, as in the case of single-feed transmitarrays. A 1296-element transmitarray, with an aperture of 90×90 mm² and a total thickness of 44 mm, has been optimized, fabricated, and experimentally characterized. A maximum gain of 32.6 dBi, corresponding to an aperture efficiency of 39.5%, has been successfully demonstrated.

SCIENTIFIC COLLABORATIONS: Radiall

Context and Challenges
High-gain backhauling operating at millimeter wave frequencies (Ka-, V-, and E-bands) are a key technology of the future 5th Generation (5G) mobile communication networks. In this context, fixed-beam antennas with wideband characteristics (10 – 20%) and high gain (30 – 43 dBi) are required. Transmitarray antennas are an excellent candidate at mmWave thanks to the spatial feeding mechanism, which allows to reduce the loss in the feeding networks if compared to classical phased array architectures. Transmitarrays for backhauling at 60 GHz, in Printed Circuit Board (PCB) technologies, have been recently demonstrated including switched-beam capability for self-alignment functions [1]-[2]. Despite the cited advantages, the required spatial feeding system considerably increases the overall profile of transmitarrays. In fact, the focal to aperture size ratio F/D is in general optimized with typical values ranging from 0.5 to 1.

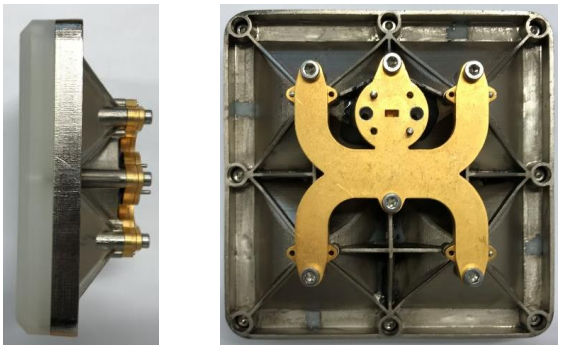

(a) (b)

Fig. 1. Photograph of the realized linearly polarized low-profile transmitarray at V-band.

Main Results
Here, a wideband transmitarray with reduced focal distance is presented [3] including experimental results (Fig. 2). The array is composed of 1296 (36×36 elements) three-metal layer unit-cells and is illuminated considering four profiled skirt focal sources (Fig. 1). This focal array is composed of elongated horns disposed in a 2×2 array configuration. Each horn has a square aperture and a rectangular waveguide input. The quad-feed architecture has been selected in order to achieve a reasonable transmitarray (i.e. around a factor 2) profile reduction if compared to the single-feed focal system [1] and simplify the power division network design. The aperture size of each elongated horn is set to 9λ×9λ (45×45 mm²) to match a quarter of the flat-lens array surface. The depth from the aperture interface and the waveguide aperture is equal to 25 mm. The proposed antenna presents a measured maximum gain of 32.6 dBi with an aperture efficiency of 39.5%. Good agreement with the numerical results has been demonstrated.

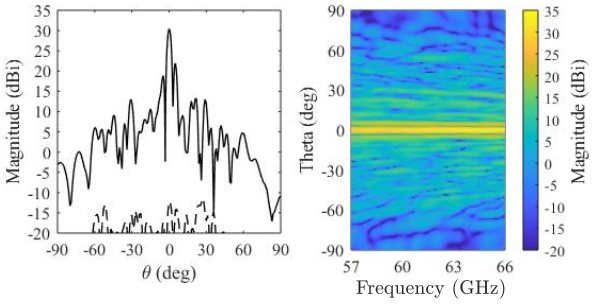

Fig. 2. Measured gain pattern of the transmitarray at 60 GHz.

Perspectives
Architectures for self-alignment and ultra-low profile transmitarrays are analyzed at Leti. The possibility to implement sub-THz (up to 300 GHz) transmitarray is also studied.

RELATED PUBLICATIONS:
[1] C. Jouanlanne, A. Clemente, M. Huchard, J. Keignart, C. Barbier, T. Le Nadan, and L. Petit, "Wideband linearly-polarized transmitarray antenna for 60 GHz backhauling," IEEE Transaction on Antennas and Propag., vol. 65, no. 3, pp. 1440-1445, Mar .2017.
[2] L. Dussopt, A. Moknache, J. Säily, A. Lamminen, M. Kaunisto, J. Aurinsalo, T. Bateman, and J. Francey, "A V-band switched-beam lineraly-polarized transmit-array antenna for wireless backhaul applications," *IEEE Trans. Antennas Propag.*, vol. 65, no. 12, pp. 6788-6793, Dec. 2017.
[3] M. Smierzchalski, A. Clemente, M. Huschard, and C. Barbier, "Wideband low-profile transmitarray antenna for backhauling at 60 GHz," in *Proc. 13th European Conf. Antennas Propag.* (*EuCAP 2018*), Mar. 2018.

DESIGN AND OPTIMIZATION OF HUYGENS SOURCE BASED SUPERDIRECTIVE ARRAYS

RESEARCH TOPIC:
Antenna theory, small antennas, superdirective arrays, IoT, RFID

AUTHORS:
Alexandre Debard, Antonio Clemente, Christophe Delaveaud

ABSTRACT:
It is well known, that a maximum directivity close to $P^2 + 2P$ could be obtained when P Huygens sources are used to implement compact end-fire arrays with reduced inter-element distance (e.g. < 0.3λ). This result has been theoretically demonstrated with infinitesimal Huygens sources, but practical antenna architectures are not yet presented. In this paper, a method to design Huygens source based superdirective arrays is numerically demonstrated through full-wave electromagnetic simulations considering a two-element array with an inter-element distance equal to 0.2λ and kr_0 = 1.33 (where r_0 indicates the radius of the minimum sphere circumscribing the antenna). End-fire directivity and gain equal to 8.7 and 7.8 dBi have been respectively obtained. These results have also been compared to the case of the two-element arrays based on magnetic and electrical dipoles.

SCIENTIFIC COLLABORATIONS: DGA

Context and Challenges
Harrington defined the antenna maximum normal directivity as $N^2 + 2N$ where $N = kr_0$ represents the maximum degree of the spherical wave expansion of the radiated field, k is the wavenumber, and r_0 indicates the radius of the minimum sphere circumscribing the antenna. For a given r_0, superdirectivity could be defined as a directivity higher than the normal directivity. Since then, the possibility of realizing superdirective and supergain arrays have been successfully demonstrated experimentally, with end-fire arrays of two, three or four closely spaced magnetic or electrical dipoles [1]. For example the directivity and gain reached for a two-dipole array was 7.2 dBi and 7.0 dBi, respectively. Furthermore, it was predicted that a maximum directivity of $P^2 + 2P$ could be achieved with end-fire array based on P Huygens source elements. For instance, for a two-element array the maximum directivity is 9.0 dBi. This fact has also been discussed and analytically demonstrated in our recent paper [2]. To the best of our knowledge, practical designs of single Huygens sources have been presented in the past, but they have never been put in an array to obtain superdirective design [3].

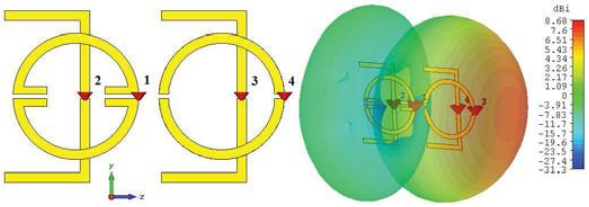

Fig. 1. Schematic view of the two Huygens source array with an inter-element spacing of 0.2λ and its simulated 3D directivity pattern.

Main Results
The synthesis method used to optimize the Huygens source based arrays is based on the algorithm previously presented in [1]. Each Huygens source is a two-port array composed of an electrical dipole and a loop antenna. The geometry of the proposed antenna is shown in Fig. 1. It is a planar structure with two copper layers printed on a 0.787 mm thick Rogers RT5880 substrate. The magnetic dipoles are achieved by a printed capacitively loaded loop (CLL) of total length equal to a half-wavelength. The electrical dipoles are a folded element also with a length of a half-wavelength. In the proposed architecture, the two elements of each Huygens source are considered as independent and can be controlled by opportunely tuning the amplitude and phase at the two ports [1]. More details are presented in [3]. The directivity and gain patterns of the single Huygens source and two Huygens-source based array are shown in Fig. 2. The 3D view of the directivity pattern at 850 MHz of the array is shown in Fig. 1. The global dimensions of the proposed array are 0.36λ×0.22λ×0.003λ which gives kr_0 = 1.33. A maximum directivity and gain of 8.7 and 7.8 dBi have been achieved, respectively.

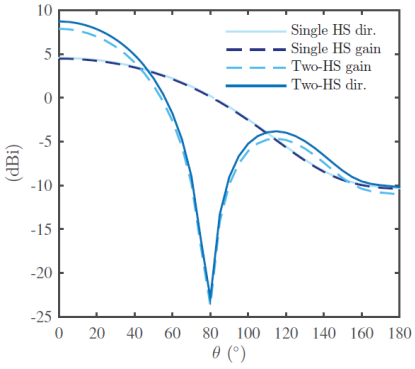

Fig. 2. Radiation directivity and gain patterns of the simulated Huygens source and two-Huygens source array.

Perspectives
The possibility of a practical implementation of this antenna and the possibility to increase the directivity will be analyzed.

RELATED PUBLICATIONS:

[1] A. Clemente, M. Pigeon, L. Rudant, and C. Delaveaud, "Design of ansuper directive four-element compact antenna array using spherical wave expansion," IEEE Transactions on Antennas and Propagation, vol. 63, no. 11, pp. 4715–4722, Nov. 2015.

[2] A. Debard, A. Clemente, C. Delaveaud, C. Djoma, P. Potier, and P. Pouliguen, "Analysis of superdirective Huygens source based endfire arrays," in 2017 11th European Conference on Antennas and Propagation (EUCAP), Mar. 2017, pp. 2983–2987.

[3] A. Debard, A. Clemente, C. Delaveaud, C. Djoma, P. Potier, and P. Pouliguen, "Design and optimization of a two-element Huygens source based superdictive array," in 2018 12th European Conference on Antennas and Propagation (EUCAP), Apr. 2018.

3D PRINTED COMPACT WIDEBAND MAGNETO-ELECTRIC DIPOLE WITH CIRCULAR POLARIZATION

RESEARCH TOPIC:

Wideband antenna, unidirectional radiation, miniaturization, 3D printing

AUTHORS:

A. S. Kaddour, S. Bories, Ch. Delaveaud

ABSTRACT:

A 3D printed compact unidirectional wideband antenna based on two crossed magneto-electric dipoles is proposed. The antenna consists in folding the electrical dipoles elements, thus the surface of the radiation element is reduced to $0.23\lambda_0*0.23\lambda_0$ where λ_0 is the wavelength at the lowest operation frequency for a standing wave ratio (SWR) <2.5. This technique leads to a reduction factor of 48%. Despite a complex 3D structure, one dipole arm is prototyped in a single piece using plastic 3D printing technology and metallization. The excellent agreement between measured and simulated results (impedance and radiation) demonstrates the quality of such realization process for low cost prototyping of such antenna structure. Circular polarization mode is obtained connecting a 90° hybrid coupler circuit. Broadside Axial Ratio (AR) is lower than 3 dB over an octave from 1.5 to 3 GHz.

SCIENTIFIC COLLABORATIONS: CNES (FRENCH SPACE AGENCY)

Context and Challenges

Recent mobile communication standards increase the demand for broadband antenna having functional characteristics such as broad impedance bandwidth, broad half power beam width and stable gain regarding frequency. State of art shows that “Magneto Electric” (ME) dipole antennas are promising solutions with excellent radiation characteristics and wide impedance matching. These antennas are based on the concept of the Huygens source [1] that presents intrinsic directivity.

Main Results

We present in [2] a novel method for reducing the occupied surface of the well-known dual-polarized wideband ME dipole antenna by transforming the electric dipole from square plates to folded square loops. Antenna miniaturization can be achieved by increasing the current path length on the electric dipoles. The proposed folded structure is very complex and expensive for fabrication using metallic plates bending or machining. Therefore, these elements were fabricated using 3D printed technology with plastic material and electroplated with copper. Furthermore, circular polarization has been generated by adding a 90° hybrid coupler circuit. The occupied surface of the proposed radiating element is only $0.23.\lambda_0 \times 0.23.\lambda_0$, which is reduced by 48% comparing with the initial design.

A 3D view of the proposed antenna is presented in Fig. 1, the antenna consists of four horizontal folded square loops operating together as two crossed electric dipoles. The folded square loops dimensions were optimized to obtain a wide impedance bandwidth while maintaining an electrically small size of the radiation element.
It is important to notice that the electrical folded dipole and vertical plates were combined in a single piece and fabricated by 3D printing technology (Laser Sintering) in Plastic PC/ABS and electroplated with a 50 µm copper thickness with no impact on the antenna radiation efficiency, Fig. 1.

In circular polarization mode, the antenna has a broadside gain varying from 7 to 10 dBic from 1.6 to 3 GHz and an axial ratio <3 dB from 1.2 to 3 GHz (85% relative bandwidth). These performance prove the feasibility and reliability of the 3D printing technology for low cost prototyping in this band.

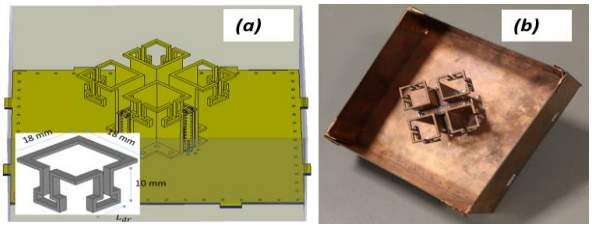

Fig. 1 (a) 3D view proposed antenna with a zoom on the folded electrical dipole. (b) picture of the prototyped antenna.

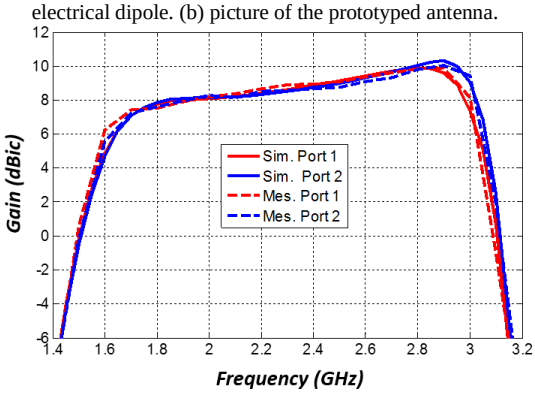

Fig. 3 Broadside measured (dash) and simulated (plain) RHCP (red), LHCP (blue) regarding frequency

Perspectives

To reach the second octave bandwidth, we plan to implement a frequency reconfigurable structure on the radiating element.

RELATED PUBLICATIONS:

[1] A. S. Kaddour, S. Bories, A. Clemente, A. Bellion and C. Delaveaud, “Radiation modes investigation of Huygens source type antenna using spherical wave expansion,” in Proc. IEEE Int. Symp. Antennas Propag. (ISAP), Okinawa, Japan, Oct. 2016, pp. 664-665
[2] A. S. Kaddour, S. Bories, A. Bellion.& C. Delaveaud, (2018). 3-D-Printed Compact Wideband Magneto-electric Dipoles with Circular Polarization. IEEE Antennas and Wireless Propagation Letters, 17(11), 2026-2030.

ULTRA MINIATURE ANTENNA FOR VHF PAGER

RESEARCH TOPIC:
Ultra Small Antennas, miniature, antenna design, VHF

AUTHORS:
Jean-François PINTOS, Cherif HAMOUDA

ABSTRACT:
For radio Pagers that require very high integration, a loaded loop antenna is a good candidate. An UMLLA (Ultra-Miniature Loaded Loop Antenna) antenna has been designed with a very small form factor (*ka*~ 0.14) for the VHF band. The shape of the antenna is printed along the outside of the plastic cover to improve radiation efficiency, and a load circuit is located on the Printed Circuit Board (PCB) inside. After calculating the optimal load, a capacity of 4.3 pF is implemented to match the antenna impedance around 170 MHz. A maximum realized gain of -12.5 dBi and a radiation efficiency of 4.2% were measured. with a bandwidth of 1.2 MHz.

SCIENTIFIC COLLABORATIONS: IPC, S2P – Smart Plastic Products

Context and Challenges

Communications in VHF band, especially those integrated in mobile devices like Pager, need the design of Electrically Small Antennas (ESA). Loaded loop antenna (LLA) is a good candidate for such devices. In [1], an LLA called Miniature IFA-Inspired Circular Antenna (MIICA) has been designed to work at 432.8 MHz with the product ka ~ 0.23 (where k is the wavenumber and a the radius of the smallest sphere that encloses the antenna) and with radiation efficiency around 38 %.

Declining such approach on a parallelepipedic form factor, an antenna design is made for the 170MHz VHF Pager to meet the POCSAG standard [2]. The Pager transverse dimensions are 97.4 x 54.7 mm2, which gives an average radius of 38 mm (~ $\lambda_0/46$ or ka ~ 0.14). The very high integration required by the context and the POCSAG standard enforce the use of an ultra-miniature 3D antenna. In order to achieve optimum performances. The antenna should occupy as much volume as possible and be placed as close as possible to the outside surface of the device. The RF parts (located on the PCB inside the terminal) act as an interface between the antenna and the RF transceiver, they also allow a tradeoff to be made between size, bandwidth and antenna efficiency by using loading lumped elements.

Main Results

The antenna system can be divided in two main parts, a radiation part, and a load circuit placed at the end. The radiation element is printed on the outside plastic cover of Pager, whereas the load is placed on the PCB. In Fig. 1, the full integrated design (left) and the simplified model (right) are illustrated.

As explained in [3], this antenna can be modeled by three cascaded matrix. The first block is associated to the feeding impedance. The second block models the antenna's behavior through its ABCD matrix extracted from the [S] parameters. Finally, the third block represents the desired load Z_{load}.

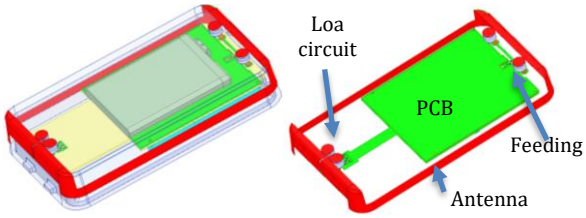

Fig. 1: Mechanical design of UMLLA

A Non Foster behavior has been observed for optimal load. In practice at 170 MHz, a 3.9pF capacitor have been implemented for the load and the results are shown In the FIg.2.

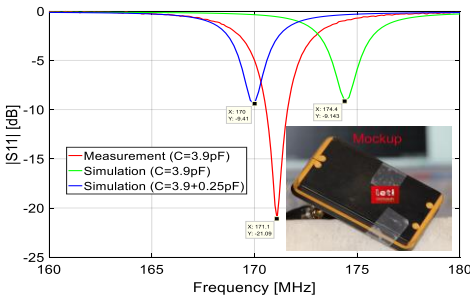

Fig. 2: Differential [S] parameters measurement

Perspectives

An Ultra miniature antenna has been designed for VHF radio pager terminal (ka=0.14). A process has been proposed to find the best antenna load and a SMD capacitor has been placed to tune antenna around 170MHz.

Good agreement (taking into account components tolerance) between measurement and simulation have been obtained for [S] parameters and radiation results (η_{tot}~4%)

The next step will be to improve antenna performances in terms of radiation efficiency.

RELATED PUBLICATIONS:

[1] F. Sarrazin, S. Pflaum and C. Delaveaud, "Radiation Efficiency Improvement of a Balanced Miniature IFA-Inspired Circular Antenna", IEEE ANTENNAS AND WIRELESS PROPAGATION LETTERS, VOL. 16, 2017 1309.

[2] C. Hamouda, J.-F. Pintos, "Ultra-Miniature Loaded Loop Antenna for VHF Pager", IEEE Antennas and Propagation Society International Symposium Boston (APS), July 8-13, USA, 2018

SUB-THZ LARGE SCALE CHANNEL CHARACTERISTICS IN INDOOR SCENARIOS

RESEARCH TOPIC:

Sub-THz communications, propagation, measurement, channel modeling

AUTHORS:

Laura Pometcul, Raffaele D'Errico,

ABSTRACT:

This paper presents the indoor sub-Terahertz channel characteristics, based on a measurement campaign realized in three indoor environments. The measurement setup is based on double steering of directive antennas. Large scale parameters and cluster characteristics are derived from measurements.

SCIENTIFIC COLLABORATIONS:

Context and Challenges

The use of the large bandwidth available at Terahertz (THz) and sub-THz frequencies represents an attractive solution for high data rate with short-range communications. Still, this technology presents some technical difficulties that must be solved before actually realizing the full capability of using high carrier frequencies.

In the last years, a large number of studies have been carried out for channel models at microwave frequencies, while only recently the development of 5G systems has been motivating the development of new channel models at millimeter-wave (mm-wave) bands. However, these studies are generally limited to frequencies below 100 GHz, and do not address the channel characterization and modeling above these frequencies.

In this paper, we present the results of an indoor channel characterization in the 126-156 GHz band for indoor scenarios (up to 10.6 m).

Main Results

The considered measurement setup is composed of a 4-port Vector Network Analyzer (VNA) with remote head frequency mm-wave converters, two high-precision antenna positioners remotely controlled. The transmitting (TX) antenna is placed on a 1-axis (azimuth) positioner, while the receiving (RX) antenna is placed on a 3-axis (x-y-Φ) positioner. This allowed us to perform a mechanical steering of 20 dBi, using horn antennas on both sides.

All measurement campaigns have been conducted at CEA-LETI. Indoor 1 scenario, represented in Fig. 1.(a), is a laboratory where a number of usual equipment like tables, chairs and closets can be encountered. The total room size dimensions are 4.3×7×2.6 m3. The Indoor 2 scenario, seen in Fig.1.(b), is a meeting room of 6×15.8 m×2.6 m3, where the antennas were placed in the middle of the room, between the tables. Indoor 3 scenario, represented in Fig. 1.(c), is an ordinary office of 7×7×2.6 m3. Measurements where performed up 10.6 m because the size of the indoor scenarios imposed it.

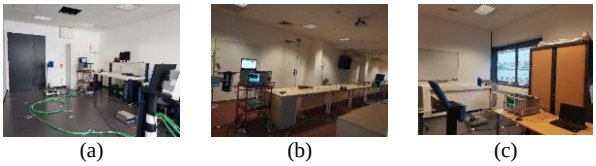

(a) (b) (c)

Fig. 1 Measurement campaign scenarios: (a) Indoor 1 scenario (laboratory), (b) Indoor 2 scenario (meeting room) and (c) Indoor 3 scenario (office).

Starting from the experimental results, the MPCs were extracted and the large scale parameters were characterized. In Fig. 2 we compare the path loss and the delay spread in the band of interest (D-band) with those obtained in previous measurement campaign at 60 GHz (V-band) and 80 GHz (E-band).

The results highlight that the Line-of-Sight path brings most of the energy contribution in the Sub-THz channel with respect to below 100 GHz channels, but multi-path components are still present and resulting into a delay spread up to 15 ns.

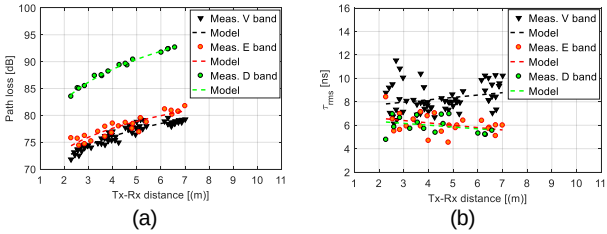

(a) (b)

Fig. 2. Path Loss (a) and delay spread (b) for Indoor 3 scenario in different frequency bands.

Perspectives

This model describes the sub-THz channel characteristics in LoS scenarios. Future work includes the extension of the characterization towards NLoS condition given by obstruction from human body and partitions. This characterization can be used for first link budget evaluation in short-range wireless communications in the D-band.

RELATED PUBLICATIONS:

[1] L. Pometcu and R. D'Errico, "Characterization of sub-THz and mmwave propagation channel for indoor scenarios," 12th European Conference on Antennas and Propagation (EuCAP 2018), London, 2018, pp. 1-4.

[2] L. Pometcu and R. D'Errico, "Large Scale and Clusters Characteristics in Indoor Sub-THz Channels," 2018 IEEE 29th Annual International Symposium on Personal, Indoor and Mobile Radio Communications (PIMRC), Bologna, 2018, pp. 1405-1409.

WIDEBAND VEHICLE TO PEDESTRIAN PROPAGATION CHANNEL CHARACTERIZATION AND MODELING

RESEARCH TOPIC:

Vehicular communication, propagation, measurement, channel modeling

AUTHORS:

Gloria Makhoul, Raffaele D'Errico, Claude Oestges

ABSTRACT:

A wide-band vehicle to pedestrian (V2P) channel model based on a measurement campaign carried out at 3.8 GHz is presented. Several propagation conditions and different mobility patterns were investigated. A stochastic channel model for line of sight (LoS) scenarios is proposed. The main path and secondary discrete components are modeled in terms of path loss (PL), large and small-scale fading.

SCIENTIFIC COLLABORATIONS: Université catholique de Louvain, Belgique

Context and Challenges

Vehicle-to-Everything (V2X) communication is a challenge for fast growing technology that has the potential to enhance road safety. Multiple communication protocols, e.g. IEEE 802.11p, 3GPP, LTE etc., were shaped to be the basic standards of intelligent transportation systems (ITS). The V2X communication is a direct link between moving vehicles and a wide set of road passengers like vehicles, pedestrian, cyclists etc. This dual mobility generates non-stationary properties of the propagation channel, which require precise modeling, for simulation network and system design.

Main Results

The limited modeling results known to vehicle to pedestrian (V2P) channels motivate the realization of V2P measurement campaign using a channel sounder. The center frequency and the bandwidth were set to 3.8 GHz and 200 MHz, respectively. The transmit power at the antenna ports was 23 dBm and a maximum excess delay of 20.47 us was measured. To achieve a high Doppler resolution, a channel sampling rate of 1062 Hz is considered which corresponds to a maximum relative speed of 150 km/h approximately. The Tx dipole antenna was mounted on the roof of a car while the Rx dipole antenna was placed on a cardboard tube carried by a human subject. Multiple V2P mobility were performed including parallel, opposite and orthogonal directions, in various propagation environments, i.e. Line-of-Sight (LoS) and Non-Line-of-Sight (NLoS) scenarios (cf. Fig. 1). The avenue includes two lanes, one for each direction. On the side of the road, there are fields of green grass and some trees. Vehicle speed was around 30 km/h and the distance between the Tx vehicle and the Rx pedestrian varied in the range of 2 m to 40 m depending on the measurement scenario.

(a) (b)

Fig. 1. Example of LoS (a) and NLoS (b) Measurements.

A stochastic modeling approach was proposed to model the measured V2P propagation channels as a combination of first path and secondary multipath components (MPCs) [1]. Its basic idea is to determine the number of contributed scatterers in each time frame, assign them different channel properties, and sum up their respective signal contributions at the Rx. The non-stationarity properties of the channel is thus formed considering the dynamic change of scatterers around the moving terminals that characterizes the appearance and disappearance of MPCs. Therefore, a detection and tracking algorithms are implemented in order to track the path components over time (cf. Fig. 2a).
The first path component mainly consists of the LoS and the ground reflection paths while the secondary MPCs result from specular reflection of scatterers. They are best fitted with a combination of path loss (PL), large-scale fading and small-scale fading. In LoS scenarios, the two rays model was considered for the PL of the first path component while a log distance model was used for the one of MPCs (cf. Fig. 2b). The small-scale fading was described with a Rice distribution and the large-scale fading was characterized in dB by a normal distribution with zero mean.

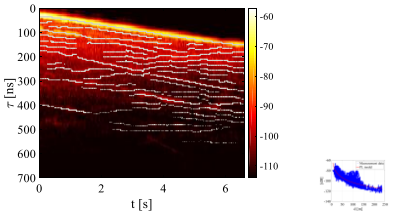

(a) (b)

Fig. 2. Outcome of MPC tracking algorithm (a) and PL model of the discrete scatterers (b) when Tx and Rx are in LoS and they are traveling in the same direction.

Perspectives

This model describes the V2P channel characteristics and its non-stationarity behavior given by the dynamic position changes of the scatterers. The preliminary evaluations reported in [1] concern the LoS scenarios. Future work includes the extension of the characterization towards NLoS and LoS/NLoS V2P links and the implementation of the model with Doppler characteristics. This model can be used for system evaluation, and OTA test for safety road applications.

RELATED PUBLICATIONS:

[1] G. Makhoul, R. D'Errico and C. Oestges, "Wideband vehicle to pedestrian propagation channel characterization and modeling," 12th European Conference on Antennas and Propagation (EuCAP 2018), London, 2018, pp. 1-4.

DESIGN OF A MONOPOLAR WIRE-PLATE ANTENNA LOADED WITH MAGNETO-DIELECTRIC MATERIAL

RESEARCH TOPIC:

Small antennas, magneto-dielectric material, antenna design.

AUTHORS:

Lotfi BATEL, Jean-François PINTOS, Christophe DELAVEAUD

ABSTRACT:

The design and performances evaluation of an electrically small Monopolar Wire-Plate (MWP) antenna loaded with magneto-dielectric material (MDM) are proposed. Changing the characteristics, the volume or the position of the material highlights a particular behavior towards MWP antenna miniaturization. A reduced volume of MDM with a suitable material's position on the antenna leads to a good compromise between antenna miniaturization and radiation performances.

SCIENTIFIC COLLABORATIONS: LabSTICC (University of Brest, France).

Context and Challenges

Antenna miniaturization for airborne systems is an important issue for reducing the weight and improving the aero dynamic shape. Nevertheless, reducing antenna size becomes critical at V/UHF bands as the wave lengths are large at those frequencies and the performances of the small antennas are reduced following the fundamental laws. Recent works dealing with material fabrication at microwave frequencies has made it possible to consider using MDM ($\varepsilon_r > 1$, $\mu_r > 1$) as a promising solution for antenna miniaturization. This opportunity led us to evaluate the performances of MWP antenna while loading by a magneto-dielectric material, which represents an original work according to the current state of the art. The goal is to show the potential of miniaturization that offers MWP antenna associated to MDM by optimizing the antenna/MDM interaction.

Main Results

The designed MWP antenna shown in Fig. 1 (a) has been studied first with a theoretical MDM load. A parametrical study based on the variation of material's properties, volume and position led us to understand the particular behavior of this specific antenna [1].

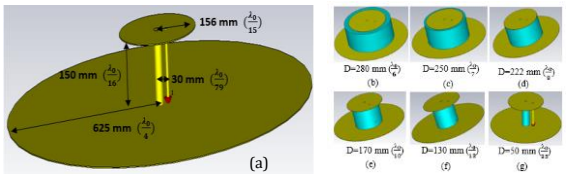

Fig. 1: MWP design (a) and variation of MDM volume (b-g)

A different behavior on impedance bandwidth is observed compared to other type of antennas loaded by MDM like patch, Planar Inverted F antenna or slot. A good tradeoff is found to perform interesting antenna properties while reducing its size and material volume by using specific materials ($\mu_r > \epsilon_r$). Typically, for a fixed resonance frequency of 100 MHz, antenna's radiation efficiency is higher for a low diameter (D) of MDM. This is particularly interesting in the context of next airborne antenna systems where small, light and low cost antennas are expected.

Considering parametrical study's results, a specific design of MWP antenna loaded with a fabricated MDM S4 [2] is proposed. The material is loaded enclosing antenna's short-circuit as it is the best position evaluated for antenna's performance in interaction with the material. The S4 material is suitable for our application since it exhibits low magnetic losses around 100 MHz (about 0.035) and its permeability (μr) close to 20 is higher than its permittivity (ε_r) close to 13. A synthesis of antenna performances (Table 1) shows the interest of using the S4 MDM for antenna miniaturization issue. Using the S4 material to load the MWP antenna has led to a reduction of 15.4% of its electrical size with a good tradeoff considering its performances (bandwidth and efficiency reduction) [3].

Table 1: Comparison between MDM loaded and unloaded MWP antenna

Antenna properties	Without material	S4 material
Hat radius	156 mm	147 mm
height	150 mm	100 mm
Sphere radius	$\frac{\lambda_0}{11}$	$\frac{\lambda_0}{13}$
% miniaturization	-	15.4%
Bandwidth	9 MHz	7 MHz
Total efficiency	99%	75%

Perspectives

A comparison between the S4 loaded and unloaded MWP antenna shows promising perspectives for airborne application in order to obtain smaller, light and low cost antenna systems. Future works will concern the experimental validation of the proposed studies to confirm the benefit of MDM with this specific antenna.

RELATED PUBLICATIONS:

[1] L. Batel, J-F.Pintos, C. Delaveaud, "Etude d'Antenne Fil-Plaque Monopolaire sur materiau magnetodielectrique", 20eme Journées Nationales des Microondes (JNM 2017), Saint-Malo, 2017.

[2] V. Doumouya, V. Laur, J.L. Mattei, P. Queffelec, L. Batel, C. Delaveaud, "Conception d'antennes miniatures accordables en bande VHF à l'aide de matériaux magnéto-diélectriques", 15eme Journées de Caractérisation Microondes et Matériaux (JCMM 2018), Paris, 2018.

[3] L. Batel, J. Pintos and C. Delaveaud, "Design of a monopolar wire-plate antenna loaded with magneto-dielectric material," *12th European Conference on Antennas and Propagation (EuCAP 2018)*, London, 2018, pp. 1-5.

FREQUENCY RECONFIGURABLE DUAL NARROW BAND ANTENNA MATCHED ON THE LOW BAND LTE FDD PHYSICAL LAYER

RESEARCH TOPIC:
Reconfigurable antenna, antenna miniaturization, LTE sub-GHz

AUTHORS:
S. Bories, F. Sarrazin, A. Giry

ABSTRACT:
The upcoming widening of the LTE frequency Low Band (LB) towards 600 MHz imposes a strong miniaturization effort to the smartphone antenna which can no more maintain its radiation efficiency performance over the full 600-960 MHz range. To overcome this issue, the design strategy consists in matching the antenna only where it is instantaneously used. Thus, based on the FDD spectrum usage, the proposed antenna presents two narrow bands that can be reconfigured independently anywhere in the whole LTE LB. The proposed design takes into account current limitations of the tunable capacitor (low Q factor). The measured total efficiency increases with frequency from 11% at 617 MHz to 60% at 960 MHz.

SCIENTIFIC COLLABORATIONS: CEA-LETI (DACLE)

Context and Challenges
The properly named LTE (Long Term Evolution) standard supports ever increasing number of E-UTRA frequency bands. In the sub-GHz bands, this is particularly relevant for network providers to improve the coverage of mobile or IoT applications due to better EM propagation properties. However, if the wavelength is increasing with coming bands (starting from 617 MHz), the terminal form-factor remains constant or even tends to shrink (cellular watch, NB-IoT sensor). These two challenges (lower band and smaller devices) can no more be faced with mere wideband passive antennas without deteriorating their performances (impedance matching and radiation efficiency). In this context, our strategy consists to match the antenna only on one single requested E-UTRA band.

Main Results
The proposed Dual Tunable Bands Antenna (DTBA) implements the concept of aperture tuning twice. It is reminded that by designing the antenna over a narrower instant bandwidth, we can expect to maintain its radiation efficiency. To match the LTE FDD scheme, the innovation consists here by matching two independent resonances of the antenna over 2 x 10 MHz: the first UL band, the second for the DL of the allocated frequency of a given network provider (Fig. 1).

This antenna is a meander monopole coupled with two tunable parasitic elements with a total volume of 40x10x6 mm3. The two obtained narrow bands can be tuned independently over the full 600-960 MHz range thanks to two tunable capacitors (TC) [1]. With small TC tuning ratio (Cmax/Cmin of 3) and despite its resistive part (ESR) that reaches a 2.5 Ω value, a very miniaturized antenna is compliant with any sub-GHz LTE FDD bands. The duplex spacing can vary from 30 MHz to 60 MHz. More important, this highly coupled antenna structure seems to be less sensitive to ESR value compared to a typical tunable notch. A lower radiation efficiency reduction is observed as TC ESR increases. However, global antenna performance seems to be still similar with the passive antenna in those frequency bands.

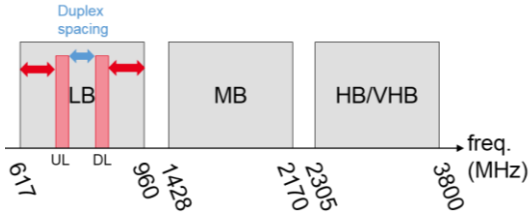

Fig. 1. Dual Tunable Bands Antenna covering two 10 MHz instant bandwidth over the whole LTE LB (617-960 MHz).

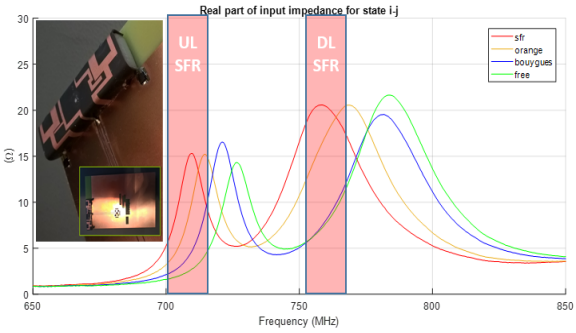

Fig. 2. Measured DTBA input impedance real part for dual band FDD matching in the LTE 700 band for the four French network providers. Insert on the tunable radiating element (left).

Perspectives
Future works will address the upper frequency bands with the same antenna structure. Ultra-miniature and ultra-narrow band agile radiating element will be also designed for LTE NB-IOT standard.

RELATED PUBLICATIONS:

[1] Bories, S., Sarrazin, F., & Giry, A. , Frequency reconfigurable dual narrow band antenna matched on the low band LTE FDD physical layer, 12th European Conference on Antennas and Propagation (EuCAP 2018) Proc., London, UK.
[2] Abdallah, E., Bories, S., Nicolas, D., Giry, A., & Delaveaud, C. Large-Signal Analysis and Characterization of a RF SOI-Based Tunable Notch Antenna for LTE in TV White Space Frequency Spectrum. In 11th Int. Conf. CROWNCOM 2016 (pp. 536-544). Springer, Proceedings, Springer International Publishing

05 SECURITY OF EMBEDDED SYSTEMS

- On-Chip Techniques
- Deployment of IoT devices & systems
- Embedded cryptography
- Side-channel attacks
- Security Testing Tools
- Blockchains

END-TO-END SECURITY AND PRIVACY BY DESIGN FOR AHA-IOT APPLICATIONS AND SERVICES

RESEARCH TOPIC:
Cybersecurity

AUTHORS:
(ST) Mario Diaz Nava, Armand Castillejo, SylvieWuidart,
(CEA) Mathieu Gallissot, Thomas Loubier,
et al.

ABSTRACT:
We present the work done as part of the Activage project and within the IRT Nanoelec to secure IoT gateways in a context where privacy and trust are essential. This security solution is based on two principles: the integrity check of the platform and the bonding of an encryption key to a physical platform instance to perform pairing. These two principles are implemented on a Raspberry Pi 3 platform that has been extended materially with a secure component supplied by STM: the STAFE-TPM. This component was used to implement a verified boot to validate the integrity of the system and to establish a unique signature of the board, in order to authenticate the removable storage. This work is intended to be deployed on 75 instances in the real world with the help of the Activage project.

SCIENTIFIC COLLABORATIONS: STMicroelectronics with the support of the Activage project and IRT Nanoelec

Context and Challenges
The Gateway in an IoT device to cloud architecture is a key element as it marks the frontier between the public and private domains. In this particular (specific) position in the architecture, the Gateway is indeed both an entry path from inside to outside and reverse. In a worst-case scenario, somebody gaining access to a gateway gains access to other gateways, by reproducing the attack at a massive scale. In the ACTIVAGE context, gateways are often deployed in homes, and thus it is not possible to master the physical access to the hardware. Moreover, the gateway, in a residential place, might be stolen more easily than a server in a data centre might.

Main Results
In order to secure IoT gateways qualified to be deployed in the Activage project, we first conducted a risk analysis to define the required security levels and prioritise the threats to be addressed. A methodology using the STRIDE and DREAD methods was used to analyse six different gateway implementations. One of the most serious and recurrent threats was the use of removable storage media on embedded platforms. The associated scenario is to drive the SD card for duplication and reverse engineering in preparation for an attack or recovery of sensitive information as for authentication on the service backend. Following this, we implemented a countermeasure to cryptographically associate removable media to a physical platform. This association is based on the contents of the physical medium by a key. The encryption key is then a function of the platform instance, this function may differ according to the capabilities of platform type and manufacture. The reference platform for this work is a Raspberry Pi 3, chosen especially for project dissemination in the project. This platform uses a removable storage medium in the form of an SD card, on which are stored the bootloader, the operating system and the applications. Raspberry Pi platforms do not have on board secured storage. A first step is to physically integrate a component to perform the primitive security functions. This component was supplied by ST Microelectronics, in the STSAFE range. It complies to the Trusted Platform Module (TPM2) specification, which provides facilities for the propagation of security functions in the firmware and user system space.

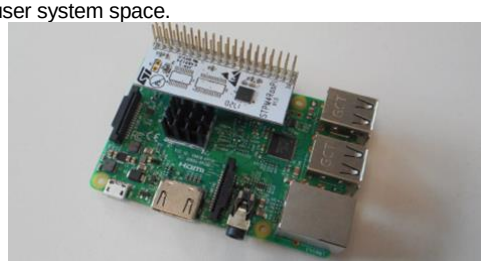

A second step is to establish the security function for generating the decryption key of the SD card. To perform this function, we used the capabilities of the STSAFE-TPM component to implement a verified boot. During start-up, the firmware analyses the integrity of the platform via Platform configuration registers (PCR). This integrity check is extended with a unique property of the board instance, in this case the serial number of the platform. This creates a generic (bootchain) and specific (serial number) integrity context on the platform. The last step is to store the decryption key in the TPM internal memory and to seal this key regarding the PCR status. Pairing is ensured by the unicity of his serial number as part of the PCR context. The threat scenario where the reverse engineering has been found to be easily reproducible becomes more complex and increases the level of protection of the solution.

Perspectives
The work carried out has made it possible to explore certain security capabilities of mainstream platforms. Other functions are being integrated, in particular to propagate the integrity measurement to the Linux kernel and the middleware running on the platform, for example using the IMA module, interfacing the TPM on PKCS11 and the use of the TrustZone ARM. A port of this work on other hardware platforms is also being investigated.

RELATED PUBLICATIONS:
Activage, H2020 agreement N°732679

ENERGY-EFFICIENT MASKING OF THE TRIVIUM STREAM CIPHER

RESEARCH TOPIC:

Lightweight Cryptography, Hardware Security, Side-channel analysis, Internet of Things

AUTHORS:

Maxime Montoya, Thomas Hiscock, Simone Bacles-Min, Anca Molnos and Jacques J.A. Fournier

ABSTRACT:

The widespread development of the Internet of Things (IoT) devices and applications raises the need for compact, efficient and secure cryptographic primitives. Trivium is a lightweight stream cipher suitable for IoT. Remarkably, no significant algebraic attack against Trivium was found since its proposal. However, many side-channel attacks are known and are a real threat for IoT devices. Countermeasures against such attacks exist, but they usually have a significant impact on the energy consumption. In this work, we propose an energy efficient implementation of the Trivium cipher provably resilient to side-channel attacks thanks to a Threshold Implementation (TI) masking scheme. Our energy-efficient approach takes advantage of the fact that the target of side-channel attacks is the initialization phase of Trivium and can reduce the power consumption of security countermeasures by 29.4%.

Context and Challenges

With the development of the IoT, a growing number of data has to be securely exchanged through wireless channels. Thus, IoT devices must embed cryptographic primitives. Unfortunately, traditional encryption methods like AES hardly meet the constraints on resource usage and power consumption required by these applications. Trivium is a hardware oriented lightweight stream cipher and finalist of the eStream competition held in 2008. Trivium remains one of the most efficient and compact stream ciphers. Therefore, it is suited to resource-constrained environments. However, many side-channel attacks have been published on Trivium so far. Most of them are able to recover its encryption key with only a few hundreds of power traces. Unfortunately, existing countermeasures usually have a high energy overhead, and thus are not suitable for IoT devices. In this work, we exploit the fact that attacks are exclusively performed during the first cycles of Trivium initialization to propose a more energy-efficient countermeasure.

Main Results

In the work [1], we studied current state-of-the-art side-channel attacks on Trivium and we observed that all of them are only applicable during the initialization phase of Trivium. More precisely, a Welch T-Test performed on power traces generated from RTL simulations of Trivium execution suggests that no leakages appear after 600 cycles as show on Fig 1.

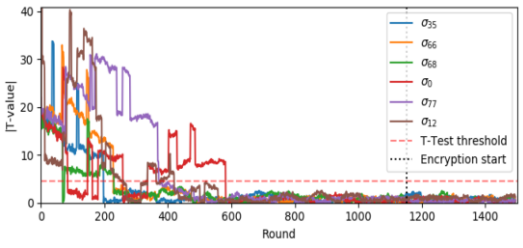

Fig 1. Welch's T-Test performed on Trivium initialization for different target variables. A value greater than the threshold of 4.5 means that there is a significant information leakage.

The countermeasure proposed in [1] is based on a Threshold Implementation masking scheme. The innovative design proposed in [1] is able to switch dynamically between protected and unprotected Trivium implementations. This design requires very few additional logic (the dotted elements in Fig. 2) and can be easily transposed to other existing stream ciphers.

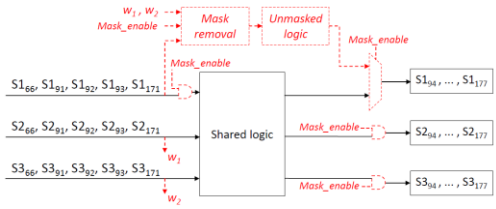

Fig 2. Architecture for mask removal. The countermeasure is enabled/removed based on the signal Mask_enable

Thanks to these dynamic switching capabilities, the power-consuming protections can be activated only during critical parts of the execution that really leak information (shown on Fig.1). Our simulations on ASIC 28 nm FDSOI technology (see Fig. 3) show that with this approach, the power consumption can be reduced by 29.4% without scarifying security.

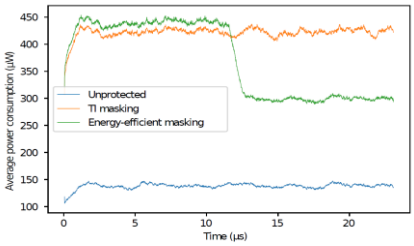

Fig 3. Power consumption of different implementations of Trivium

Perspectives

This work suggests that adapting the security level dynamically is a promising approach to embed hardened cryptographic primitives in IoT devices. Further work will investigate how to add more security levels and switch based on more advanced criteria.

RELATED PUBLICATIONS:

[1] Energy Efficient Masking of the Trivium Stream Cipher. Maxime Montoya, Thomas Hiscock, Simone Bacles-Min, Anca Molnos, and Jacques J.A. Fournier. 25th IEEE International Conference on Electronics Circuits and Systems Bordeaux, 2018

THWARTING FAULT ATTACKS AGAINST LIGHTWEIGHT CRYPTOGRAPHY USING SIMD INSTRUCTIONS

RESEARCH TOPIC:

Cybersecurity, hardware security, cryptography, fault attacks.

AUTHORS:

Benjamin Lac, Anne Canteaut, Renaud Sirdey & Jacques J.A. Fournier

ABSTRACT:

Several lightweight ciphers are intended for connected objects with high performance and low-resource constraints. Thereby, they are physically accessible to attackers and susceptible to fault attacks which quite often allow to retrieve the secrets they use with a relatively low complexity and cost. In this paper, we describe a new generic software countermeasure to thwart most fault attacks while preserving the performances of the underlying cipher: we call it the Internal Redundancy Countermeasure (IRC). We report practical experiments showing that IRC successfully thwarts fault attacks on the block cipher PRIDE and on the stream cipher TRIVIUM for which we protect both the initialization and keystream generation.

SCIENTIFIC COLLABORATIONS: Inria, CEA List

Context and Challenges

The expansion of the Internet of Things (IoT) brings many benefits but also raises a number of issues with respect to security and privacy. Lightweight cryptography (LWC) is investigated in order to address IoT security issues while seeking the best trade-off between security, power consumption, performance and footprint. Symmetric ciphers are the most used ciphers in IoT devices. During the last few years, several lightweight block and stream ciphers have been proposed. These ciphers are mainly designed to resist black-box mathematical attacks. However, since they are used in IoT devices in pervasive environments, we ought to also look at implementation-related attacks like side-channel attacks and fault attacks. However, even if many attacks have been introduced few low-cost countermeasures or designs have been proposed to thwart them. We hereby introduce a new paradigm for using spatial redundancies to thwart fault attacks, called the Internal Redundancy Countermeasure (IRC) for software implementations of embedded cryptography.

Main Results

Protecting the implementations of cryptographic algorithms against fault attacks, especially in software, is a complex and challenging issue whenever performance issues can be critical and given that, for a high level of protection, both spatial and temporal redundancies may be needed. In this respect, we propose a new approach, called IRC, which consists in taking advantage of *Single Instruction Multiple Data* (SIMD) instructions that are available in many 32-bit embedded processors (like an ARM Cortex-M4). The principle consists in implementing the cryptographic algorithm by representing each 32-bit register as an array of 4 bytes on which operations are executed in parallel. Hence four encryptions are executed in parallel, two working on the input data to be encrypted and two working on reference data used to detect any injected fault.

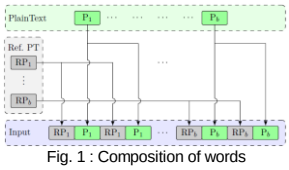

Fig. 1 : Composition of words

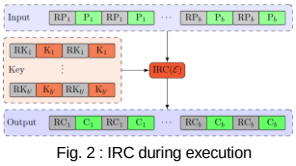

Fig. 2 : IRC during execution

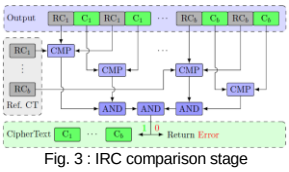

Fig. 3 : IRC comparison stage

The approach has been implemented and tested on two exemplars light weight ciphers like the block cipher PRIDE [2] and the stream cipher TRIVIUM [3]. On PRIDE, the countermeasure doubles the time for encryption for a 50% rise in code size. On TRIVIUM however, for a similar impact on the code size, the secure implementation is 7 times slower than the one without countermeasures. In both cases, we tested the secure implementations against fault attacks generated using EM pulses. All the attempts of fault injections were detected, leaving not more for any form of Differential Fault Attack.

Perspectives

Those first versions of IRC-based secure implementations of LWC have demonstrated the approach's efficiency against fault injections. However, to limit the impact of the countermeasure in terms of code size and performance, LWC might be designed to be more friendly with this approach. Hence a next step might be to design a new light weight cipher, based on so far mathematically proven principles, which might facilitate secure implementations against fault attacks based on IRC. Another perspective would be to see how IRC can be tweaked to efficiently implement countermeasures against side-channel attacks.

RELATED PUBLICATIONS:

[1] "Thwarting Fault Attacks against Lightweight Cryptography using SIMD Instructions" Benjamin Lac, Anne Canteaut, Jacques Fournier and Renaud Sirdey, in the proceedings of the IEEE ISCAS 2018, Florence (Italy), May 2018.

[2] M. R. Albrecht, B. Driessen, E. B. Kavun, G. Leander, C. Paar, and T. Yalçin, "Block ciphers - focus on the linear layer (feat. PRIDE)," in CRYPTO 2014, Part I, ser. LNCS, J. A. Garay and R. Gennaro, Eds., vol. 8616. Santa Barbara, CA, USA: Springer, Berlin, Germany, Aug. 17–21, 2014, pp. 57–76.

[3] C. De Cannière, "Trivium: A stream cipher construction inspired by block cipher design principles," in Information Security: 9th International Conference, ISC 2006, ser. LNCS, S. K. Katsikas, J. López, M. Backes, S. Gritzalis, and B. Preneel, Eds., vol. 4176. Springer, 2006, pp. 171–186.

PROTECTING PERSONAL DATA IN IOT PLATFORM SCENARIOSTHROUGH ENCRYPTION-BASED SELECTIVE DISCLOSURE

RESEARCH TOPIC:

Reference Architecture for IoT, Protection of the Personal Data, Privacy by design, Attribute-Based Encryption

AUTHORS:

J. L. Hernandez-Ramos, S. Pereza, C. Hennebert (CEA),
J. Bernal Bernabe, B. Denis (CEA), A. Macabies, A. F. Skarmeta

ABSTRACT:

This paper aims at experimenting a new technique enabling privacy by design in a data-centric IoT architecture. The work has been carried in the context of the FP7 SocIoTal project in cooperation with the University of Murcia. A sensor network composed of OpenMote devices has been deployed in a building of the CEA-LETI to test and evaluate the introduced solutions. The data collected in the field are aggregated by the gateway at the edge to deduce the location of people wearing sensors. The location information is encrypted using an attribute-based encryption algorithm and shared with the members of the group having the same attributes. This experiment brings the experiment and the know-how of the implementation of a complete IoT platform. As feedback, it highlights the difficulty to handle privacy by design in a data-centric architecture.

SCIENTIFIC COLLABORATIONS:

Context and Challenges

This paper introduces a way to share data generated by personal devices through an IoT platform protecting by design the privacy of the users. This is achieved with a key management scheme based on attributes encryption, which allows to form groups using common characteristics between the members. A pairing approach is used to securely exchanged data between groups. This new technique of management of encrypted data has been experimented in a smart-building. As the building is equipped of anchors distributed in the corridors and the offices, the people owns emitters enabling to track their movements (Figure 1). The signals emitted are collected by the anchors, securely transmitted to a sink gateway, treated to compute the location of the people, and relayed to the context manager located in the cloud. As the location information is personal data, the privacy is protected through the CP-ABE technique before sharing with the members of the community of their owner

Main Results

The CEA-LETI was involved in realising a proof-of-concept of the attribute-based encryption technique in a complete IoT platform. The WSN nodes are IEEE 802.15.4-enabled devices using OpenMote hardware. The embedded application is Contiki-based. The user position is derived from its distance to anchor nodes. Such distance is computed using RSSI. The user carries a special device called the mobile node, along with a smartphone for graphical feedback. The goal is to display the real-time user's location on a map on the smartphone (Fig 2).

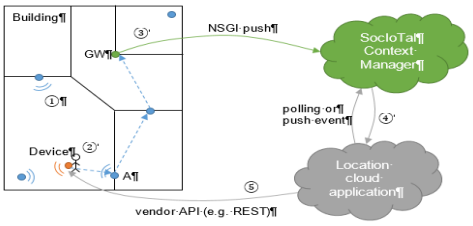

Figure 1: The radio localization scenario

Furthermore, the computed location is pushed to the Context Manager by using OMA NGSI-9/10 messages. Then, the third party \Location application,' hosted in the cloud, receives the updated location of the user/device, and finally, the graphical front-end running on the user's smartphone updates the position (protocol is application specific).

The platform aims to embrace different components to enable the creation and management of groups of members in the proposed scenario. By taking into account the addition of the CP-ABE Assistant component, the implementation details for each component are provided in the wiki : https://github.com/sociotal/SOCIOTAL/wiki.

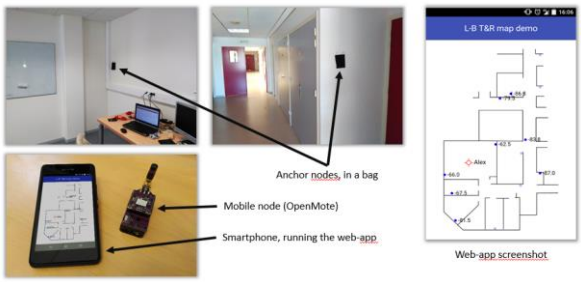

Figure 2: Deployment of the radio localization demonstrator in an indoor environment

The experiments have been performed with the OpenMote hardware that is narrowband IEEE 802.15.4 devices operating at 2.4 GHz in the ISM band. Furthermore, the gateway functionality was implemented on a Raspberry PI3.

Perspectives

This experiment highlights that privacy by design is difficult to handle in a data-centric IoT platform. The need for protection of the confidentiality of the data makes them difficult to share with others. New architectures of system user-centric orchestrate around a distributed ledger will be investigated in the following in order to implement solutions easier to scale for the protection of the personal data.

RELATED PUBLICATIONS:

[1] Christine Hennebert, Jessye Dos Santos, "Security Protocols and Privacy Issues into 6LoWPAN stack: A synthesis", *IEEE Internet of Things Journal Issue*, vol. 1, no. 5, pp. 384-398, october 2014

[2] J. Dos Santos, C. Hennebert, C. Lauradoux, "Preserving privacy in secured ZigBee wireless sensor networks", *2015 IEEE 2nd World Forum on Internet of Things (WF-IoT)*, pp. 715-720, 2015.

[3] B. Denis, L. He, L. Ouvry, A flexible distributed maximum log-likelihood scheme for UWB indoor positioning, in: 2007 4th Workshop on Positioning Navigation and Communication, 2007, pp. 77-86.

BINARY EDWARDS CURVES FIR INTRINSICALLY SECURE ECC IMPLEMENTATION FOR THE IOT

RESEARCH TOPIC:
Cryptography and embedded systems security.

AUTHORS:
Antoine Loiseau, Jacques Fournier

ABSTRACT:
Even if recent advances in public key cryptography tend to focus on algorithms able to survive the post-quantum era. At present, there is an urgent need to propose fast, low power and securely implemented cryptography to address immediate security challenges of the IoT. To achieve this challenge we have built a new set of Binary Edwards Curves up to the highest security levels (284-bit security level) and whose parameters have been defined to fit IoT device embedding 32-bit general-purpose processors. On top of the performance benefits, cryptography over such curves have some intrinsic security properties against physical attacks.

SCIENTIFIC COLLABORATIONS: These works have been done with JOE's project.

Context and Challenges
The rising amount of connectivity and number of connected devices has given rise to the concept of the "Internet of Things". One of the biggest challenges of the IoT is the Security and Privacy. The main difficulties with deploying security for the IoT come from the heterogeneity of this "system of systems". One of the key aspects of such systems is that end-to-end security has to be enforced, which means that the end-nodes of an IoT infrastructure shall also embed security features and applications. Asymmetric cryptography is one of such security tools and given the size, power and performance constraints pertaining to IoT end-nodes. Elliptic Curves Cryptography (ECC) is by far the best fit for such use cases and this despite the recently growing fear of quantum computer.

Main Results
Koblitz and Miller introduced ECC in 1987 and 1986, where the Elliptic Curve Discrete Logarithm Problem (ECDLP) is presented and its exploitation for doing cryptography over elliptic curves is explained. The main standardization effort for ECC has been through the FIPS 186 by the NIST. However, alternative approaches have been proposed like the Edwards Curve of Bernstein. These alternatives are more efficient than NIST's curves in terms of performance and security. Unfortunately, these works do not consider the challenge of IoT.

In these works, we propose a new set of elliptic curves with the alternative model of Binary Edwards Curves (BEC). This model fit with the constraints of IoT in terms of time computing and security. Moreover, we consider the constraint of the architecture during the generation of this new set. Finally, we have additional optimizations and this new set of elliptic curves admits an efficient implementation for general 32-bit architecture. To the generation algorithm, we have performed a completely new optimization to reduce the time computation by 20%.

Finally, after almost three months of computing over a cluster of 80 cores. We propose a new set of BEC for all security levels. The set is composed of 49 new curves. However only eight curves should use for optimal efficiency.

A software implementation of this new set has been done on a 32-bit RISC V core running at 100 MHz. The implementation is the fattest ECC library over 32-bit architectures. In fact, for 128 bits security level, which is the standard level to consider, *we performed a signature operation in 58 ms where the mbedTLS library perform the same operation with the standard curve P256 on a Cortex-M3 at 96 MHz in 122 ms. We gain almost 53% of time computing*. For the verification operation in the same conditions, we need 139 ms where mbedTLS needs 458 ms. We gain 70% of time computing. Moreover, against the Curve25519 of Bernstein, which is the main alternative of NIST's standards curves, we perform the first step of the key exchange protocol (ECDH) in 46 ms and the Curves25519 Google's implementation in 94 ms.

In terms of physical security, our new set of BEC and the implementation embed intrinsically security against a set of physical attacks. All these security properties were verified in real conditions. Additional countermeasures should be added to the implementation to protect the library against advanced attacks.

Perspectives
In future works, we plan to perform a hardware implementation of this new set of BEC over a FPGA. Moreover, additional studies shall be done over physical security of the implementation and the Binary Edwards Curves model.

RELATED PUBLICATIONS:
[1] "Binary Edwards Curves for intrinsically secure ECC implementations for the IoT", Antoine Loiseau and Jacques J. A. Fournier, SECRYPT 2018.
[2] "Binary Edwards Curves", D. Bernstein, T. Lange and R. Rezaeian Farashahi, LCNS volume 5154, 2008.
(3] "Batch binary Edwards", D. Bernstein, LCNS volume 5677, 2009.
[4] "Use of Elliptic-Curves in Cryptography", V. Miller, LCNS volume 218, 1986.
[5] "Elliptic curve cryptosystem", N. Koblitz, Mathematics of Computation volume 48, 1987.
[6] "A normal form for elliptic curves", Bulletin of the American Mathematical Society, 2007.

IOT SECURITY ASSESSMENT THROUGH THE INTERFACES
P-SCAN TEST BENCH PLATFORM

RESEARCH TOPIC:
Internet Of Things, IoT security assessment, automated security testing, interface testing, vulnerability detection

AUTHORS:
Thomas MAURIN (CEA), Laurent-Frédéric DUCREUX (CEA), George CARAIMAN (LCIE), Philippe SISSOKO (LCIE)

ABSTRACT:
The recent, massive and always-growing usage of communicating objects over interconnected networks enhances their vulnerability to cyber-attacks. The P-SCAN test platform is designed to democratize connected objects security assessment. Associated with security guidelines and a library of test suites, the scalable and customizable platform enables automating the process of testing security features on the device's communication interfaces to detect potential vulnerabilities.
This paper exposes the identified business needs and the corresponding provided technical solution.

SCIENTIFIC COLLABORATIONS: Univ. Grenoble Alpes, F-38000, Grenoble, France - CEA, LETI, MINATEC Campus, F-38054, Grenoble, France - LCIE Bureau Veritas, Fontenay-aux-Roses, France

Context and Challenges
The Internet of Things (IoT) has been a hot topic for the past several years and its adoption is rapid. As IoT spreads in virtually any kind of installations, it is now perceived as a new entry door for malicious people or organizations.
Cyberattacks examples mentioned in mass-media definitely raise public awareness on the threats of unsecured IoT. Mainstream security is now mandatory to ensure sustainability of all IoT businesses, making the security assessment of this wide, heterogeneous market a real challenge. Bureau Veritas (BV) and CEA Leti joined forces to develop an innovative approach to tackle this issue, tailored to the market needs [1].

The IoT is built upon the concept of remotely monitoring and controlling something via a connected solution. This is made possible by embedding connectivity features in new devices or enhancing legacy ones with added sensors, actuators and communication capabilities.
The attack surface is the whole set of vulnerabilities that can be potentially exploited by an attacker. The huge and increasing number of connected Things [2] expands the overall attack surface of the global IoT world into unprecedented proportions.
Consumers or industrial users of IoT devices may not all be aware of requirements this induces such as deep state-of-the-art knowledge of cyber-attacks and accordingly up-to-date dedicated tools. But tools or methodologies to assert protocol implementation correctness are not always publicly available. Then, security complexity must be abstracted to them. They should be able to rely on third-parties who provide trustworthy security assessments, labels and certifications [3].
Some international security evaluation frameworks such as Common Criteria (CC) exist but their associated complexity, delays and costs are too restrictive in regards of most IoT commercial and technical requirements. Some standards are emerging to complement legacy ones or attempting to structure a minimum baseline assessment upon private scheme [4].
In this global context, we envision a growing market niche where security evaluations are tailored to meet the concerns of the IoT providers.

Main Results
The P-SCAN offer is based on a highly automated cybersecurity service where (i) assessment of security features is performed through the communication interfaces (ii) with respect to the device's complexity and relevant low-to-medium security level (iii) in accordance to IoT business constraints (quick-to-market, incremental, low-cost) and (iv) managed and provided by a renowned and trusted third-party.
P-SCAN is a highly configurable and scalable automated test-bench. Its architecture is inspired from research work conducted in the Security dept. of CEA Leti [5]. It challenges security functions implemented in the evaluated device through all its interfaces. Collections of security test cases are available in an incremental library. An evaluation methodology is also specified in order to define specific security targets, to ensure that technical and documentary requirements are met to enable relevant evaluations. The BV's operator/evaluator defines the appropriate test plan by selecting and parametrizing the relevant test cases from the test library. This library is regularly updated by CEA-Leti's security engineers. Once parametrized accordingly, the test plan is automatically run and P-SCAN produces an evaluation report with clear Boolean verdicts for all executed test cases.

Perspectives
We describe here some aspects related to the cybersecurity for IoT. We identify a niche in a promisingly growing market and tailor an offer to respond to the associated segments' needs: (i) a rigorous methodology defined by seasoned security experts, (ii) a strong partnership between CEA-Leti and BV, which combines scientific and technical excellence, worldwide recognition in the security and evaluation areas, and (iii) a powerful tool which will meet demanding technical and business requirements such as high automation and incremental scalability capabilities with optimized operational costs.
We believe that with such an approach, we will help providers in their device development and deployment, even with evolving technologies and security threats.
The issuance of a future label would also bridge the gap towards the current security assessment certifications.

RELATED PUBLICATIONS:

[1] R. Hooper, A. Dell "Bureau Veritas to Unveil Disruptive Approach to Cyber Security Testing and Innovative Smart Wear Testing Solution at Mobile World Congress", February 2017
[2] Gartner "Gartner Says 8.4 Billion Connected "Things" Will Be in Use in 2017, Up 31 Percent From 2016", Feb. 2017
[3] ENISA "Infineon – NXP – STMicroelectronics – ENISA Common Position On Cybersecurity", December 2016
[4] UL "UL2900-1 Outline of Investigation for Software Cybersecurity for Network-Connectable Products, Part 1: General Requirements", Sept. 2016
[5] J.C. Fonbonne, "Automated and Remote Security Fuzz Testing Tool for IoT Devices", Computer & Electronics Security Applications Rendezvous (C&ESAR 2016), November 2016

ON THE IMPORTANCE OF ANALYSING MICROARCHITECTURE FOR ACCURATE SOFTWARE FAULT MODELS.

RESEARCH TOPIC:

Hardware fault injection, software fault model, cross-layer analysis, RISC-V processor, software countermeasures.

AUTHORS:

Johan Laurent, Vincent, Beroulle, Christophe Deleuze, Florian Pebay-Peyroula

ABSTRACT:

Fault injection is a powerful technique for attacking digital systems. Software developers have to take into account fault effects when system security is a concern. To this end, software fault models have been developed. However, these models are often designed independently of any hardware consideration and thus raise the problem of realism. The generality of these models cannot account for the specificities of each architecture. As a consequence, software countermeasures based on such software fault models do not guarantee a good protection against faults. Processor microarchitecture should be precisely analyzed to better understand faulty behaviors and design stronger software countermeasures. To illustrate this assumption, we show some faulty behaviors that have been observed on a RISC-V processor, and their consequences on typical software countermeasures.

SCIENTIFIC COLLABORATIONS: Univ. Grenoble Alpes, Grenoble INP, LCIS

Context and Challenges

Hardware fault injection has been an important threat to digital systems since the seminal work from Bellcore Lab [1]. To protect against this kind of threat, countermeasures can be built at the software level. To do this, it is necessary to rely on software fault models that represent the effects of a hardware fault on the software. Typical software fault models include instruction skip, test inversion or register corruption. These models, although interesting, are very general and are applied regardless of the processor microarchitecture under attack. This raises the question of their generality and if they can account for every possible faulty behavior? The answer is of course no, but so far, related works mainly show the inaccuracies in a quantitative manner [2]. In this work, we dive in the microarchitecture of a RISC-V processor (Rocket-core) to actually understand what can happen when a bit-flip is injected, and to build new software fault models from that.

Main Results

The analysis of a RISC-V microarchitecture showed that many weird behaviors can happen when the processor is attacked with a single bit-flip. It is for example possible to make a branch instruction modify the register-file, or to force the result of the ALU to 0 or 1. The most interesting effects happen when the fault makes use of some optimization structures in the processor. With branch prediction, it is possible to commit the result of a speculated (but wrong) instruction. With forwarding, it is possible to make an instruction "transient", meaning that its result can be seen by the following one or two instructions, but not the ones after. These last two effects happen because in the processor, instructions are not executed atomically, but are pipelined. This non-atomicity makes an important difference with the software point of view. A difference that is not considered in typical software fault models and that leads to interesting attacks [3].

The effects that are not taken into account by typical software fault models can make some software countermeasures ineffective. In particular, in [4], we show different ways to attack an instruction duplication countermeasure (an assembly instruction is executed twice, and results are compared).

Overall, we can say that many different behaviors are possible, and they depend heavily on the software that is being executed. The same bit-flip can have different effects depending on the instruction, the values used, and even the context of execution (faulting an isolated instruction can give different results when the same instruction is executed after other instructions). This multiplicity of faulty behaviors, coupled with the fact that these behaviors are very different from one another, means that it is difficult to find a general way to protect the processor. Moreover adding lots of countermeasures to try to thwart every possible scenario is not only difficult, but also costly. Furthermore, since certain types of faults can only occur under specific circumstances, many countermeasures would be useless most of the time. In light of this remark, we argue that the design of countermeasures should come after a cross-layer analysis of the whole system. By that we mean that only after having studied conjointly the hardware and the software parts of the system the developer can design cost-effective countermeasures. This kind of analysis does not aim at replacing existing methodologies, but acting as a complement. Existing analyses often focus on the quantitative side while we propose to add a qualitative analysis: faults are fewer but real.

Perspectives

The first perspective that comes from this preliminary work is to find a way to automatically extract software fault models from a given processor microarchitecture. In this way, we could have a set of accurate fault models that cover many possible faulty behaviors. A second perspective is to study the impact of multi-bit faults to see what kind of complex behaviors can be induced. Finally, a last perspective is to build a tool that could analyze the vulnerability of an application against the fault models extracted from the microarchitecture.

RELATED PUBLICATIONS:

[1] D. Boneh, R. A. DeMillo, and R. J. Lipton, “On the Importance of Checking Cryptographic Protocols for Faults,” in *Advances in Cryptology — EUROCRYPT ’97*, 1997, pp. 37–51.

[2] H. Cho, S. Mirkhani, C. Y. Cher, J. A. Abraham, and S. Mitra, “Quantitative evaluation of soft error injection techniques for robust system design,” in 2013 50th ACM/EDAC/IEEE Design Automation Conference (DAC), 2013, pp. 1–10.

[3] B. Yuce, N. F. Ghalaty, H. Santapuri, C. Deshpande, C. Patrick, and P. Schaumont, “Software Fault Resistance is Futile: Effective Single-Glitch Attacks,” in *2016 Workshop on Fault Diagnosis and Tolerance in Cryptography (FDTC)*, 2016, pp. 47–58.

[4] J. Laurent, V. Beroulle, C. Deleuze, F. Pebay-Peyroula and A. Papadimitriou, “On the Importance of Analysing Microarchitecture for Accurate Software Fault Models,” DSD-ASHA 2018.

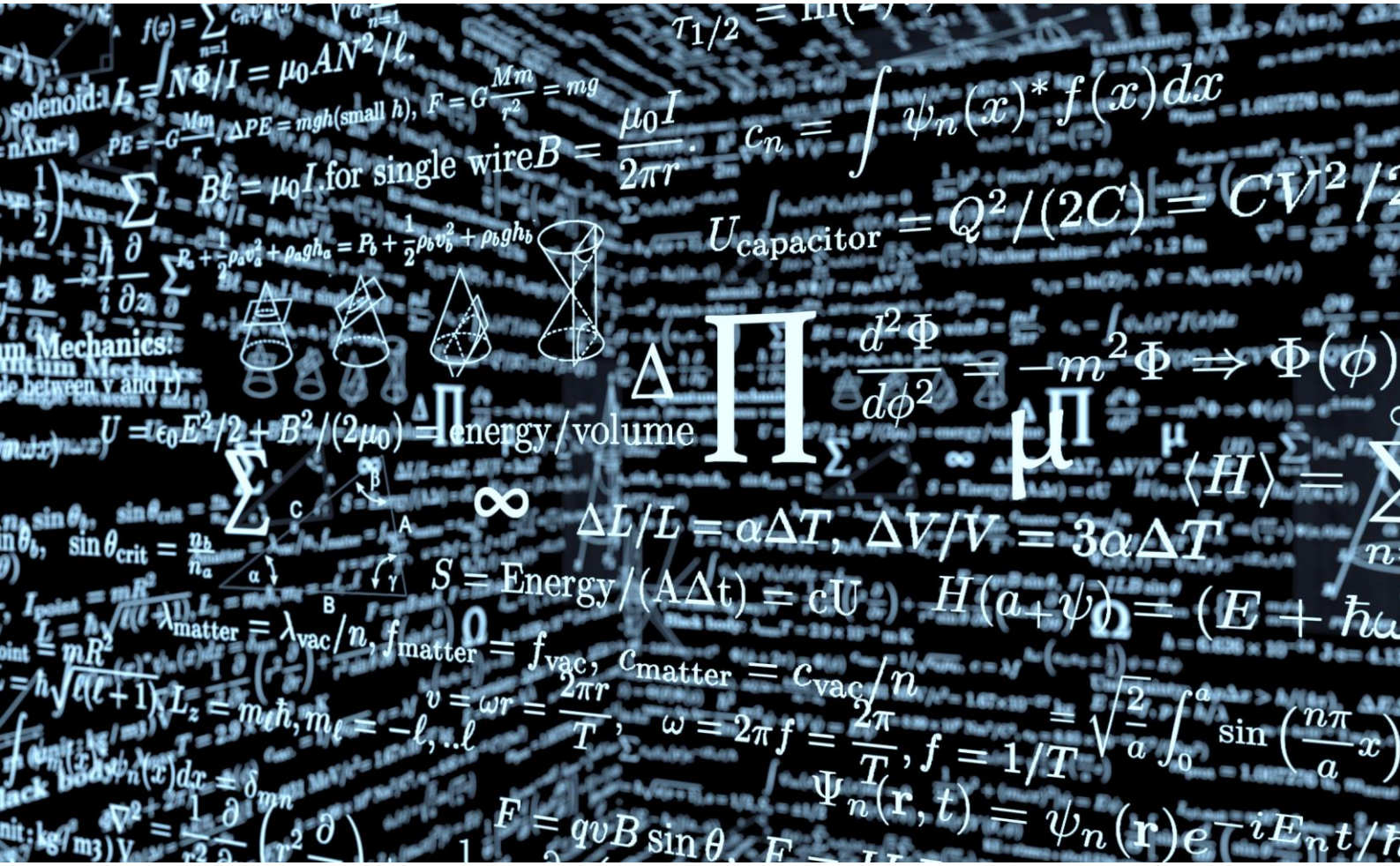

06 PHD DEGREES AWARDED IN 2018

- **Eleonora CAGLI**
- **Léo STERNA**
- **Gloria MAKHOUL**
- **Nebil KRISTOU**
- **Mouhcine MENDIL**
- **Fatimata DIABY**
- **Elodie MORIN**
- **Abdoul Sattar KADDOUR**
- **Kersane ZOUBERT-OUSSENI**

ELEONORA CAGLI

FEATURE EXTRACTION FOR SIDE-CHANNEL ATTACKS

Sorbonne Université (France)

Cryptographic integrated circuits may be vulnerable to attacks based on the observation of information leakages conducted during the cryptographic algorithms' executions, the so-called Side-Channel Attacks. Nowadays the presence of several countermeasures may lead to the acquisition of signals which are at the same time highly noisy, forcing an attacker or a security evaluator to exploit statistical models, and highly multi-dimensional, letting hard the estimation of such models.

In this thesis we study preprocessing techniques aiming at reducing the dimension of the measured data, and the more general issue of information extraction from highly multi-dimensional signals. The first works concern the application of classical linear feature extractors, such as Principal Component Analysis and Linear Discriminant Analysis. Then we analyse a non-linear generalisation of the latter extractor, obtained through the application of a Kernel Trick, in order to let such preprocessing effective in presence of masking countermeasures. Finally, further generalising the extraction models, we explore the deep learning methodology, in order to reduce signal preprocessing and automatically extract sensitive information from rough signal. In particular, the application of the Convolutional Neural Network allows us to perform some attacks that remain effective in presence of signal desynchronisation.

LEO STERNA

STUDY AND IMPLEMENTATION OF NEW BIDIRECTIONAL GAN TRANSISTORS WITHIN HIGH PERFORMANCES POWER ELECTRONICS STRUCTURES

Université Grenoble Alpes (France)

CEA-Leti offers bidirectional current-voltage transistors based on the HEMT GaN technology recently applied to the power switch design. The 4-segment bidirectional feature opens new perspectives in terms of power electronics structures and leads to explore the topologies that require this type of switches, allowing to design single-stage AC-DC or AC-AC conversion systems. These structures, which then require fewer switches, offer potential benefits in terms of compactness and efficiency. The 4-segment CEA Leti switch has the particularity of being single-gate type, which allows to control one bidirectional switch with just one control signal. On the other hand, this specificity leads to avoid classical control strategies and to explore new modes of control: in this context, this PhD work was interested in automatic switching strategies applied to the single gate bidirectional switch. A specific "switch frame" has been defined as a preliminary condition for the definition of any topology implementing this type of switch in order to implement ZCS or ZVS self-switching strategies. On this basis, two topologies, one ZCS, the other ZVS, were studied in the context of an AC/DC conversion with PFC function and power reversibility. The ZVS switching topology has been selected for experimental implementation. In this perspective, a specific ZVS auto-switching driver circuit has been designed. The converter operation, in ZVS auto-switching, is validated by tests on a prototype in

GLORIA MAKHOUL

RADIO PROPAGATION CHANNEL MODELING FOR MOBILE-TO-MOBILE COMMUNICATIONS

Université catholique de Louvain (Belgique)

Mobile-to-Mobile (M2M) communication is a challenge, but fast growing since it has the potential to enhance the quality of data service with low energy consumption. This dual mobility generates non-stationarity properties of the propagation channel, which requires precise modeling, for simulation network and system design.

This thesis aims for characterization and modeling of M2M channels based on stochastic approaches. Some common M2M aspects like the non-stationarity, Doppler and correlation properties were also analyzed. Stochastic channel models were proposed for Body-to-Body (B2B) and Vehicle to Pedestrian (V2P) channels based on measurements. The non-stationary fading behavior were observed as a function of mutual body orientation and the relative Tx-Rx distance. A general model for the auto-correlation function of the fading channel was derived assuming a typical M2M scenario in the presence of moving scatterers; and a simplify Doppler spectrum model was also developed for indoor M2M scenarios. Both models allow to reproduce with good accuracy the correlation and Doppler properties of different M2M scenarios including line-of-sight (LoS) and non-line of sight (NLoS) environments. Finally, implementation techniques able to reproduce the fading characteristics of M2M channels including the Doppler and correlation characteristics were proposed and successfully compared to the measurements.

NEBIL KRISTOU

STUDY AND DESIGN OF TUNABLE METAMATERIALS FOR THE MINIATURIZATION OF MICROWAVE FREQUENCY ANTENNAS

Rennes 1 University (France)

Antennas are now very integrated in several connected systems like cars, airplanes and trains. Many antenna miniaturization techniques exist and all go through a compromise between size and performance (bandwidth and/or radiation efficiency). For the systems mentioned above, the antennas are often placed near a metallic reflector (vehicle roof, aircraft cabin). Within this context, Artificial Magnetic Conductors (AMC) present an attractive reflector for low profile antennas which can take advantage of intrinsic zero reflection phase response to boost antenna performance without the need for thick quarter wave backplane. However, for sub-GHz applications (RFID, LTE, PMR ...), AMC are limited by the size of the unit cells necessary for their implementation ($\lambda g/4$) as well as their reduced operating bandwidth. AMC miniaturization makes their use compatible with small antennas. Adding tunability restores the possibility of adjusting the operating frequency over a large bandwidth. This PhD thesis proposes to study and develop a new electrically small, low-profile antenna based on miniaturized and tunable AMC for the NB-IoT standard in low LTE band (700 MHz – 960 MHz).

MOUHCINE MENDIL

JOINT RADIO AND POWER RESOURCE OPTIMAL MANAGEMENT FOR WIRELESS CELLULAR NETWORKS INTERCONNECTED THROUGH SMART GRIDS

Université Grenoble Alpes (France)

Mobile Network Operators (MNOs) are densifying their networks through the deployment of Small-cell Base Stations (SBSs), low-range radio-access transceivers that offer enhanced capacity and improved coverage. This infrastructure raise a crucial concern regarding their energy consumption and carbon footprint. In this context, the integration of renewable energy and energy storage capability in SBSs is a relevant solution allowing to gain in efficiency thanks to the technological enablers brought by the Smart Grid (SG). However, the obtained architecture, which we call Green Small-cell Base Station (GSBS), is complex. Thus, we have elaborated pre-deployment and post-deployment optimization frameworks for GSBSs that allow the MNOs to jointly reduce their electricity expenses and the equipment degradation. The pre-deployment optimization consists in an effective sizing of the GSBS that accounts in particular for the battery aging. The post-deployment scheme relies on learning capabilities to dynamically adjust the GSBS energy management to its environment (weather conditions, traffic load, battery status, and electricity cost). The solution developed consists in tuning a fuzzy inference system with the Q-learning algorithm. Results show that, by considering the battery aging and the system environment and interconnexion, the optimal sizing of the GSBS is able to maximize the return on investment. Also, thanks to its learning capabilities, the GSBSs can be deployed with the ability to self organize, improve the operating energy cost of the system, and preserves the battery lifespan.

FATIMATA TATA DIABY

ELECTRONICALLY RECONFIGURABLE TRANSMITARRAY ANTENNAS WITH BEAM-FORMING AND BEAM-STEERING AT MILLIMTRE WAVE FREQUENCIES

Université Grenoble Alpes (France)

The telecommunications domain has greatly evolved in the last decades with the advent of a wide range of applications such as satellite communication (SatCom) systems, wireless fixed and mobile networks, and broadcast services. However, this abundance of emerging applications is not without consequence; it is accompanied with a global bandwidth scarcity at lower frequencies. Nowadays, the millimeter wave frequencies, spanning from 30 GHz to 300 GHz, are increasingly explored to overcome the limitation of spectrum resources.

The aim of the PhD thesis, which has been founded by the French Research Agency (ANR) in the framework of the project TRANSMIL, was to implement high-gain fixed beams and electronically reconfigurable transmitarrays. The antennas developed in this thesis operate in Ka-band (27-40 GHz) and are based on standard Printed Circuit Board manufacturing technology. The Ka-band has been selected in this thesis because of the numerous applications developed there. Among these applications, we can mention the 5th–Generation mobile wireless networks, SatCom systems, and the Internet of Space (IoS).

The major contributions of this PhD thesis was: (i) the development of an optimization and simulation tool for multi-facetted transmitarrays, (ii) the demonstration of fixed- or multi-beam wideband transmitarrays with circular-polarization, and (iii) the demonstration of a 2-bit electronically-steerable transmitarray. The results demonstrate in this work are at the

ÉLODIE MORIN

INTEROPERABILITY OF ADAPTIVE LOW POWER COMMUNICATION PROTOCOLS FOR WIRELESS SENSORS NETWORKS

Université Grenoble Alpes (France): Laboratoire d'Informatique de Grenoble (LIG), CEA-Leti Grenoble, STMicroelectronics Crolles.

The growth of various technologies dedicated to sensor networks (WSN) has led to the development of platforms capable of operating in two different technologies, adaptive to transmission contexts. Such platforms open the door to the design of multi-technology networks, which we proposed to exploit to reduce overall energy consumption.
First, we described the main Internet of Things (IoT) technologies, comparing them on an equal footing thanks to the analyzer we developed, and we classified them according to the MAC mechanisms they use and the application context (latency and frequency of data generation).
Secondly, as sparse application traffic management are mainly based on always-on platform (in reception mode), we proposed to exploit the multi-technology platforms to build a synchronous network in which each node distributes its activity over time to globally save energy by replacing the role of the always-on platform, while guaranteeing the delivery of the latency-constrained asynchronous traffic.
Lastly, as currently standardized network attachment procedures are naïve and energy-greedy, we proposed to exploit the synchronous network joining phase to route latency-constrained traffic originating from asynchronous nodes through the synchronous network. Two approaches to reduce the cost of the TSCH network attachment procedure were proposed: The first one is based on the use of mathematical sequences which distribute the periods of activity over time, while minimizing the impact on the latency of the procedure, in order to reduce the overall energy cost of the attachment procedure. The second proposed method exploits the acknowledgement frames (ACK) of TSCH data communications to embed the date of the next synchronization frame transmission on the same physical channel as the ACK frame. Thanks to the development of a simulator of the TSCH joining phase, we show that the proposed protocols achieve better performance, in terms of joining latency or overall energy consumption, than the standard joining protocols used in WSN.

ABDUL SATTAR KADDOUR

EMBEDDED BROADBAND MEASUREMENT OF ELECTRICAL IMPEDANCE : APPLICATION TO BATTERY

CEA Leti / CNES / Université Grenoble Alpes (France)

These past years, the space sector is experiencing rapid growth (new players, new technologies) that tend to reduce the cost of telecom and observation applications via smaller satellites. In particular, reducing the size and weight of circularly polarized broadband antennas at VHF-UHF frequencies is a major challenge. However the miniaturization of an antenna is generally accompanied by a degradation of its efficiency and its bandwidth. In order to overcome this problem, the frequency agility technique constitutes an interesting solution to maintain the performance of the miniaturized antenna on a sub-band that can be driven on a wider frequency tuning range.
The "crossed magneto-electric dipole" antenna based on the Huygens source
concept is part of the most compact broadband antennas with excellent unidirectional radiation. The first objective of this thesis is to study and develop original miniaturization techniques. Then frequency agility is implemented on the miniaturized antenna to cover several octaves.
Several miniaturization techniques (geometric folding, capacitive loading) were developed based on 3D EM simulations, theoretical

KERSANE ZOUBERT-OUSSENI

POST-PROCESSING INDOOR LOCALIZATION ALGORITHMS

Université de Rennes 1 (France)

Indoor localization has received a growing interest with the massive use of smartphones, as they provide a powerful and rich platform to sense the environment through sensors, Wifi/BLE, GNSS and to access extra information like the map of the venue.

Although most the studies have focused on real-time fusion algorithms that use map-matching or fingerprinting technics, real-time positioning is not required for some applications like user behavior analysis or crowd sourcing applications.

In this study, a post-processing framework for indoor localization based on pedestrian dead reckoning (PDR) fusion with Wifi / BLE and map information is developed.

A first approach without floorplan based on an adaptive pathloss model for RSS measurements and on a piecewise parametrization for the PDR trajectory, has resulted in an average error of 6.2mfor the off-line estimation against 12.5m for the real-time estimation.

A second approach that accounts for map constraints and using particle smoother and a Viterbi algorithms has been introduced. Some other heuristics, like the map-less initialization and the repetition of the particle filter with score based selection have further improved the performances up to 3.6m against 5.8m for real time approaches.

A statistical machine learning algorithm has then be implemented to detect and reject all trajectories with a too low confidence level.

SYSTEMS

ANNUAL
RESEARCH REPORT
2018

Contacts

Sébastien DAUVÉ
Head of Systems Division
sebastien.dauve@cea.fr

Jean-Louis AMANS
Deputy Head of Systems Division
jean-louis.amans@cea.fr

Emilio CALVANESE-STRINATI
Scientific Manager
emilio.calvanese-strinati@cea.fr

Jean-Michel LÉGER
Program Manager
jean-michel.leger@cea.fr

Dimitri KTENAS
Head of Telecom Department
dimitri.ktenas@cea.fr

thierry BOUDET
Head of Energy Electronics & Sensor Systems Department
thierry.boudet@cea.fr

Bruno CHARRAT
Head of Electronics and components Department
bruno.charrat@cea.fr

Discover the CEA-Leti's Research Reports

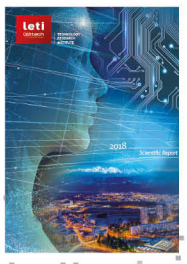

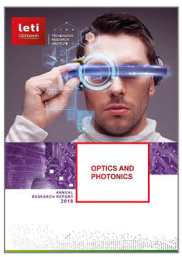

Leti, technology research institute
Commissariat à l'énergie atomique et aux énergies alternatives
Minatec Campus | 17 rue des Martyrs | 38054 Grenoble Cedex 9 | France
www.leti-cea.com

@CEA_Leti Leti

INSTITUT CARNOT Leti